

University of Alberta

**Unconstrained nonlinear state estimation for chemical  
processes**

by

**Arjun V Shenoy**

A thesis submitted to the Faculty of Graduate Studies and Research in partial  
fulfillment of the requirements for the degree of

**Master of Science**

in

**Process Control**

Department of Chemical and Materials Engineering

©Arjun V Shenoy  
Fall 2010  
Edmonton, Alberta

Permission is hereby granted to the University of Alberta Libraries to reproduce single copies of this thesis and to lend or sell such copies for private, scholarly or scientific research purposes only. Where the thesis is converted to, or otherwise made available in digital form, the University of Alberta will advise potential users of the thesis of these terms.

The author reserves all other publication and other rights in association with the copyright in the thesis and, except as herein before provided, neither the thesis nor any substantial portion thereof may be printed or otherwise reproduced in any material form whatsoever without the author's prior written permission.

## **Examining Committee**

Dr. Sirish L Shah, Chemical and Materials Engineering (co-supervisor)

Dr. Vinay Prasad, Chemical and Materials Engineering (co-supervisor)

Dr. Japan Trivedi, School of Mining and Petroleum Engineering (external examiner)

To Mummy, Papa, Archu and my lovely grandparents

# Abstract

Estimation theory is a branch of statistics and probability that derives information about random variables based on known information. In process engineering, state estimation is used for a variety of purposes, such as: soft sensing, digital filter design, model predictive control and performance monitoring. In literature, there exist numerous estimation algorithms. In this study, we provide guidelines for choosing the appropriate estimator for a system under consideration. Various estimators are compared and their advantages and disadvantages are highlighted. This has been done through case studies which use examples from process engineering. We also address certain robustness issues of application of estimation techniques to chemical processes. Choice of estimator in case of high plant-model mismatch has also been discussed. The study is restricted to unconstrained nonlinear estimators.

# Acknowledgements

Firstly, I would like to thank my co-supervisors Dr Sirish L. Shah and Dr Vinay Prasad, for all the time that they have invested in guiding me through my studies. I would like to thank them for all the wonderful opportunities that they have provided me with, during the course of my study at the University of Alberta. The experience that I have gained from these opportunities have helped me grow academically and more importantly as a person. It has helped me realize my own strengths and it has given me a confidence to face life with all its joys and sorrows. I need to thank them for the fact that the knowledge I have gained, is much more than what has been presented in this thesis. I would like to thank Dr Prakash from Madras Institute of Technology (India) for his guidance during my research. The numerous discussions with him have helped me gain a better understanding of state estimation theory. I would like to thank Dr Kim McAuley of Queen's University (Canada) for the resources that she has provided, to conduct research on the polyethylene reactor. I need to thank Dr Dave Shook, who has been a constant source of inspiration for me. The opportunities presented to me by him have helped me look at things practically. During the course of my study, many a times, I have landed myself in a penrose triangle where it has seemed that research has no end, leading to frustration. It is the company of my friends that has kept me running during this time. I would like to thank my friends: Xing, Anuj, Dru, Johnny, Yash, Sam, Bhushie, Shishir, Ganesh, Nagi, Sunil, Mranal, Rithika, Amit, JT, Mridul, Sandy and SKP for the wonderful time I have had in Edmonton. A special thanks to Saneer for his guidance during my research. Last but not the least, I need to thank my wonderful family, who have always been very supportive and who love so much.

# Contents

|          |  |           |
|----------|--|-----------|
| <b>1</b> | <b>Introduction</b>  | <b>1</b>  |
| 1.1      | Motivation . . . . .   | 1         |
| 1.2      | The state estimation problem . . . . .                                 | 2         |
| 1.3      | State estimation of polymer reactors . . . . .                         | 3         |
| 1.4      | Thesis overview . . . . .  | 4         |
| 1.4.1    | Thesis outline . . . . .   | 4         |
| 1.4.2    | Thesis contributions . . . . .   | 7         |
| <b>2</b> | <b>State estimation techniques</b>                                     | <b>8</b>  |
| 2.1      | State estimation for linear systems . . . . .                          | 9         |
| 2.1.1    | Kalman filter . . . . .  | 10        |
| 2.2      | Unconstrained state estimation techniques for nonlinear systems . . .  | 14        |
| 2.2.1    | Kalman update based estimators . . . . .                               | 15        |
| 2.2.2    | Monte Carlo technique based estimator . . . . .                        | 22        |
| 2.2.3    | Combination of Monte Carlo and Kalman update based estimator . . . . . | 25        |
| 2.3      | Constrained filtering . . . . .  | 28        |
| <b>3</b> | <b>Comparison of unconstrained state estimation techniques</b>         | <b>30</b> |
| 3.1      | Introduction . . . . .   | 30        |
| 3.2      | Literature review on comparison of state estimation techniques . . . . | 31        |
| 3.3      | Methyl methacrylate (MMA) polymerization CSTR . . . . .                | 35        |
| 3.3.1    | Process description . . . . .  | 35        |
| 3.3.2    | Modeling the PMMA reactor . . . . .                                    | 36        |
| 3.3.3    | Estimation framework . . . . .   | 37        |
| 3.3.4    | Observability . . . . .  | 38        |
| 3.4      | Filter performance under different noise statistics . . . . .          | 38        |
| 3.4.1    | Case studies . . . . .   | 38        |

|       |  |    |
|-------|--|----|
| 3.4.2 | Analysis of case studies . . . . .   | 39 |
| 3.5   | EKF versus UKF : Effect of process noise to measurement noise co-<br>variance ratios (Q/R) ratio on filter performance . . . . . | 45 |
| 3.5.1 | Noise statistics and tuning parameters . . . . .   | 45 |
| 3.5.2 | Case 1 - Low Q/R ratio . . . . .   | 46 |
| 3.5.3 | Case 2 - Q and R ratios are comparable . . . . .   | 47 |
| 3.5.4 | Case 3 - High Q/R ratio . . . . .  | 51 |
| 3.5.5 | Analysis and Concluding remarks - EKF versus UKF . . . . .   | 52 |
| 3.5.6 | Heuristic tuning of Kalman update based filters . . . . .  | 57 |
| 3.6   | Ensemble Kalman filter for state estimation . . . . .  | 58 |
| 3.6.1 | Analysis of the application of EnKF to a PMMA reactor . . . . .  | 58 |
| 3.7   | State estimation in case of non-Gaussian posterior . . . . .   | 60 |
| 3.7.1 | Application of particle filters . . . . .  | 62 |
| 3.7.2 | Filter tuning and performance . . . . .  | 63 |
| 3.7.3 | Concluding remarks for the particle filter . . . . .   | 64 |
| 3.8   | Proportional-integral based Kalman filters . . . . .   | 69 |
| 3.8.1 | PI-KF algorithm . . . . .  | 69 |
| 3.8.2 | PI-KF algorithm on two tank system . . . . .   | 69 |
| 3.8.3 | Similarity between integral action and state augmentation . . . . .  | 73 |
| 3.8.4 | Concluding remarks . . . . .   | 73 |
| 3.9   | Point estimate extraction from full state distributions . . . . .  | 74 |
| 3.9.1 | Non-stationary growth model . . . . .  | 74 |
| 3.9.2 | Non-Gaussian posteriors . . . . .  | 75 |
| 3.9.3 | Methods of information extraction . . . . .  | 76 |
| 3.9.4 | Summary on point estimate extraction from full state distri-<br>butions . . . . .  | 80 |

|          |  |           |
|----------|--|-----------|
| <b>4</b> | <b>State and parameter estimation of a gas phase polyethylene reactor<br/>using particle filters</b> | <b>82</b> |
| 4.1      | Literature review . . . . .  | 83        |
| 4.2      | Gas phase polyethylene reactor . . . . .   | 85        |
| 4.2.1    | Process description . . . . .  | 85        |
| 4.2.2    | Reactor modeling . . . . .   | 85        |
| 4.2.3    | Estimation framework . . . . .   | 89        |
| 4.3      | Application of particle filters . . . . .  | 93        |
| 4.4      | Unscented particle filters for high plant-model mismatch . . . . .                                   | 98        |

|       |  |     |
|-------|--|-----|
| 4.4.1 | Analysis of application of UPF to gas phase polyethylene FBR | 101 |
| 4.5   | Concluding remarks . . . . .                                 | 101 |

**5 Concluding remarks and future work 105**

|       |  |     |
|-------|--|-----|
| 5.1   | Concluding remarks . . . . .                           | 105 |
| 5.2   | Future work . . . . .                                  | 107 |
| 5.2.1 | Nonlinear observability . . . . .                      | 107 |
| 5.2.2 | Issues with particle filters . . . . .                 | 108 |
| 5.2.3 | Subspace identification for state estimation . . . . . | 108 |
| 5.2.4 | Proportional integral based estimators . . . . .       | 109 |
| 5.2.5 | Polyethylene FBR : future work . . . . .               | 109 |
| 5.2.6 | Estimation of MWD and PSD . . . . .                    | 109 |
| 5.2.7 | Tuning of filters . . . . .                            | 110 |

# List of Tables

|     |  |    |
|-----|--|----|
| 3.1 | Operating parameters for the simulated PMMA CSTR . . . . .             | 37 |
| 3.2 | Summary of case studies ( $G = Gaussian$ ; $NG = Non-Gaussian$ ) . . . | 40 |
| 3.3 | EKF versus UKF for varying process-measurement noise ratio . . . .     | 56 |
| 3.4 | MSE values for tuning of particle filter . . . . .                     | 68 |
| 3.5 | Comparison of EKF , UKF and PF MSE values . . . . .                    | 68 |
| 3.6 | Tabulation of variables for two tank system . . . . .                  | 71 |

# List of Figures

|     |  |    |
|-----|--|----|
| 1.1 | State estimation schematic . . . . .   | 2  |
| 1.2 | State estimation of a two tank system . . . . .  | 3  |
| 1.3 | Off-specification polymer produced during steady state operation of polymer reactors illustrates the importance of monitoring polymer product quality variables . . . . .  | 4  |
| 1.4 | State estimation for detection of product quality variables . . . . .  | 5  |
| 1.5 | Off-specification polymer produced during grade transition in polymer reactors illustrates the importance of monitoring polymer product quality variables during grade transition . . . . .  | 5  |
| 1.6 | State estimation for product quality control in polymer reactors . . . . .   | 6  |
| 2.1 | Flowchart of state estimation techniques. . . . .  | 9  |
| 2.2 | Schematic of the Extended Kalman Filter. . . . .   | 18 |
| 2.3 | The principle of the unscented transform (adapted from Julier and Uhlmann (1997)). Sigma points are used to represent the variable under consideration in the $x$ -space. These are then passed through the nonlinear transformation $F$ to get transformed points in the $y$ -space. The statistics calculated using transformed points, represent the statistics of the variable under consideration in the $y$ -space . . . . . | 19 |
| 2.4 | Prediction - correction formulation of the unscented Kalman filter with equations. . . . .   | 20 |
| 2.5 | Schematic of the unscented Kalman filter. . . . .  | 21 |
| 2.6 | Schematic of the particle filter (adapted from der Merwe et al. (2000)).   | 25 |
| 2.7 | Combining Monte Carlo technique with Bayes rule to derive the Sequential Monte Carlo technique (PF) . . . . .  | 26 |
| 3.1 | MMA polymerization reactor schematic . . . . .   | 36 |

|      |  |    |
|------|--|----|
| 3.2  | State estimation in the presence of zero process noise, Gaussian measurement noise (standard deviation (std) of 0.01), and a 10% positive step in cold water flow rate. . . . .  | 41 |
| 3.3  | State estimation in the presence of Gaussian state noise (std of 1 and 0.01 on the monomer and initiator concentrations respectively), Gaussian measurement noise (std of 0.01 on the temperatures), and a 10% positive step in cold water flow rate. . . . .                                | 42 |
| 3.4  | State estimation in the presence of non-Gaussian state (multimodal with std of 1 and 0.01 on the monomer and initiator concentrations respectively), non-Gaussian measurement noise (multimodal with std of 0.01 on the temperatures) and a 10 % positive step in monomer flow rate. . . . . | 43 |
| 3.5  | State estimation in the presence of non-Gaussian measurement noise (multimodal with std of 0.01 on the temperatures) and a 10 % positive step in monomer flow rate. . . . .  | 44 |
| 3.6  | Distribution of noise sequences used in the simulation studies that follow. . . . .  | 46 |
| 3.7  | Case 1 - Estimation under low process-measurement noise ratio. . . .   | 48 |
| 3.8  | Case 1 - Covariance propagation under low process-measurement noise ratio. . . . .   | 48 |
| 3.9  | Case 1 - Kalman gain propagation of measured states under low process-measurement noise ratio. The figure shows the Kalman gains tend to zero. . . . .   | 49 |
| 3.10 | Case 2 - Kalman gain propagation of measured states under unit process-measurement noise ratio. The figure shows the Kalman gain lies between 0 and 1. . . . .   | 50 |
| 3.11 | Case 2 - Estimation under unit process-measurement noise ratio. . . .  | 50 |
| 3.12 | Case 2 - Plots to show biased EKF estimates compared to UKF estimates for monomer concentration under unit process-measurement noise ratio. The bias is not more than that seen in case 3. . . . .   | 51 |
| 3.13 | Case 2 - Covariance propagation under unit process-measurement noise ratio. . . . .  | 52 |
| 3.14 | Case 3 - Kalman gain propagation of measured states under high process-measurement noise ratio. The figure shows the Kalman gain approaches 1. . . . .   | 53 |

|      |   |    |
|------|---|----|
| 3.15 | Case 3 - Estimation under high process-measurement noise ratio. . . .   | 53 |
| 3.16 | Case 3 - Plots to show biased EKF estimates compared to UKF estimates for monomer concentration under high process-measurement noise ratio. . . . .   | 54 |
| 3.17 | Case 3 - Covariance propagation under high process-measurement noise ratio. . . . .   | 54 |
| 3.18 | Estimation intervals for temperatures (measured states). Intervals obtained as maximum and minimum values at each time instant for 1000 Monte Carlo simulations. Plant (blue), EKF (Red) and UKF (green). The solid blue line that runs through the center is the average of plant values. $Q/R \sim 1$ . . . . .     | 56 |
| 3.19 | Estimation intervals for concentrations (unmeasured states). Intervals obtained as maximum and minimum values at each time instant for 1000 Monte Carlo simulations. Plant (blue), EKF (Red) and UKF (green). The solid blue line that runs through the center is the average of plant values. $Q/R \sim 1$ . . . . . | 57 |
| 3.20 | Box plots for 100 Monte Carlo simulations for the case where $Q/R$ ratio $\sim 1$ . . . . .   | 58 |
| 3.21 | EnKF estimation plots for 1 minute of time run . . . . .  | 60 |
| 3.22 | MSE values of UKF/EnKF for the case study on comparison of UKF and EnKF performances on a PMMA reactor. . . . .   | 61 |
| 3.23 | CPU run times of UKF and EnKF for the case study on comparison of UKF and EnKF performances on a PMMA reactor. . . . .  | 61 |
| 3.24 | Evolution of posterior for $C_m$ . The posterior is either skewed or multimodal. The overlying Gaussian distribution fails to describe the histogram accurately. . . . .  | 63 |
| 3.25 | Evolution of posterior for $C_m$ . The posterior is either skewed or multimodal. The overlying Gaussian distribution fails to describe the histogram accurately. . . . .  | 64 |
| 3.26 | Evolution of posterior for $C_i$ . The posterior is either skewed or multimodal. The overlying Gaussian distribution fails to describe the histogram accurately. . . . .  | 65 |
| 3.27 | Particle filter performance for Case 1 under high process covariance. .   | 66 |
| 3.28 | Distribution of weights for particle filter application for Case 2 (under reduced process covariance). . . . .  | 66 |

|      |   |    |
|------|---|----|
| 3.29 | Particle filter performance for Case 2 (under reduced process noise covariance). . . . .  | 67 |
| 3.30 | Distribution of weights for particle filter application for Case 3 (under increased measurement noise covariance). . . . .  | 67 |
| 3.31 | Particle filter performance for Case 3 (under increased measurement noise covariance). . . . .  | 68 |
| 3.32 | Schematic of two tank system used to study the PF-KF problem . . .  | 70 |
| 3.33 | State estimates for the two tank system with Kalman filter . . . . .  | 72 |
| 3.34 | State estimates for the two tank system response with proportional integral Kalman filter . . . . .   | 72 |
| 3.35 | Importance of point estimate extraction from non-Gaussian posteriors. Notice that the mode and mean do not match for non-gaussian distributions. . . . .                | 74 |
| 3.36 | Evolution of non-Gaussian posteriors at specific time instants for non-stationary growth model. . . . .   | 75 |
| 3.37 | Poor performance of EKF for non-stationary growth model. . . . .  | 76 |
| 3.38 | Superior performance of PF in comparison to EKF for non-stationary growth model. . . . .  | 77 |
| 3.39 | PF with mean and mode as point estimates for non-stationary growth model. . . . .   | 78 |
| 3.40 | Failure in information extraction from full state distribution provided by particle filter. . . . .   | 79 |
| 3.41 | Information extraction using k-means clustering from full state distribution provided by particle filter. . . . .   | 79 |
| 3.42 | 'K-means' clustering from full state distributions provided by particle filter. . . . .   | 80 |
| 4.1  | Schematic of a gas phase fluidized bed reactor for polyethylene production . . . . .  | 86 |
| 4.2  | Estimation framework for the gas phase fluidized bed reactor for polyethylene production . . . . .  | 92 |
| 4.3  | Plot of inlet feeds for gas phase FBR for polyethylene production (plots have been scaled due to the proprietary nature of the data) . .                                | 93 |
| 4.4  | Measurement smoothing using particle filters for gas phase FBR for polyethylene production (plots have been scaled due to the proprietary nature of the data) . . . . . | 94 |

|      |  |     |
|------|--|-----|
| 4.5  | Estimation of polymer product properties using particle filters for gas phase FBR for polyethylene production (plots have been scaled due to the proprietary nature of the data) . . . . .           | 95  |
| 4.6  | Estimation of unmeasured state using particle filters for gas phase FBR for polyethylene production (plots have been scaled due to the proprietary nature of the data) . . . . .                     | 95  |
| 4.7  | Parameter estimation using particle filters for gas phase FBR for polyethylene production (plots have been scaled due to the proprietary nature of the data) . . . . .                               | 96  |
| 4.8  | Problem of particle degeneracy due to overlap of likelihood and prior near tail of likelihood or no overlap at all. (idea for figures adapted from der Merwe et al. (2000)) . . . . .                | 97  |
| 4.9  | Incorporating feedback into prior particles using Kalman update based filters for proposal generation. (figure adapted from der Merwe et al. (2000)) . . . . .                                       | 99  |
| 4.10 | Estimation of polymer product properties using unscented Kalman filters for gas phase FBR for polyethylene production (plots have been scaled due to the proprietary nature of the data) . . . . .   | 100 |
| 4.11 | Measurement smoothing using unscented particle filters for gas phase FBR for polyethylene production (plots have been scaled due to the proprietary nature of the data) . . . . .                    | 102 |
| 4.12 | Estimation of polymer product properties using unscented particle filters for gas phase FBR for polyethylene production (plots have been scaled due to the proprietary nature of the data) . . . . . | 103 |
| 4.13 | Estimation of unmeasured state using unscented particle filters for gas phase FBR for polyethylene production (plots have been scaled due to the proprietary nature of the data) . . . . .           | 103 |
| 4.14 | Parameter estimation using unscented particle filters for gas phase FBR for polyethylene production (plots have been scaled due to the proprietary nature of the data) . . . . .                     | 104 |
| 5.1  | Flowchart to help in the decision for choice of state estimation technique   | 106 |

# List of Symbols

|                  |   |
|------------------|---|
| $x_k$            | state at time instant $k$   |
| $F_k$            | state transition model at time instant $k$  |
| $G_k$            | control-input model at time instant $k$   |
| $w_k$            | process at time instant $k$   |
| $y_k$            | measurement at time instant $k$   |
| $H_k$            | observation model at time instant $k$   |
| $v_k$            | measurement noise at time instant $k$   |
| $Q$              | process noise covariance matrix   |
| $R$              | measurement noise covariance matrix   |
| $N(0, Q)$        | Normal distribution with mean 0 and covariance $Q$                                      |
| $x(k k-1)$       | predicted state of time instant $k$ with known information upto time instant $k-1$      |
| $\hat{x}(k k-1)$ | expected values( $E$ ) of $x(k k-1)$  |
| $P$              | state covariance matrix   |
| $K_k$            | Kalman gain at time instant $k$   |
| $I$              | Identity matrix   |
| $p(x_k Y_k)$     | conditional density of $x(k)$ , given all measurement information ( $Y$ ) upto time $k$ |
| $\Theta_k$       | parameters at time instant $k$  |

# List of Abbreviations

|             |   |
|-------------|---|
| <i>KF</i>   | Kalman Filter                                 |
| <i>EKF</i>  | Extended Kalman Filter                        |
| <i>UKF</i>  | Unscented Kalman Filter                       |
| <i>EnKF</i> | Ensemble Kalman Filter                        |
| <i>PF</i>   | Particle Filter                               |
| <i>UPF</i>  | Unscented Particle Filter                     |
| <i>MSE</i>  | Mean Square Error                             |
| <i>RMSE</i> | Root Mean Square Error                        |
| <i>MMA</i>  | Methyl Methacrylate                           |
| <i>PMMA</i> | Poly Methyl Methacrylate                      |
| <i>CSTR</i> | Continuous Stirred Tank Reactor               |
| <i>SIR</i>  | Sequential Importance Resampling              |
| <i>ASIR</i> | Auxiliary Sequential Importance Resampling    |
| <i>SMC</i>  | Sequential Monte Carlo                        |
| <i>PID</i>  | Proportional Integral Derivative (Controller) |
| <i>PI</i>   | Proportional Integral (Controller)            |
| <i>GRV</i>  | Gaussian Random Variable                      |
| <i>FBR</i>  | Fluidized Bed Reactor                         |

*PSD* Particle Size Distribution

*MWD* Molecular Weight Distribution

*MI* Melt Index

# Chapter 1

## Introduction

### 1.1 Motivation

Estimation theory is a powerful tool that has been used in most fields of science and engineering. Signal processing, economics, robotics, aeronautics, medicine, telecommunications are a few of the fields that use estimation theory. In process industries, estimation is widely used to infer accurate measurements from noisy sensor data, i.e., as a soft sensor to predict variables that are not measurable online and/or to estimate parameters to obtain accurate dynamic process models, and for model predictive control. This not only provides improved control, but assists in fault detection and process monitoring. Most chemical processes exhibit highly nonlinear dynamics, and the extended Kalman filter (EKF) has been widely used to solve the related estimation problems. Though numerous algorithms exist, process engineering continues to lag behind in the implementation and use of advanced estimation techniques. Over the past decade, the literature on the application of estimation theory in process engineering has been receiving increasing attention. However, to the knowledge of the author, the literature lacks a direct comparison of all techniques to process engineering examples. The objective of this work is to study the application of various estimation techniques and to evaluate them by application to benchmark (polymer) process engineering systems. We differentiate estimators based on their advantages and disadvantages, and provide guidelines on which estimator to use under which circumstance, depending on specific features (process dynamics) of the application under consideration. We also address certain issues with respect to tuning of the filters and their robustness. This thesis aims to provide a framework for the selection of the appropriate unconstrained estimator for different chemical processes.

## 1.2 The state estimation problem

Estimation theory is the science of estimating the values of variables and parameters of a model (that describe a system) using measured or empirical data. A state-space model is used to describe the system under consideration, and model parameters and variables are obtained using state estimation algorithms. Fig 1.1 shows a schematic of the state estimation problem. Known quantities such as system inputs and measurements are fused with a model of the system to give smoothed measurements and estimates of unmeasured parameters and states. For example, in a two-tank non-interacting system, if the height of liquid in the second tank were to be measured, the estimation algorithms would compute the smoothed measurements of the level in tank 2 and provide an estimate of level of liquid in tank 1 (Fig 1.2).

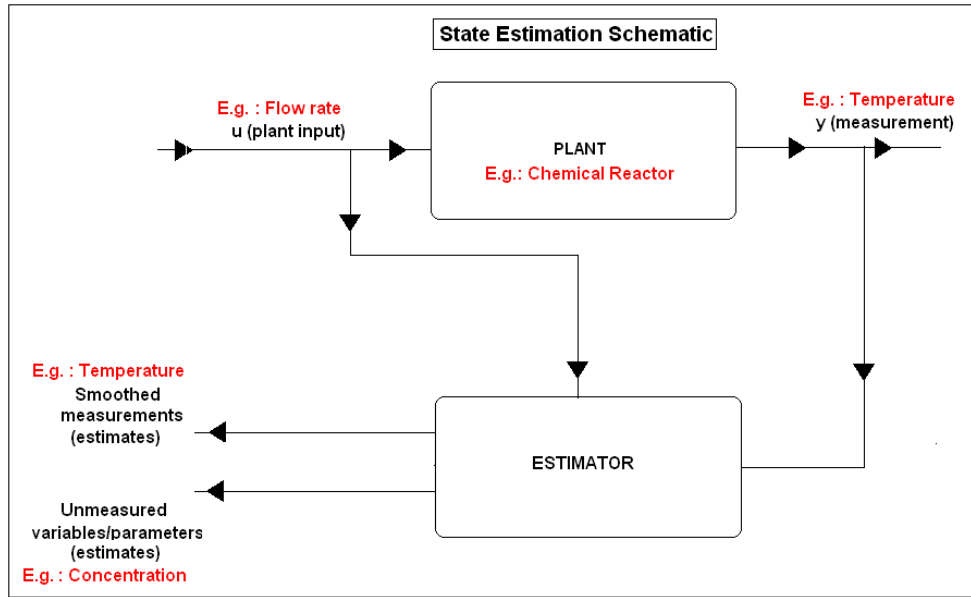


Figure 1.1: State estimation schematic

In a mathematical sense, if a process were to be described by a state-space model as described by eqs. 1.1 and 1.2 (or a nonlinear model), where  $x$  represents the states of the system,  $u$  the inputs and  $y$  the measurements, estimation theory predicts  $p(x(k)|Y)$ , where  $k$  represents a discrete instance in time;  $p(x(k)|Y)$  is the conditional probability density function of the state conditioned over all measurements up to time  $k$ ; and  $w$  and  $v$  represent the uncertainty in state transition and measurement models respectively.

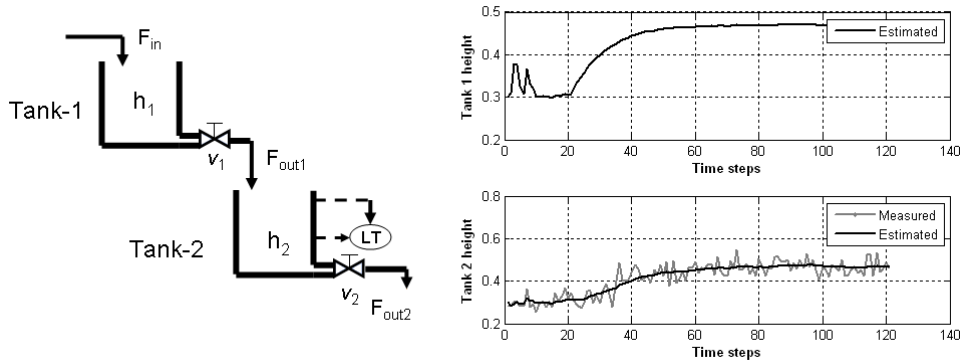


Figure 1.2: State estimation of a two tank system

$$x(k) = F_k x(k-1) + G_k u(k) + w(k) \quad (1.1)$$

$$y(k) = H_k x(k) + v(k) \quad (1.2)$$

State estimation depends on the properties of the system under consideration. More information on full state estimation (estimation of all states) and its dependence on the properties of the system can be obtained from Ray (1981). Estimation of states of a system depends on the observability of the dynamic equations used to represent it. Observability is a measure of how many of the internal states of a system may be calculated from measurements. If a state is unobservable based on the dynamic model of the system and its measurements, then the internal state cannot be estimated. Therefore there is a need for good dynamic models which fuse the measurements to achieve full state observability.

### 1.3 State estimation of polymer reactors

Ohshima and Tanigaki (2000), Asua (2007), Embirucu et al. (1996), Kiparissides and Morris (1996) and Soroush (1998) have highlighted the importance of state estimation algorithms in the polymer industry. Polymerization reactors are a good platform to study the application of different estimation techniques as they exhibit highly nonlinear dynamics. Moreover, polymerization kinetics can take place through many mechanisms, and these processes are carried out in different types of reactors. Therefore, such systems provide a broad range of cases studies to evaluate the state estimation algorithms. Also, polymer quality variables such as melt index and polymer density are not measurable online. If at any instance of time,

the polymer quality variables extend beyond the client specifications, the product may be rendered as an off-specification polymer which is of no use to both the polymer vendor and the client (Fig 1.3). Hence, monitoring of process variables is of utmost importance (Fig 1.4). Also, the polymer product specifications requested by different vendors may be different. Hence, transition from one grade of polymer to the other needs to be done in an optimal manner. The polymer that is produced during transition is off-specification polymer (Fig 1.5) and clearly given the state estimates, one can develop control strategies to minimize the off-spec product during and between grade transitions. Such methods would then improve the economic and monetary gains of polymer production by effective utilization of resources and decrease of transition time. For optimization algorithms to be effective, it is critical that they receive accurate estimates of process and polymer quality variables (Fig 1.6).

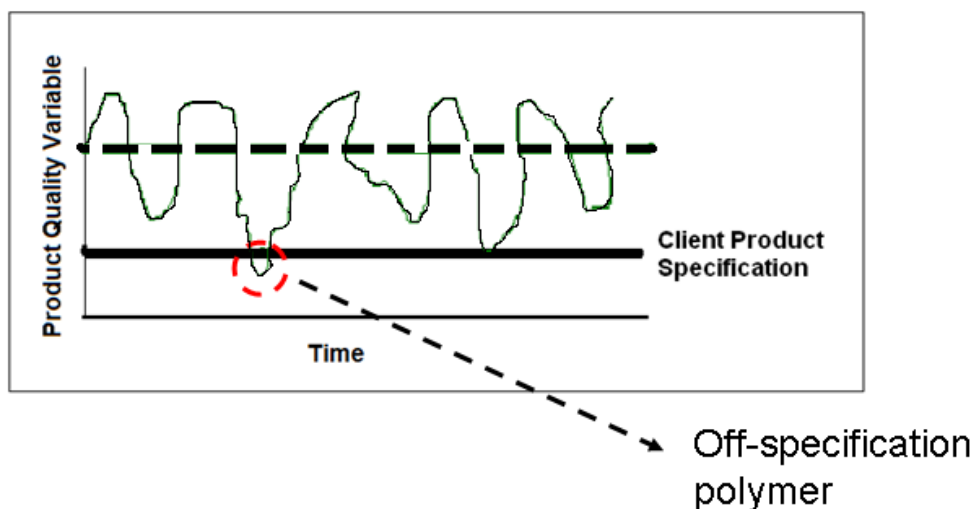


Figure 1.3: Off-specification polymer produced during steady state operation of polymer reactors illustrates the importance of monitoring polymer product quality variables

## 1.4 Thesis overview

### 1.4.1 Thesis outline

The thesis is organized as follows: Algorithms for advanced state estimation are discussed in chapter 2 of the thesis. Chapter 3 contains results for comparison of

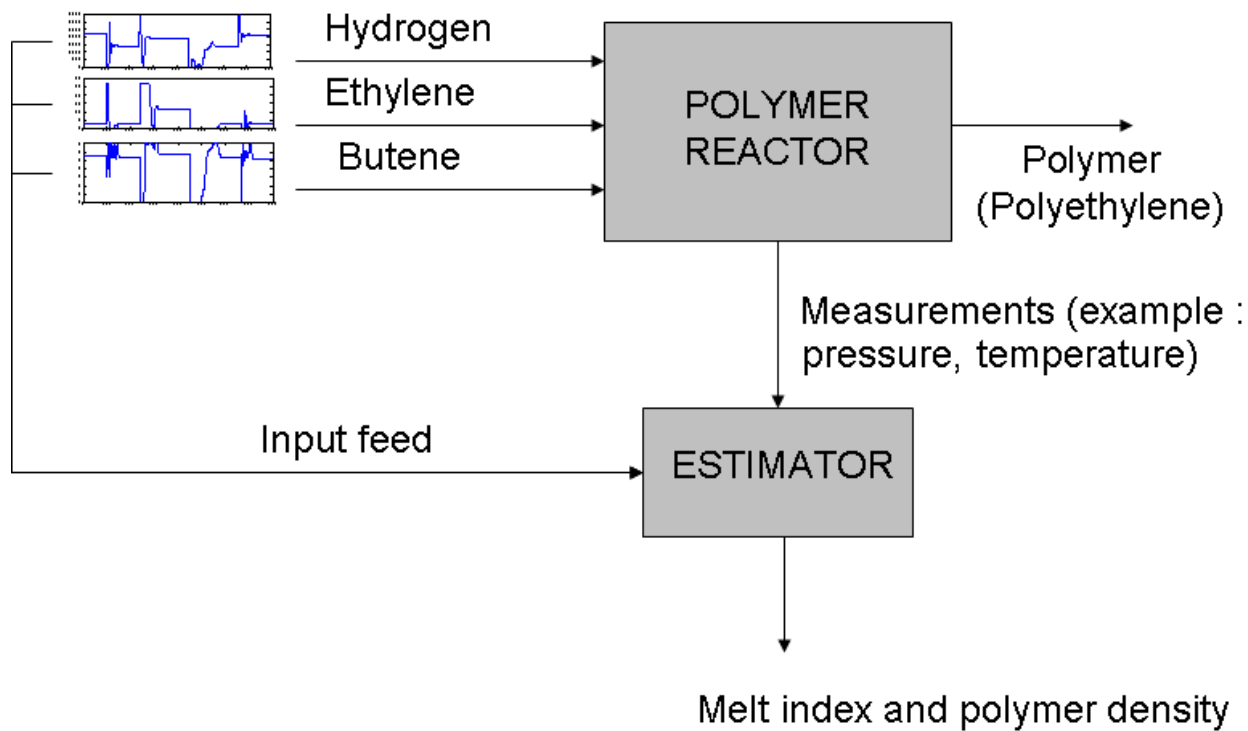


Figure 1.4: State estimation for detection of product quality variables

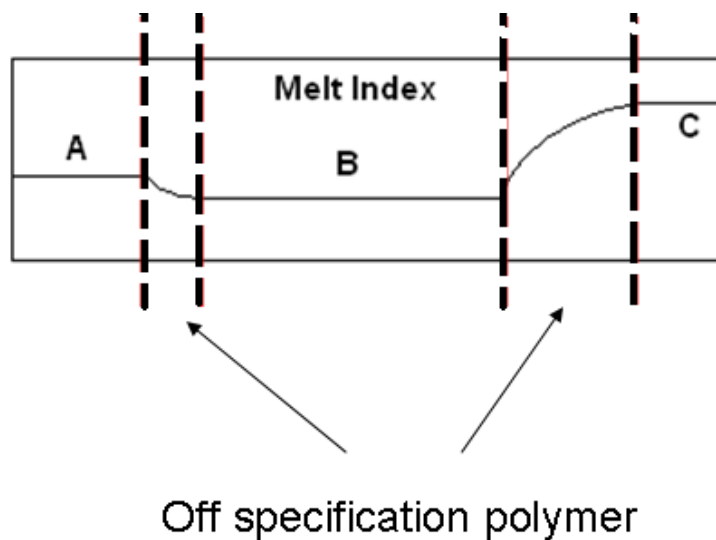


Figure 1.5: Off-specification polymer produced during grade transition in polymer reactors illustrates the importance of monitoring polymer product quality variables during grade transition

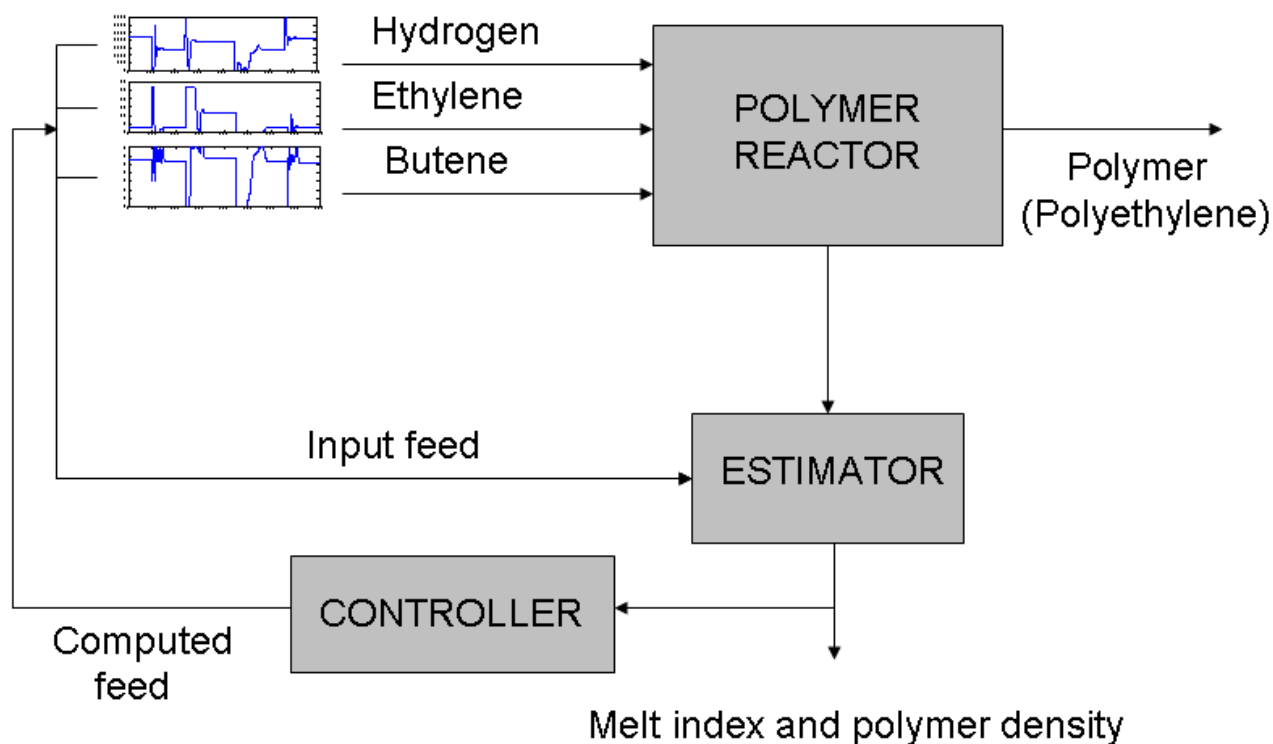


Figure 1.6: State estimation for product quality control in polymer reactors

unconstrained state estimation techniques. First, a comprehensive literature review on comparison of estimation algorithms is presented. Advanced estimation techniques are applied onto a MMA polymerization CSTR, and their results are compared. The EKF, UKF and PF are compared on the basis of system properties, i.e., different noise sequences (Gaussian and non-Gaussian). Later, the EKF and UKF are compared with respect to their tuning parameters (process to measurement noise ratios). State estimation using the EnKF and its comparison to the UKF is also presented in chapter 3. The use of PF's for state estimation of full state distributions and non-Gaussian sequences is also highlighted. The importance of introducing integral action to state estimation algorithms and its reduction to state augmentation formulation is discussed. Clustering techniques to extract point estimates from full state distributions is documented in the last part of chapter 3. Chapter 4 introduces a gas phase fluidized bed reactor for polyethylene production. The application of PF and UPF to this system is presented in chapter 4. Chapter 5 contains some concluding remarks, and recommendations for future study.

## 1.4.2 Thesis contributions

Comparison of state estimation techniques have been presented by many researchers. A collection of past and recent literature in this research area is listed in the next chapter. The main thesis contribution that distinguishes this piece of work from current and past studies are as follows:

(1) This thesis provides detailed guidelines for the selection of appropriate unconstrained estimators (EKF, UKF, EnKF, PF, UPF) for chemical processes. This is done through a case study approach.

(2) In chapter 2, a systems analysis approach to state estimation of a polymethyl methacrylate (PMMA) continuous stirred tank reactor (CSTR) has been presented. Case studies have been conducted to exhibit the performance of estimation algorithms under different Gaussian and non-Gaussian noise sequences. This part of the thesis has been presented as a publication at the IFAC-DYCOPS 2010 meeting in Leuven, Belgium.

(3) The EKF linearization error in the form of bias has been characterized by application on the PMMA reactor. This study successfully differentiates linearization error from approximation errors.

(4) In a novel study of tuning particle filters, Imtiaz et al. (2006) presented a method using distribution of weights applied to *a priori* state estimates to tune particle filters. In our work, we have extended this method to a PMMA reactor, demonstrating the ease of implementation of this algorithm.

(5) The importance of introducing integral action in state estimation, and its reduction to state augmentation is a practical contribution demonstrated in chapter 3.

(6) In chapter 3, we demonstrate alternate approaches to using the expectation ( $E$ ) as the point estimate in Bayesian estimation (especially for the PF). We demonstrate the use of 'k-means' clustering for modal analysis of the probability distribution of the estimate.

(7) In chapter 4, the importance of proposal generation in particle filters for cases of large plant-model mismatch is illustrated. In this case study, we have applied the particle filter to a polyethylene polymerization reactor under a high dimensional plant-model and reduced order estimation model framework.

(8) Using a polyethylene reactor as an example, Kalman update based filters are shown to be more stable than particle filters in case of high plant-model mismatch. The unscented particle filter, a modification of the generic particle filter using the UKF to generate the proposal is shown to be a robust estimator.

# Chapter 2

## State estimation techniques

In the previous chapter, the state estimation problem was introduced. In this chapter, various estimation algorithms are discussed. Fig. 2.1 provides an overview of different estimation techniques under the stochastic framework. Estimation techniques are first differentiated based on the type of system dynamics they are applied to - as linear and nonlinear estimators. The next differentiation is by the nature of the algorithm - as constrained or unconstrained based filters. Under the unconstrained framework, the Kalman filter provides the optimal solution to the linear state estimation problem. The need for an optimal solution to the nonlinear estimation problem has led to the derivation of numerous estimation algorithms each under different fundamentals, principles and assumptions. Kalman update based nonlinear estimators include the extended Kalman filter (EKF) and the unscented Kalman filter (UKF). The particle filter (PF) and its variants, such as the sequential importance resampling (SIR) based PF, the auxiliary SIR (ASIR) particle filter and the unscented or ensemble based PF (UPF, EnKF-PF) are Monte Carlo based nonlinear estimators. The ensemble Kalman filter is a nonlinear estimator that combines the Kalman update with Monte Carlo based techniques. Under the constrained framework, estimation algorithms include moving horizon estimation (MHE), nonlinear dynamic data reconciliation (NDDR), recursive NDDR (RNDDR) and constrained versions of the unconstrained techniques such as the constrained KF and the constrained EKF.

Section 2.1 introduces the linear state estimation problem and the Kalman filter. The linear Kalman filter forms the basis for derivation and understanding of most nonlinear estimators. Hence, it is discussed in detail here. The nonlinear estimation problem and the different techniques used are introduced later in section 2.2. Section 2.3 is a brief note on unconstrained state estimation techniques.

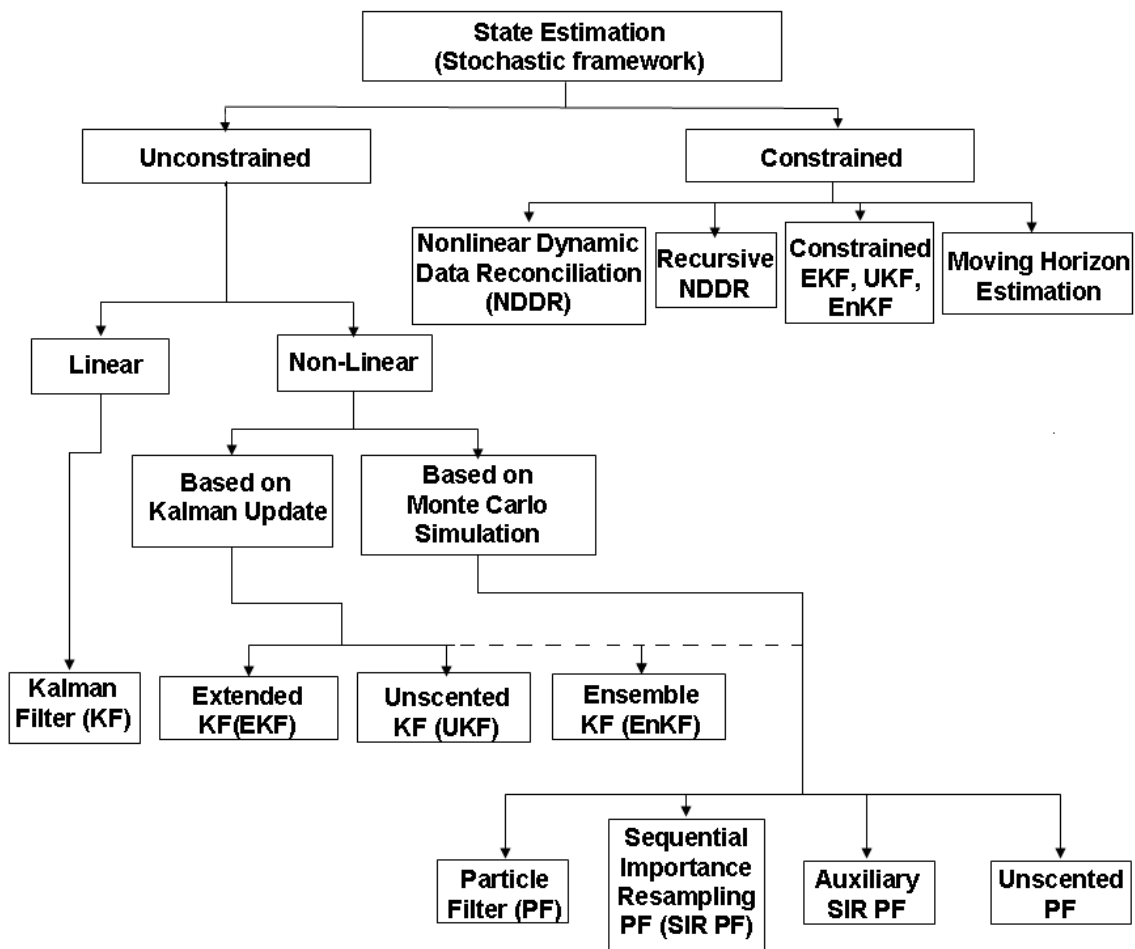


Figure 2.1: Flowchart of state estimation techniques.

## 2.1 State estimation for linear systems

Under the discrete time framework, a linear dynamical system can be described by equations 2.1 and 2.2.  $w$  and  $v$  are uncertainties associated with the process and measurement respectively.  $F_k$  is the state transition matrix applied to the previous state  $x_{k-1}$ .  $G_k$  is the control-input matrix applied to the input vector  $u_k$ .  $H_k$  is the observation model which relates the state vector to the measured variables ( $y_k$ ).

$$x(k+1) = F_k x(k) + G_k u(k) + w(k) \quad (2.1)$$

$$y(k) = H_k x(k) + v(k) \quad (2.2)$$

Under the stochastic estimation framework, the optimal solution to the dynamic estimation problem was described by Kalman (1960). Details of the Kalman filter and its evolution are described in the next section.

### 2.1.1 Kalman filter

The study of revolution of heavenly bodies lead to the evolution of a new branch of mathematics called estimation theory. The earliest work in estimation theory was introduced by Friedrich Gauss in the form of a least squares problem (Sorenson (1985)). Subsequent improvements in the field of estimation theory lead to the development of one the most powerful algorithms in history: published by R E Kalman in 1960 as the Kalman Filter (Kalman (1960)). The Kalman filter provided state estimates using noisy measurement data. It was based on a framework of optimality and it provided the optimal solution to the state estimation problem for linear stochastic systems. This new method was based as a recursive prediction - correction algorithm unlike previous algorithms that used a batch of past and current data. Under its assumptions, the Kalman filter provides the optimal solution to the linear state estimation problem (Maybeck (1979)). It can be either formulated as a minimum mean squared error problem or as a maximum likelihood estimation algorithm under the Bayesian framework. In Kalman (1960), the idea of Kalman filter was devised by combining the state transition matrix with orthogonal projections. A collection of early work on Kalman filtering, its derivatives and its applications is provided by Sorenson (1985). Jazwinski (1970) and Gelb (1974) provide further information on the KF algorithm and its implementation. Maybeck (1979) provides an introduction to the estimation problem and basics of the Kalman filter, including its implementation and its underlying assumptions. In a tutorial, Welch and Bishop (2001) introduce the Kalman filter equations with its assumptions as a novel solution to the linear filtering problem. The application of the KF to a problem is system specific, and this has lead to development of a wide range of derivatives of the traditional KF. A comprehensive review of the KF and its derivatives with examples and its derivations based on when one or more of its assumptions are violated can be obtained in Simon (2006). The derivation of the KF as an optimal recursive data processing algorithm is documented below. The KF differs from its earlier counterparts as it does not require batches of data. It can be represented as a Markov process where the current information can be derived based on the information at the previous time instant. First, the KF is derived as a minimum mean squared error estimator. Later, the KF derivation is discussed under the Bayesian framework. With respect to eqs. 2.1 and 2.2, the assumption is that  $w$  and  $v$  are zero mean Gaussian noise with covariances  $Q$  and  $R$  respectively. The noise is assumed to be white and uncorrelated at each time instant.

$$w_k \sim N(0, Q_k)$$

$$v_k \sim N(0, R_k)$$

Under these assumptions, the objective of the Kalman filter is to obtain the conditional pdf  $p[x(k)|Y^k]$ . The KF is a predictor-corrector method, i.e., it involves a prediction step (time update) where state predictions are obtained without incorporating the most recent measurements, followed by a correction step (measurement update) where the predictions are corrected based on the incoming measurements.

### Time update

The first step is to predict the state and covariance estimates at each instant in time. This step is prior to the measurement becoming available. Eq. 2.3 represents the one step ahead prediction of the state  $x$  using the model of the process that the estimator uses.

$$\hat{x}(k|k-1) = E[x(k)|k-1] = F_{k-1}\hat{x}(k-1|k-1) + G_{k-1}u(k-1) \quad (2.3)$$

The next step is to derive the one step ahead predicted covariance. The following steps lead to equation. 2.16 which is the simplified expression of the predicted covariance.

$$P_{k|k-1} = E[(x(k) - \hat{x}(k|k-1))(x(k) - \hat{x}(k|k-1))^T]$$

$$P_{k|k-1} = E[(F_{k-1}x(k-1) + G_{k-1}u(k-1) + w(k-1) - F_{k-1}\hat{x}(k-1|k-1) - G_{k-1}u(k-1))(\dots\dots\dots)^T]$$

$$P_{k|k-1} = E[(F_{k-1}(x(k-1) - \hat{x}(k-1|k-1)) + w_{k-1})(\dots\dots\dots)^T]$$

$$P_{k|k-1} = E[F_{k-1}(x(k-1) - \hat{x}(k-1|k-1))(x(k-1) - \hat{x}(k-1|k-1))^T F_{k-1}^T + w_{k-1}w_{k-1}^T + F_{k-1}(x(k-1) - \hat{x}(k-1|k-1))w_{k-1}^T + w_{k-1}(x(k-1) - \hat{x}(k-1|k-1))^T F_{k-1}^T]$$

$$P_{k|k-1} = F_{k-1}P_{k-1|k-1}F_{k-1}^T + Q_{k-1}$$

$$P_{k|k-1} = F_{k-1}P_{k-1|k-1}F_{k-1}^T + Q_{k-1} \quad (2.4)$$

### Measurement update

Once the time update is complete, the incoming measurement information is employed to obtain the measurement update steps. The equation for the state estimate is obtained by weighing the prediction error from the model and the innovation error using the Kalman gain. Eq. 2.5 represents this equation.

$$\hat{x}(k|k) = \hat{x}(k|k-1) + K_k(y_k - H_k\hat{x}(k|k-1)) \quad (2.5)$$

Based on this proposed equation, the covariance update and Kalman gain expressions can be derived under an optimization framework as a minimum mean squared error (MMSE) estimator.

First the covariance expression is derived. Equation. 2.6 represents the expression for covariance measurement update

$$\begin{aligned} P(k|k) &= cov(x_k - \hat{x}(k|k)) \\ P(k|k) &= cov(x_k - (\hat{x}(k|k-1) + K_k(y_k - H_k\hat{x}(k|k-1)))) \\ P(k|k) &= cov(x_k - (\hat{x}(k|k-1) + K_k(H_kx(k) + v(k) - H_k\hat{x}(k|k-1)))) \\ P(k|k) &= cov((I - k_k H_k)(x_k - \hat{x}(k|k-1)) - K_k v_k) \\ P(k|k) &= (I - k_k H_k)cov(x_k - \hat{x}(k|k-1))(I - k_k H_k)^T + K_k cov(v_k) K_k^T \\ P(k|k) &= (I - k_k H_k)P_{k|k-1}(I - k_k H_k)^T + K_k R_k K_k^T \end{aligned} \quad (2.6)$$

Next, the Kalman gain expression is derived. The objective is to obtain an MMSE estimate represented by the expression given in equation. 2.7.

$$min E[|x(k) - \hat{x}(k|k)|^2] = min tr P_{k|k} \quad (2.7)$$

$$\begin{aligned} P_{k|k} &= P_{k|k-1} - k_k H_k P_{k|k-1} - P_{k|k-1} H_k^T k_k^T + K_k (H_k P_{k|k-1} H_k^T + R_k) K_k^T \\ P_{k|k} &= P_{k|k-1} - k_k H_k P_{k|k-1} - P_{k|k-1} H_k^T k_k^T + K_k (S_k) K_k^T \\ \frac{\partial tr P_{k|k}}{\partial K_k} &= -2(H_k P_{k|k-1})^T + 2K_k S_k = 0 \\ K_k &= P_{k|k-1} H_k^T S_k^{-1} \end{aligned}$$

Eq 2.8 is the derived Kalman gain expression under the optimal framework.

$$K_k = P_{k|k-1} H_k^T S_k^{-1} \quad (2.8)$$

where  $S_k$  is given by  $H_k P_{k|k-1} H_k^T + R_k$

Based on the Kalman gain expression, the covariance update equation can be simplified (eq. 2.9).

$$\begin{aligned}
K_k S_k K_k^T &= P_{k|k-1} H_k^T K_k^T \\
P_{k|k} &= P_{k|k-1} - k_k H_k P_{k|k-1} - P_{k|k-1} H_k^T k_k^T + K_k (S_k) K_k^T \\
P_{k|k} &= P_{k|k-1} - k_k H_k P_{k|k-1} \\
P_{k|k} &= P_{k|k-1} (I - K_k H_k)
\end{aligned}$$

$$P_{k|k} = P_{k|k-1} (I - K_k H_k) \quad (2.9)$$

Eq's. 2.3 to 2.9 represent the Kalman filter equations that are used to implement the KF on any system. There are three variables/parameters that can be used to tune the filters: the initial state matrix ( $x_0$ ), the initial state covariance matrix ( $P_0$ ), and the ratio of noise covariance matrices ( $Q/R$ ).

The KF can also be derived under the Bayesian framework using maximum likelihood statistics. The true state  $x$  is assumed to be a Markov process, i.e., the current state ( $x(k)$ ) can be calculated from the state of the process at the previous time step ( $x(k-1)$ ). It does not require information of any other previous states ( $x(k-2), \dots, x(0)$ ). The measurement  $y$  is assumed to be a hidden Markov process, i.e., the observable states of a Markov process. Due to the Markov assumption, the following equations hold:

$$\begin{aligned}
p(x(k)|x(k-1)x(k-2)\dots x(0)) &= p(x(k)|x(k-1)) \\
p(y(k)|x(k)x(k-1)\dots x(0)) &= p(y(k)|x(k-1))
\end{aligned}$$

Based on the above equations, the probability distribution over all states of the hidden Markov process can be obtained :

$$p(x(0), \dots, x(k), y(1), \dots, y(k)) = p(x(0)) \prod_{i=1}^k p(y(i)|x(i)) p(x(i)|x(i-1))$$

The Chapman-Kolmogorov equation, which uses the Markov property is given by equation. 2.10. It provides a recursive relationship relationship between the posterior densities of the states at two different time instants based on the the previous measurement.

$$p(x(k)|Y(k-1)) = \int p(x(k)|x(k-1)) p(x(k-1)|Y(k-1)) dx(k-1) \quad (2.10)$$

$Y(k)$  = the measurement set up to time  $k = y(1), y(2), \dots, y(k)$

Using Bayes rule, eq. 2.11 can be derived

$$p(x(k)|Y(k)) = \frac{p(y(k)|x(k))p(x(k)|Y(k-1))}{p(y(k)|Y(k-1))} \quad (2.11)$$

The expression for  $p(y(k)|Y(k-1))$  is given by eq. 2.12

$$p(y(k)|Y(k-1)) = \int p(y(k)|x(k))p(x(k)|Y(k-1))dx(k) \quad (2.12)$$

Using the above equations with the following densities gives the Kalman filter under Bayesian framework

$$\begin{aligned} p(x(k)|x(k-1)) &= N(F_k x(k-1), Q_k) \\ p(Y(k)|x(k)) &= N(H_k x(k), R_k) \\ p(x(k)|Y(k-1)) &= N(\hat{x}(k-1), P_{k-1}) \end{aligned}$$

The Kalman filter has been the basis for the development of a large number of algorithms in estimation theory. Ever since its introduction in 1960, it has been the most widely applied algorithm to obtain smoothed measurements and estimates of hidden state variables. In the subsequent section we discuss a number of estimation techniques for nonlinear systems, most of which use the Kalman update.

## 2.2 Unconstrained state estimation techniques for nonlinear systems

In the previous section, the Kalman filter algorithm was discussed in detail. As illustrated, the Kalman filter is the optimal solution to the linear estimation problem. However, most processes exhibit highly nonlinear dynamics. A nonlinear system can be represented by equations. 2.13 and 2.14.

$$x(k) = F(x(k-1), u(k)) + w(k) \quad (2.13)$$

$$y(k) = H(x(k)) + v(k) \quad (2.14)$$

In certain cases, the process nonlinearity can be captured very accurately by linear

models. A Kalman filter would be adequate in this case. However, if linear models cannot be used to represent the system, a nonlinear estimator is required for estimation purposes. In the earliest efforts, numerous versions of the Kalman filter were proposed to solve the nonlinear estimation problem. However, until now, no general optimal solution is available for the estimation of nonlinear systems, and it is an open research problem. In this section, some of the most commonly used nonlinear estimators are discussed. In section 2.2.1 the Kalman update based filters are discussed. In section 2.2.2 Monte Carlo based methods are discussed, followed by section 2.2.3 that highlights a filter that combines the Kalman update with Monte Carlo techniques.

### **2.2.1 Kalman update based estimators**

In this section, two commonly used Kalman update based nonlinear estimators are illustrated. These filters use the Kalman update for point estimate calculation and covariance update as represented by equations. 2.5 to 2.9. The Gaussian assumption is used in all of these filters. First, the extended Kalman filter is introduced, followed by the unscented Kalman filter. In each of these filters, the nonlinearity is approximated in different ways for the time update, followed by the measurement update adapted exactly from the generic Kalman filter.

#### **Extended Kalman Filter**

As pointed out earlier, most processes exhibit highly nonlinear dynamics, and the Kalman filter does not always provide a satisfactory solution to this problem. Early attempts to solve the nonlinear estimation problem involved linearizing the nonlinear equations around a nominal state trajectory and then applying the Kalman filter (linearized Kalman filter). Later, it was proposed that the nonlinear equations could be linearized around the Kalman filter estimate, thus forming a dynamic linearization approach. This filter commonly became known as the Schmidt-Kalman filter (Schmidt (1966)) or the extended Kalman filter (EKF). Further information on the EKF can be found in Maybeck (1979) , Jazwinski (1970), Gelb (1974), Welch and Bishop (2001) and Simon (2006).

In this section, the EKF has been derived under the continuous-discrete framework, as this is the most commonly used form of the estimator. It can however be derived under the continuous or discrete formulations. In the continuous-discrete framework, the system is treated as a continuous time system with measurements taken

at discrete time intervals. The system is modeled under the nonlinear framework represented by equations. 2.13 and 2.14. The steps involved in the EKF are the same as the KF, except for the linearization step (jacobian calculation) at each discrete instant of time.

### Time Update

$$\hat{x}(k|k-1) = F(\hat{x}(k-1|k-1), u(k-1)) \quad (2.15)$$

The covariance time update is the same as for the KF.

$$P_{k|k-1} = A_{k-1}P_{k-1|k-1}A_{k-1}^T + Q_{k-1} \quad (2.16)$$

In equation. 2.15,  $F_{k-1}$  is the linearization of nonlinear function  $F$  around the current state estimate ( $\hat{x}_{k-1|k-1}$ ) and model inputs ( $u_{k-1}$ ).

$$A_{k-1} = \frac{\partial A}{\partial x} |_{\hat{x}(k-1|k-1), u(k-1)}$$

### Measurement Update

The measurement update is also similar to the KF except that the nonlinear measurement function  $H$  is used to predict the measurements. A linearized form of  $H$  is required for the calculation of Kalman gain as represented in equation. 2.17. Hence, at each instant in time,  $H$  is linearized around the predicted estimate ( $\hat{x}(k|k-1)$ ).

$$C_k = \frac{\partial H}{\partial x} |_{\hat{x}(k|k-1)}$$

$$K_k = P_{k|k-1}C_k^T S_k^{-1} \quad (2.17)$$

where  $S_k$  is given by  $C_k P_{k|k-1} C_k^T + R_k$

$$\hat{x}(k|k) = \hat{x}(k|k-1) + K_k(y_k - H(\hat{x}(k|k-1))) \quad (2.18)$$

$$P_{k|k} = P_{k|k-1}(I - K_k C_k) \quad (2.19)$$

Eqs. 2.15 to 2.19 represent the extended Kalman filter equations. The assumptions made in the KF hold for the EKF as well (i.e. Gaussian white noise sequences).

Implementation of the EKF can be understood from the schematic presented in fig. 2.2. The estimator is initialized with guess values of state ( $x(0)$ ) and covariance ( $P_0$ ) matrices. The nonlinear system propagation model is linearized around the initial state and input variables. The linearized model is used in the one step ahead covariance prediction ( $P_{k|k-1}$ ). The state space model of the process is used to obtain the one step ahead predicted state estimate ( $\hat{x}(k|k-1)$ ).  $\hat{x}(k|k-1)$  and  $P_{k|k-1}$  are the prior estimates obtained from the time update step. The correction part of the algorithm begins with the linearization of measurement propagation equation around the predicted state (to obtain  $C_k$ ). This is used in the Kalman gain ( $K_k$ ) calculation. The state estimate at time  $k$  ( $\hat{x}_{k|k}$ ) is obtained by weighing (using the calculated Kalman gain,  $K_k$ ) the predicted estimate and the measurement innovation. Note that the most recent measurement ( $y_k$ ) is incorporated in this calculation. The covariance estimate at time  $k$  ( $P_{k|k}$ ) is then obtained.  $K_k$ ,  $\hat{x}_{k|k}$  and  $P_{k|k}$  are known as the posterior estimates. These steps are repeated in time in a recursive formulation. In this algorithm, the tuning parameters are the noise covariance matrices. The estimator is sensitive to the initial state vector and the initial state covariance matrix based on the system dynamics.

The EKF is the most widely used estimator in chemical processes. In fields such as navigation and aerospace, the EKF seems to be losing out to more recently developed techniques which have demonstrated certain advantages in comparison. For highly nonlinear systems, the linearization performed by the EKF is unable to represent the true system dynamics (Romanenko and Castro (2004)). It has been shown to diverge or produce biased estimates under certain cases of nonlinear dynamics. The drawbacks of the EKF and its application to chemical processes with comparison to other estimators are discussed in later chapters.

### Unscented Kalman Filter

The EKF is based on a simple linear approximation that represents the system nonlinearity at each time instant. This however leads to linearization bias when the linearized set of equations are unable to represent the nonlinear dynamics accurately. Need for an alternate method to represent system nonlinearity has led to a novel algorithm called the unscented Kalman filter (UKF). The UKF is based on the principle of the unscented transform. As stated by Julier and Uhlmann (1997), the unscented transform is founded on the premise that it is easier to approximate a Gaussian distribution than it is to approximate a nonlinear function or transforma-

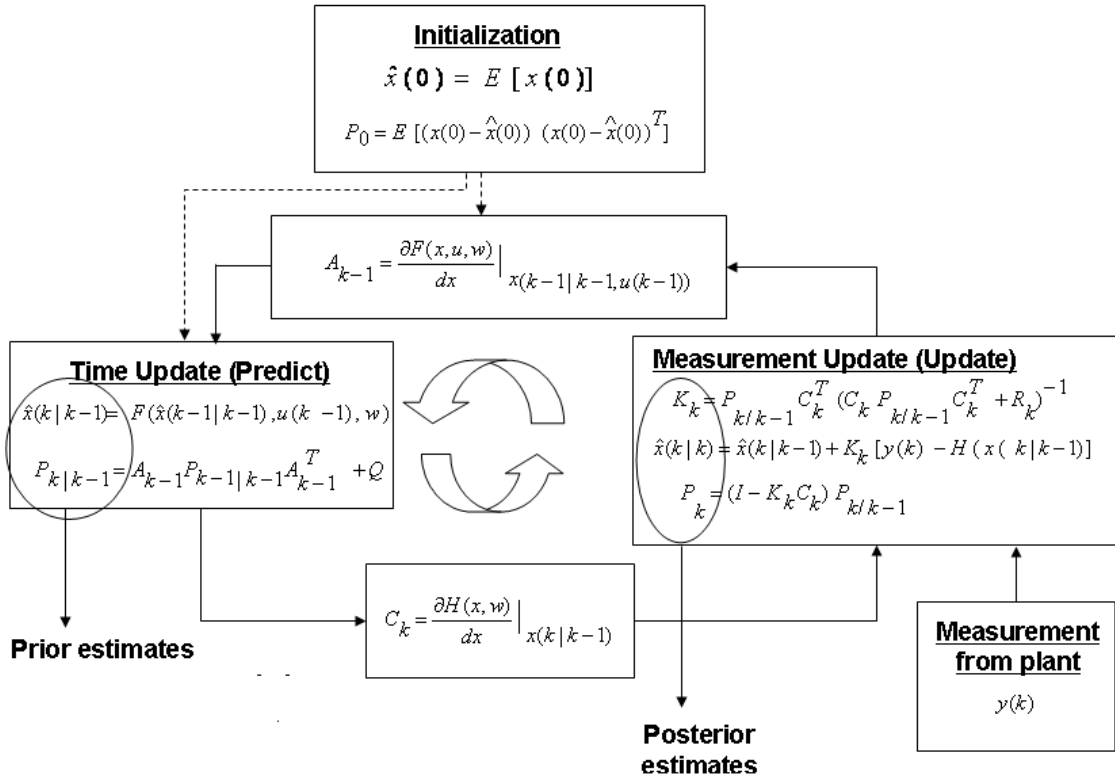


Figure 2.2: Schematic of the Extended Kalman Filter.

tion. Fig. 2.3 illustrates this principle. A variable with known Gaussian statistics (mean and variance) in the space of  $x$  undergoes a nonlinear transformation ( $F$ ) in the space of  $y$ . The EKF would simply linearize  $F$ , and pass the mean through the linearized set of equations to obtain the mean in the  $y$ -space. In contrast, in the unscented transform, points (sigma points) are deterministically chosen from the Gaussian distribution based on its mean and covariance. These points are passed through the nonlinear transformation to the  $y$ -space. The known distribution in  $x$  is now represented in the  $y$ -space by these transformed points. The approximate Gaussian statistics of the transformed distribution can now be obtained using these transformed points.

Julier and Uhlmann (1997) introduced the unscented transform for use in state estimation. The unscented transform is coupled with the Kalman update to give the UKF. A comprehensive review of the UKF algorithm is provided in Wan and van der Merwe (2000). Daum (2005) presents a short illustration on the importance of the UKF in nonlinear filtering. Kandepe et al. (2008) have compared the UKF performance to other estimator algorithms for several dynamic systems. A literature

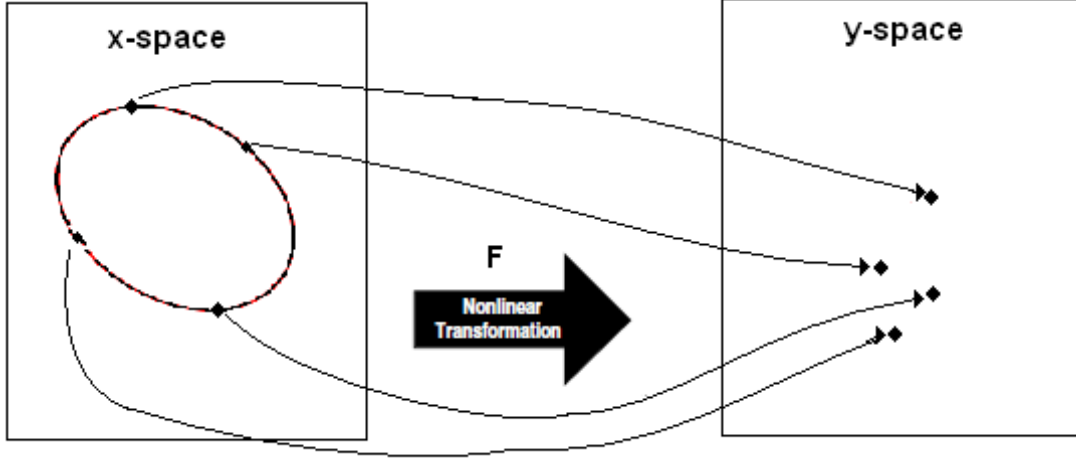


Figure 2.3: The principle of the unscented transform (adapted from Julier and Uhlmann (1997)). Sigma points are used to represent the variable under consideration in the  $x$ -space. These are then passed through the nonlinear transformation  $F$  to get transformed points in the  $y$ -space. The statistics calculated using transformed points, represent the statistics of the variable under consideration in the  $y$ -space

review on application and comparison of UKF to other estimation algorithms is presented in Chapter 3.

Fig. 2.4 represents the prediction - correction formulation of the UKF with its equations. Fig. 2.5 provides a schematic of the UKF. The UKF requires an initial guess of the state and covariance matrices, as represented by Eq. 2.20 and Eq. 2.21. In the following algorithm, the variable  $x$  represents the augmented states, i.e., system states and the disturbance, which is also modeled as a state.

$$\hat{x}_0 = E[x_0] \quad (2.20)$$

$$P_0 = E[(x_0 - \hat{x}_0)(x_0 - \hat{x}_0)^T] \quad (2.21)$$

### Calculation of sigma points:

Sigma points along with their corresponding weights provide a deterministic method of representing the state distribution.  $\mathcal{X}$  represents the sigma points, while  $W$  represents the weights. Eq's. 2.22 to 2.25 are used to calculate sigma points and the weights associated with them.

$$\mathcal{X}_{k-1} = [\hat{x}_{k-1} \quad \hat{x}_{k-1} \pm \sqrt{(L + \lambda)P_{k-1}}] \quad (2.22)$$

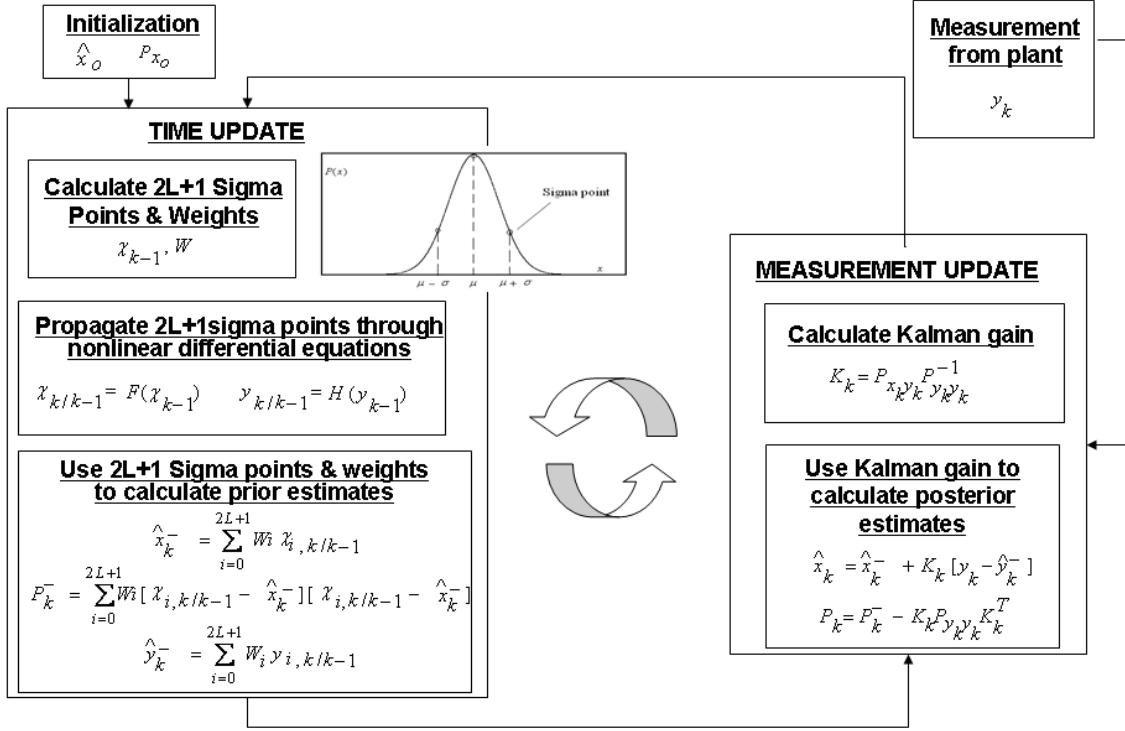


Figure 2.4: Prediction - correction formulation of the unscented Kalman filter with equations.

$$W_0^{(m)} = \lambda / (L + \lambda) \quad (2.23)$$

$$W_0^{(c)} = \lambda / (L + \lambda) + (1 - \alpha^2 + \beta) \quad (2.24)$$

$$W_i^{(m)} = W_i^{(c)} = 1 / (2(L + \lambda)) \quad i = 1, \dots, 2L \quad (2.25)$$

$L$  represents the number of states.  $\lambda = \alpha^2(L + \kappa) - L$  is a scaling parameter where  $\kappa$  (generally set to 0) and  $\beta$  (incorporates knowledge of prior distribution of  $x$ ) are secondary scaling parameters. The number of sigma points is  $2L + 1$ .

### Time update:

This step involves calculation of the prior estimates, obtained by propagating the sigma points through the non-linear system dynamics. Eq. 2.26 represents the non-linear transformation of the sigma points. The output vector represented by each sigma point is obtained using equation. 2.27. The weights associated with each transformed sigma point are known from equation. 2.23 to equation. 2.25. The

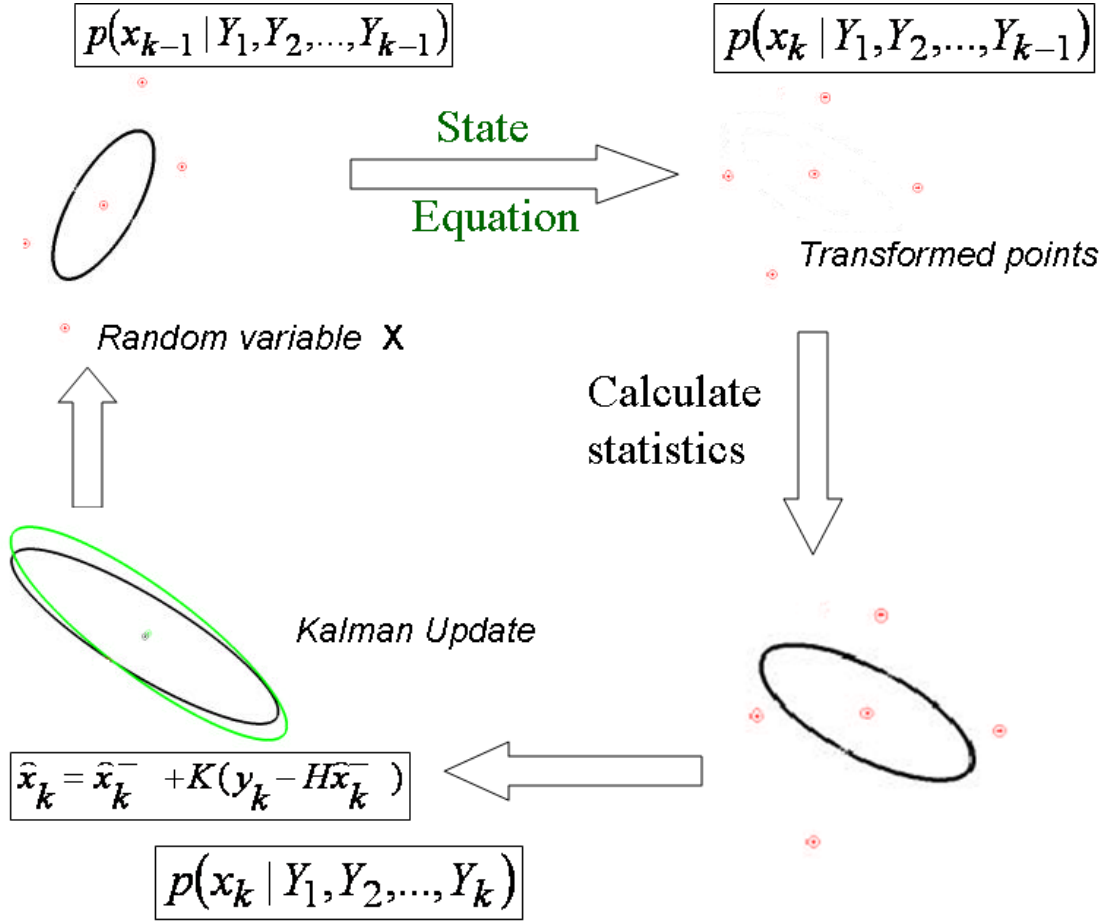


Figure 2.5: Schematic of the unscented Kalman filter.

weights and transformed sigma points are used to calculate the *a priori* estimates (equation. 2.28 and equation. 2.30) and *a priori* covariance matrix (equation. 2.29).

$$\mathcal{X}_{k/k-1} = F(\mathcal{X}_{k-1}) \quad (2.26)$$

$$\mathcal{Y}_{k/k-1} = G(\mathcal{X}_{k/k-1}) \quad (2.27)$$

$$\hat{x}_{k/k-1} = \sum_{i=0}^{2L} W_i^{(m)} \mathcal{X}_{i,k/k-1} \quad (2.28)$$

$$P_{k/k-1} = \sum_{i=0}^{2L} W_i^{(c)} [\mathcal{X}_{i,k/k-1} - \hat{x}_{k/k-1}] [\mathcal{X}_{i,k/k-1} - \hat{x}_{k/k-1}]^T \quad (2.29)$$

$$\hat{y}_{k/k-1} = \sum_{i=0}^{2L} W_i^{(m)} \mathcal{Y}_{i,k/k-1} \quad (2.30)$$

### Measurement update:

The measurement update in the UKF is similar to the Kalman update except that the cross-covariances are used instead of the auto-covariance. However, it has been shown that there is an increased efficiency of the measurement update step in the case of the UKF (Kandepu et al. (2008)). Posterior estimates of the state are calculated by using the Kalman gain to weight the measurement innovations with the state estimates.

$$\mathcal{K} = P_{x_k y_k} P_{y_k y_k}^{-1} \quad (2.31)$$

$$\hat{x}_{k/k} = \hat{x}_{k/k-1} + \mathcal{K}(y_k - \hat{y}_{k/k-1}) \quad (2.32)$$

$$P_k = P_{k/k-1} - \mathcal{K} P_{y_k y_k} \mathcal{K}^T \quad (2.33)$$

The UKF estimates are said to be accurate upto  $3^{rd}$  order statistics for Gaussian distributions and upto  $2^{nd}$  order statistics for non-Gaussian distributions (Julier and Uhlmann (1997)). The true mean and covariance estimates of the UKF are more accurate than those obtained through the EKF. In addition, it does not require computation of the Jacobian, thereby reducing the computational complexity of the problem. However, it must be noted that both the EKF and UKF make an assumption that the underlying distributions are all Gaussian and hence can be accurately represented by  $2^{nd}$  order statistics.

### **2.2.2 Monte Carlo technique based estimator**

Monte Carlo techniques use repeated random sampling, i.e., a trial of all or most possible cases to obtain aggregate statistics for processes. For example, if one were to find the probability of landing the number six in a single role of a die, one could do that by repeated throwing the die about 100 times, and computing the probability by dividing the number of times the die rolled the number 6 by 100. Monte Carlo techniques are repeated sequentially (Sequential Monte Carlo : SMC) to obtain solutions to the nonlinear estimation problem. SMC methods are more commonly known as particle filters, and are discussed in the following section.

## Particle filters

Particle filtering is a method of recursive Bayesian filtering by Monte Carlo simulations, or, in other words, a sequential Monte Carlo (SMC) technique. In a Bayesian approach to state estimation, the entire information of the state is represented in the form of a posterior probability density function (pdf) based on the measurements obtained at that time instant. The pdf is represented by using Monte Carlo techniques in which a set of random samples (particles) with associated weights are generated. The particles are similar to the sigma points of the UKF, except that the particles are not computed deterministically. As the number of particles increases, the exact posterior density is approached. The algorithm is based on calculating the entire posterior distribution of the state rather than finding a single point estimate at each sampling instant.

As pointed out in Ristic et al. (2004), SMC techniques were introduced as early as in the 1950s. However, these were not popular due to their requirement of high computational power. The early algorithms of the particle filter were based on sequential importance sampling (SIS). An increase in the use of particle filtering algorithms was seen with the introduction of the resampling technique by Gordon et al. (1993). Arulampalam et al. (2002) and Doucet et al. (2001) give a comprehensive review of the particle filtering techniques. Sequential importance sampling (SIS), sequential importance resampling (SIR), auxiliary sequential importance resampling (ASIR) and regularized particle filtering are some of the common SMC techniques. The SIR algorithm is the most commonly used technique today. However it has certain drawbacks which are illustrated in later chapters.

The basic SMC algorithm is described below (adapted from Ristic et al. (2004)). The posterior density of the state at time instant  $k$  is represented by  $p(x_k|Y_k)$  and the joint posterior density is represented by  $p(X_k|Y_k)$  (i.e. probability of  $X$  occurring, given  $Y$  occurred).  $p(X_k|Y_k)$  can be approximated by a set of particles  $X_k^i, i = 1, \dots, N$  and a set of weights  $w_k^i, i = 1, \dots, N$  :

$$p(X_k|Y_k) \approx \sum_{i=1}^N w_k^i \delta(X_k - X_k^i)$$

According to the principle of importance sampling, since the exact distribution  $p(X_k|Y_k)$  is unknown, we draw samples from an importance distribution  $q(X_k|Y_k)$ . The weights are now given by the expression  $w_k^i \propto p(X_k^i|Y_k)/q(X_k^i|Y_k)$ . The importance density is a known distribution, drawing samples from which is similar to drawing samples from the actual posterior distribution. Suppose the posterior den-

sity at time step  $k - 1$  has been computed. Once the measurement  $y_k$  is obtained, we compute the importance density:

$$q(X_k|Y_k) = q(x_k|X_{k-1}, Y_k)q(X_{k-1}|Y_{k-1})$$

The posterior density can be represented as :

$$\begin{aligned} p(X_k|Y_k) &= p(y_k|X_k, Y_{k-1})p(X_k|Y_{k-1})/p(y_k|Y_{k-1}) \\ &\propto p(y_k|x_k)p(x_k|x_{k-1})p(X_{k-1}|Y_{k-1}) \end{aligned}$$

The weight update equation can hence be derived as :

$$w_k^i \propto p(X_k^i|Y_k)|q(X_k^i|Y_k) = w_{k-1}^i p(y_k|x_k^i)p(x_k^i|x_{k-1}^i)|q(x_k^i|X_{k-1}^i, Y_k)$$

The posterior density can now be approximated as :

$$p(x_k|Y_k) \approx \sum_{i=1}^N w_k^i \delta(x_k - x_k^i)$$

The steps described above represent the sequential importance sampling algorithm and form the basis for derivation of most sequential Monte Carlo methods. It has been shown that as  $N \rightarrow \infty$ , the true posterior density is obtained. However, a large number of particles are required to avoid particles with zero weights. This depends on the variance of the posterior density and its computation. To eliminate degeneracy, the resampling step was introduced. Ever since its introduction by Gordon et al. (1993), the particle filter has become a popular tool in state estimation. It involves sampling of  $N$  particles from the posterior distribution such that all  $N$  particles have equal weights ( $1/N$ ). The posterior particles  $\{x_k^i\}$  and their corresponding weights  $\{w_k^i\}$  are used to construct the cumulative distribution function (cdf), followed by which,  $N$  particles of equal weights are drawn based on the constructed cdf. The  $N$  particles are represented as  $\{x_k^i, 1/N\}$ . The generic particle filter combines the SIS algorithm with a resampling step. The sequential importance resampling (SIR) algorithm is the most basic and widely used version of the particle filter, and it uses the prior distribution to be the importance distribution. Under these assumptions, the equations involved with the SIS algorithm simplify to:

$$q(x_k|X_{k-1}^i, Y_k) = p(x_k, x_{k-1}^i)$$

$$w_k^i \propto w_{k-1}^{i-1} p(y_k|x_k^i)$$

The SIR PF algorithm is described in fig. 2.6 and fig. 2.7. Initial particles are

passed through the system dynamics. The obtained transition particles are the importance particles. The likelihood function uses the incoming measurement information to calculate the importance weights. The importance weights and particles are combined to produce the posterior distribution. Resampling from this distribution is done such that the new set of particles are all of equal weights and they are concentrated in regions of high probability. These particles form the prior particles for the subsequent time instant run of the particle filter. The algorithm is repeated itself at each time instant.

The disadvantages of the SIR PF are loss of diversity of particles due to resampling at every step and sensitivity to outliers, as no measurement is incorporated in the likelihood function. Other versions of the PF have been developed to obtain optimal solutions to the nonlinear state estimation problem. An application of the auxiliary SIR-PF with its basic algorithm is available in Chen et al. (2005). Particle filters with EKF, EnKF or UKF to compute the proposal distribution are described in der Merwe et al. (2000) and Prakash et al. (2008). Extensive literature is present and maybe accessed through online journals for more information on particle filters.

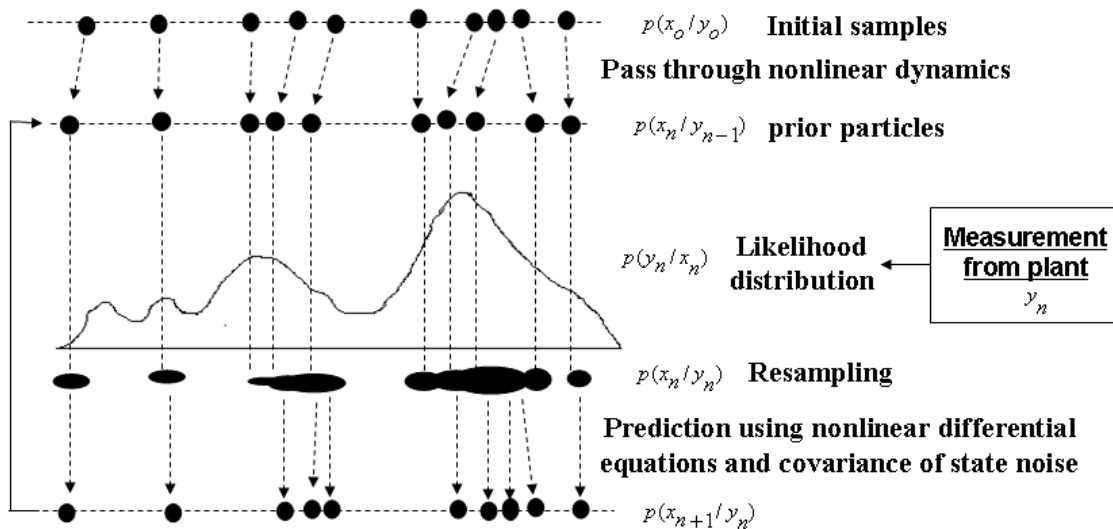


Figure 2.6: Schematic of the particle filter (adapted from der Merwe et al. (2000)).

### 2.2.3 Combination of Monte Carlo and Kalman update based estimator

In this section, an estimator which represents a hybrid between the Kalman update and the Monte Carlo technique is described. In such techniques, N Kalman

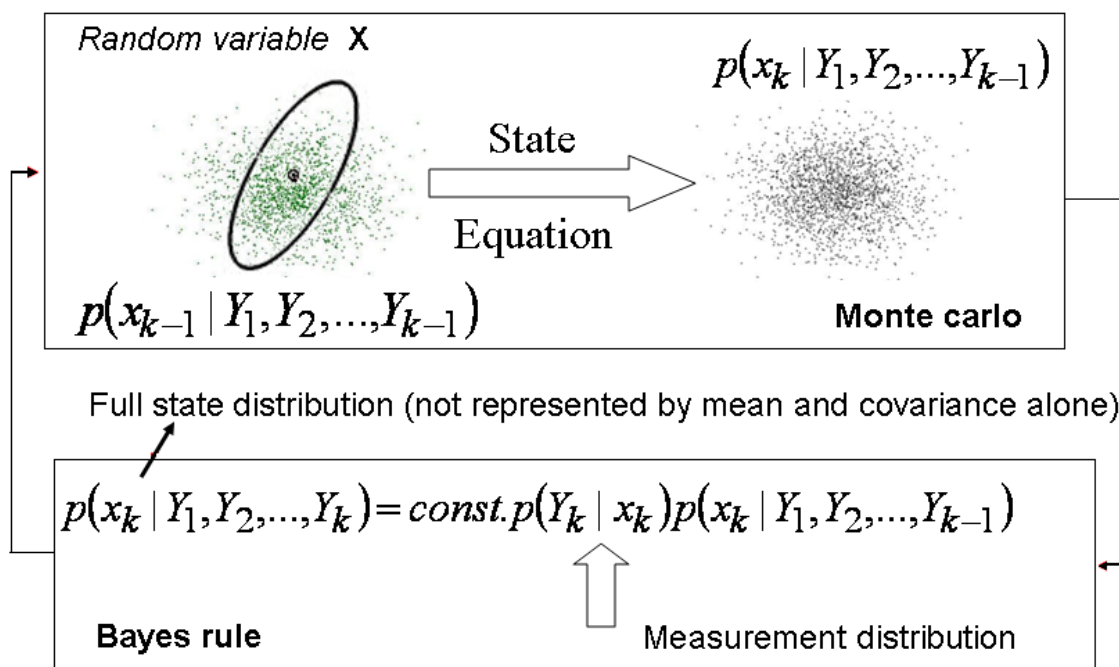


Figure 2.7: Combining Monte Carlo technique with Bayes rule to derive the Sequential Monte Carlo technique (PF)

updated based filters are run in parallel to approximate the population statistics of the Gaussian random variable under consideration. In other words, at each time instant, a Kalman update based filter is run in a Monte Carlo fashion (N times). One of the most commonly used methods to do this is the ensemble Kalman filter and is illustrated below.

### Ensemble Kalman filter

The ensemble Kalman filter (EnKF) is an algorithm that combines two powerful techniques - Monte Carlo and Kalman update. The EnKF was first introduced by Evensen (1994b) for application to ocean models which are large scale nonlinear systems. The EnKF has been used for other large scale systems such as weather predictions and reservoir simulations (Evensen (1994a)). Monte Carlo samples called ensembles are used to represent the statistics of a variable. The sample mean of these ensembles gives the state estimate, and the sample covariance gives the covariance matrix. Each ensemble point is used to predict individually its prior estimate and measurement estimate using the extended Kalman filter algorithm. The N prior and measurement estimates are then used to calculate auto-covariance and cross-

covariance matrices. A comprehensive review of the EnKF algorithm may be found in Gillijns et al. (2006) and Baker (2007). The EnKF algorithm is described below:

$$\hat{X}(k-1|k-1) \equiv (x^1(k-1|k-1), x^2(k-1|k-1), \dots, x^N(k-1|k-1)) \quad (2.34)$$

where  $x^i(k-1|k-1)$  represents a Monte Carlo sample (an ensemble) obtained from the state and covariance estimate at time step  $k-1$ .  $N$  is the number of ensembles. Each member of the ensemble is propagated forward in time.

$$\hat{x}^i(k|k-1) = F(\hat{x}^i(k-1|k-1), u(k-1)) + w^i(k) \quad (2.35)$$

Eq. 2.35 is applied to each member of the ensemble, i.e., from  $i = 1, \dots, N$ , where  $w(k)^i$  is a random sample from  $N(0, Q)$ .

The state prediction error covariance matrix  $\hat{P}(k+1|k)$  is approximated as the sample covariance of  $\hat{X}(k|k-1)$  around the sample mean  $\mu^x(k|k-1)$

$$\mu^x(k|k-1) = \frac{1}{N} \sum_{i=1}^N x^i(k|k-1) \quad (2.36)$$

$$P^{xx}(k|k-1) = \frac{1}{N-1} \sum_{i=1}^N ((x^i(k|k-1) - \mu^x(k|k-1))((x^i(k|k-1) - \mu^x(k|k-1)))^T \quad (2.37)$$

### Prediction step

Measurement predictions are performed using the measurement model of the system under consideration.

$$y^i(k|k-1) = H(x^i(k|k-1)) + v_k^i \quad (2.38)$$

$v_k^i$  is a Monte Carlo sample from  $N(0, R)$ . An ensemble of predicted measurements is now obtained

$$\hat{Y}(k|k-1) = (y^1(k|k-1), \dots, y^N(k|k-1)).$$

The output error covariance can be calculated as the sample covariance of  $y^i(k|k-1)$  using the sample mean  $\mu^y(k|k-1)$

$$\mu^y(k|k-1) = \frac{1}{N} \sum_{i=1}^N y^i(k|k-1) \quad (2.39)$$

$$P^{yy}(k|k-1) = \frac{1}{N-1} \sum_{i=1}^N ((y^i(k|k-1) - \mu^y(k|k-1))((y^i(k|k-1) - \mu^y(k|k-1)))^T \quad (2.40)$$

Similarly, a cross-covariance between the prediction error and output error can be calculated

$$P^{xy}(k|k-1) = \frac{1}{N-1} \sum_{i=1}^N ((x^i(k|k-1) - \mu^x(k|k-1))((x^i(k|k-1) - \mu^y(k|k-1)))^T \quad (2.41)$$

### Update step

The Kalman gain is obtained from combination of the auto and cross-covariance matrices.

$$K_k = P^{xx}(k|k-1)(P^{xy}(k|k-1))^{-1} \quad (2.42)$$

The updated ensemble is given by  $\hat{X}(k|k) = (x^1(k|k), \dots, x^N(k|k))$  where

$$x^i(k|k) = x^i(k|k-1) + K_k(y(k) - y^i(k|k-1)) \quad (2.43)$$

This estimate is used to reinitialize the algorithm for the next step. The optimal estimate is chosen to be the mean of the updated ensemble

$$\hat{x}^*(k|k) = \frac{1}{N} \sum_{i=1}^N x^i(k|k) \quad (2.44)$$

The covariance for the updated state ensemble can be computed as below

$$P^*(k|k) = \frac{1}{N-1} \sum_{i=1}^N (x^i(k|k) - \hat{x}^*(k|k))(x^i(k|k) - \hat{x}^*(k|k))^T \quad (2.45)$$

The EnKF avoids the problem of calculation of the Jacobian. It also has advantages over the UKF, as it does not involve a deterministic sampling and re-calculation of initial points to be propagated at the next time step. It has been used for large scale systems and under the Gaussian assumption, it is a very powerful estimation algorithm in terms of quality of estimates and computational cost. Although it is unable to handle highly non-Gaussian behavior unlike the particle filter, it is generally more robust than the PF and has been used to generate the proposal distribution for particle filter applications.

## 2.3 Constrained filtering

Model computations often end up moving towards regions where the solutions are physically not realizable (example: the height in the two tank system becomes negative). This may be due to noise, incorrect assumptions of Gaussian behavior, etc.

In these cases, it is important to consider the estimation problem under a constrained framework. One of the most commonly used methods is applying clipping constraints to unconstrained estimation algorithms (such as setting the height to zero when it goes negative). However, the need for sophisticated ways to introduce constraints has led to the development of rigorous methods of constrained state estimation. The commonly used methods are illustrated in Fig. 2.1. A good review of moving horizon estimation (MHE) can be found in Rawlings and Bakshi (2006) and Haseltine and Rawlings (2005). Recursive data reconciliation (RNDDR) methods have been illustrated by P. Vachhani and Rengaswamy (2006). Constrained versions of unconstrained algorithms can be found in literature by Kolas et al. (2009), Shao et al. (2010), Prakash et al. (2008) and Prakash et al. (2010). It must be noted that constrained state estimation is beyond the scope of this thesis.

# Chapter 3

## Comparison of unconstrained state estimation techniques

### 3.1 Introduction

In the previous chapter, linear and nonlinear estimation algorithms were discussed. In this chapter, various unconstrained estimation methods are compared. Section 3.2 contains an extensive literature survey comparing these techniques. Section 3.3 contains details of the polymethyl methacrylate (PMMA) polymerization reactor that has been used as a case study example for comparison of various estimation algorithms. The behavior of estimation algorithms under different noise sequences that may occur in the PMMA reactor is studied in section 3.4. This section has been presented and appears in the proceedings of the IFAC DYCOPS 2010 conference held in Leuven, Belgium. In section 3.5, the two Kalman update based filters (EKF and UKF) are studied under different cases of noise covariance ratios (process to measurement noise covariances). Heuristic tuning of these filters is also established in this section. Section 3.6 highlights the advantages and disadvantages of the EnKF over other Kalman update based filters. The importance of particle filters for estimation of non-Gaussian posteriors is illustrated in section 3.7. Section 3.4 to 3.7 contains results for comparison of unconstrained state estimation techniques. In section 3.8, the importance of integral action in estimation algorithms is highlighted using the example of a two tank system. The algorithm used incorporates integral action in a manner that is similar to that used in a proportional-integral type controller. Section 3.9 highlights the importance of efficient point estimate extraction from full state distributions. A novel method for extracting point estimates using k-means clustering has been illustrated.

## 3.2 Literature review on comparison of state estimation techniques

In the past, a lot of attention was paid towards the comparison of different estimation algorithms on various systems under different scenarios of noise statistics and process dynamics. Most comparative studies involve simple examples (small state systems - 2 to 3 states) with little or no model-plant mismatch.

The EKF has been the most widely used estimator in process engineering. Only recently has there been literature on application of alternate methods on chemical process systems. The EKF has been preferred owing to its ease of implementation, and the unavailability of alternate methods to address its drawbacks until recent years. Extensive literature may be found on the implementation of EKF on process systems. In one of the first works on estimation in polymerization reactors, Jo and Bankoff (1976) used an extended Kalman filter to estimate the conversion and weight average molecular weight of a vinyl acetate polymerization continuous stirred tank reactor (CSTR) system with free-radical polymerization mechanism. Results obtained using the EKF were compared to values obtained from an experimental setup. Kozub and MacGregor (1992) used an EKF to estimate states in a semi-batch emulsion copolymerization of styrene/butadiene rubber (SBR) system. McAuley and MacGregor (1991) soft sensed the melt index and polymer density values of a polyethylene reactor by using an EKF. Srinivas et al. (1994) used an EKF to estimate the states from multi-rate sampled measurements with variable dead times on an industrial gas-phase co-polymerization reactor model. Prasad et al. (2002) used a multi-rate EKF for state and parameter estimation of a styrene polymerization reactor to monitor polymer quality variables. Gudi et al. (1994) used a multi-rate EKF to monitor biomass profiles and critical fermentation parameters in an antibiotic fermentation reactor.

Wilson et al. (1998) provide a critical review on the industrial implementation of EKF. In their work, they have documented the application of EKF to different process engineering systems such as polymerization reactors, pulp & paper processes, and biotechnology and nuclear industries. These systems have been compared with respect to different criteria such as the type of dynamic and measurement models, sensitivity of estimation results, and the comparison of open loop predictions to estimator results. They also assessed the feasibility of using an estimator for an industrial scale reactor using an industrial pilot semibatch reactor. Results based on an online run of the two step exothermic reaction lead Wilson et al. (1998) to believe

that the EKF is not robust enough to be implemented online, and that modifications are required to avoid filter divergence. The paper concludes with critical evaluations of the EKF for industrial scale estimation and future recommendations for industrial applications.

In one of the the earliest works on comparison of state estimation techniques, Romanenko and Castro (2004) compared the performance of the EKF and UKF in a nonlinear environment with perfect plant-model match. A fair comparison of ideally tuned filters was conducted under three different case studies of measurement to process noise covariance ratio ( $Q/R$ ) scenarios. Under high noise ratios (low measurement noise), similar filter performances of the estimators were established. As the noise ratios were decreased, the EKF performance degraded and it finally diverged completely, in contrast to the performance of the UKF. The reason for the poor performance of the EKF was attributed to the linearization error that propagated through the covariance matrix calculations; this was supposed to be efficiently handled in the UKF. A critical evaluation of similar case studies has been conducted in section 3.5 of this thesis. It has been established in section 3.5, that the cause of divergence of the EKF in the Romanenko and Castro (2004) study should be attributed to the approximation error rather than the linearization error.

In a recent study, Kandepu et al. (2008) established that the UKF performed better than the EKF in terms of robustness and speed of convergence. The conclusions were established using four different simulation studies. Using the example of a van der Pol oscillator, the EKF is shown to diverge under conditions of plant-model mismatch, unlike the UKF. However, we believe that further tuning of the EKF might produce better results than those exhibited in their paper. Under no plant-model mismatch, the UKF has a slight advantage over the EKF. Kandepu et al. (2008) demonstrate the advantage of using the unscented transform as a nonlinear approximation by showing faster convergence of the UKF against the EKF using the example of an induction machine with poor initial state estimates. In a separate case study using an SOFC hybrid system, the faster convergence of the UKF with respect to the EKF has been established under poor initial state estimates. The system contains 3 known inputs and 14 measurements to estimate 18 states.

In the work by Kolas et al. (2009), different versions of the UKF algorithm have been documented and compared with the EKF. First, the algorithm for a generic UKF with symmetric sigma points is documented. Later, the UKF with augmented state noise and the fully augmented UKF algorithms are illustrated. In addition,

the generic UKF is reformulated to improve its numerical behavior and constraint handling; i.e., instead of the generic Kalman measurement update, sigma points are used to calculate the posterior statistics (rather than using prior statistics obtained from the sigma points). The authors use case studies to establish that the EKF fails to converge under constraints while the UKF converges for the same case. However, in the unconstrained case, both filters fail to converge. The literature provides a good review of the different versions of the generic UKF. However, the comparison of the performance of the EKF and the UKF is established based on convergence under constraints, and the authors do not address linearization errors.

Using a CSTR and batch reactors as examples, Qu and Hahn (2009) have shown that the UKF performs similar to the EKF when process nonlinearities are not significant. In the case of severe nonlinearity and high noise levels, the UKF outperforms the EKF.

The above documented literature by Kolas et al. (2009), Romanenko and Castro (2004), Kandepu et al. (2008), Qu and Hahn (2009) compare the performance of the EKF and the UKF. Performance comparisons of the UKF and the PF are very rare. Shao et al. (2010) have compared the performance of the PF against the EKF, UKF and moving horizon estimation (MHE) under constraints. Using three different examples : a two state batch reaction, a three state batch reaction and a three state CSTR, it has been established that the PF provides flexibility for constrained nonlinear Bayesian state estimation in comparison to other estimators. Novel methods of handling constraints have been established. A hybrid method that combines acceptance/rejection of particles, and clipping of particles that fall outside the region obtained using optimization strategies is proposed.

In two separate contributions, Haseltine and Rawlings (2005) and Rawlings and Bakshi (2006) have compared the EKF to the constrained MHE and later, the MHE with the PF. In Haseltine and Rawlings (2005), examples have been used to show that the EKF may fail even in cases where there is no plant-model mismatch. The poor performance of the EKF with respect to the MHE in the demonstrated examples are due to poor constraint handling methods in the EKF in comparison to the MHE. Rawlings and Bakshi (2006) have introduced the particle filter as a new tool in the field of nonlinear state estimation. The authors state that the MHE is a well-established tool for constrained systems. But in case of multimodal distributions, the PF may have an advantage over the MHE and hence a hybrid version of PF and MHE is proposed by the authors in these cases.

Chen et al. (2004) have compared the performance of the EKF, MHE and sequential Monte Carlo methods (PF) for three different examples. In the first case study, the estimators are compared for a linear system under Gaussian noise statistics. The EKF is shown to perform the best, as it reduces to the KF for the linear case. The MHE performance is very similar to that of the PF while they differ in computational time. In the second case study, a non-stationary time series model which forms a nonlinear one state dynamic model is used to compare estimator performance. The posterior distributions have been shown to be non-Gaussian (skewed or bimodal). It is clear that under these circumstances, the filters that assume Gaussian statistics for random variables will underperform (EKF and MHE). The PF is shown to give much lower mean squared error value in comparison to the EKF and MHE. However, in terms of computation time, the EKF takes far lesser time than the SMC which in turn takes lesser time than the MHE. This establishes that in cases where non-Gaussian distributions may be closely represented by Gaussian distributions, the EKF can be used as an adequate choice of estimator. In the third case study, a two state CSTR is used as the example. This model exhibits multimodality of posterior distributions at certain steady states. It has been shown that in this case, the PF performance is similar to the EKF and the MHE. This however is a contradiction to the expected behavior of Monte Carlo based techniques as they should be able to handle the multi-modality. We believe that the reason for similar performance is due to the fact that the extent of multi-modality is low and it can be represented adequately by Gaussian unimodal distributions. In a second case study of the same example under a different steady state with more or less unimodal distributions, it has again been shown that the filters perform similarly with respect to mean squared error values.

In one of the first papers to apply the particle filter to a process system, Chen et al. (2005) have compared the performance of an auxiliary particle filter (ASIR-PF) with an EKF for a batch polymerization reactor. A polymethyl methacrylate process similar to the one used here was used for this case study. The temperatures of the reactor are measured while the concentrations are estimated. It has been shown that the root mean square error values (RMSE) are lower for the ASIR filter in comparison to the EKF. CPU times are, however, much lower for the EKF than for the ASIR filter. In a separate case study, the termination rate constant of the monomer was considered to be a time varying parameter and parameter estimation results were compared. The RMSE values for polymer properties were much lower

in the case of the ASIR establishing that the estimated parameter values of the ASIR filter were more accurate. In conclusion, the ASIR filter was determined to be the estimator choice for highly non-linear batch processes.

In recent years, there has been an increase in the literature related to comparison of different estimation techniques particularly in context of process engineering. The well cited recent literature is restricted to the above cited papers. The above-cited literature indicates that there are few, if any, instances where multiple unconstrained estimators are compared with the EKF, especially for chemical process systems. Most of the literature indicates the comparison of a single unconstrained (UKF, PF) or constrained (MHE) estimator with the EKF. In this chapter, we describe the application of all unconstrained estimators on the same example, a PMMA CSTR. The comparison of the UKF and the EnKF with each other and the PF including heuristic tuning of these filters is also established.

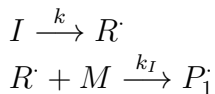
### 3.3 Methyl methacrylate (MMA) polymerization CSTR

This chapter involves the study of estimation techniques on a methyl methacrylate polymerization reactor. This is a 6 state plant model, and the model used by the estimator has the same structure as the plant model, that is no structural model-plant mismatch is assumed.

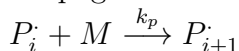
#### 3.3.1 Process description

A free-radical MMA polymerization process is used in this study. Polymerization takes place in a CSTR with azo-bis-isobutyronitrile (AIBN) as an initiator and toluene as a solvent. Fig. 3.1 provides a schematic of the reactor. The reactions are exothermic, and a cooling jacket is used to remove heat. The details of the model can be obtained from Silva et al [13]. The reaction mechanism for MMA free-radical polymerization is as follows:

Initiation:



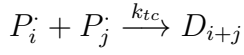
Propagation:



Monomer transfer:



Addition termination:



Disproportionation termination:

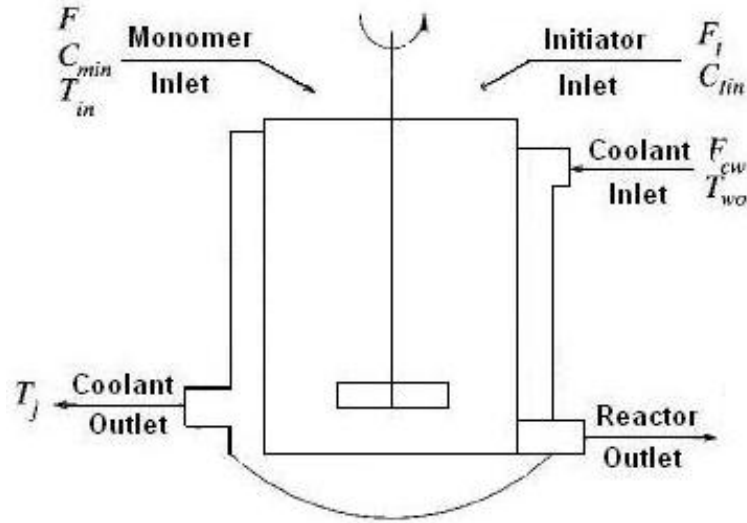


Figure 3.1: MMA polymerization reactor schematic

### 3.3.2 Modeling the PMMA reactor

A mathematical model of the process is developed based on the following assumptions: (a) constant volume of the reactor, (b) reactor contents are perfectly mixed, (c) no gel effect, (d) uniform cooling fluid temperature, (e) heat capacity and density of cooling fluid and reactor mixture remain constant. The mass and energy balance equations are as follows:

$$\frac{dC_m}{dt} = -(k_p + k_{fm})C_m P_0 + \frac{F(C_{min} - C_m)}{V} \quad (3.1)$$

$$\frac{dC_I}{dt} = -k_I C_I + \frac{(F_I C_{Iin} - F C_I)}{V} \quad (3.2)$$

Table 3.1: Operating parameters for the simulated PMMA CSTR

|                             |   |
|-----------------------------|---|
| $F = 1.0m^3/h$              | $Mm = 100.12 \text{ kg/kgmol}$                                |
| $F_I = 0.0032m^3/h$         | $f^* = 0.58$  |
| $F_{cw} = 0.1588m^3/h$      | $R = 8.314 \text{ kJ/(kgmol.K)}$                              |
| $C_{min} = 6.4678kgmol/m^3$ | $-\Delta H = 57800 \text{ kJ/kgmol}$                          |
| $C_{Iin} = 8.0kgmol/m^3$    | $E_p = 1.8283 \times 10^4 \text{ kJ/kgmol}$                   |
| $T_{in} = 350K$             | $E_I = 1.2877 \times 10^5 \text{ kJ/kgmol}$                   |
| $T_{w0} = 293.2K$           | $E_{fm} = 7.4478 \times 10^4 \text{ kJ/kgmol}$                |
| $U = 720kJ/(h.K.m^2)$       | $E_{tc} = 2.9442 \times 10^3 \text{ kJ/kgmol}$                |
| $U = 2.0m^2$                | $E_{td} = 2.9442 \times 10^3 \text{ kJ/kgmol}$                |
| $V = 0.1m^3$                | $A_p = 1.77 \times 10^9 \text{ m}^3/(\text{kgmol.h})$         |
| $V_0 = 0.02m^3$             | $A_I = 3.792 \times 10^{18} \text{ l/h}$                      |
| $\rho = 866kg/m^3$          | $A_{fm} = 1.0067 \times 10^{15} \text{ m}^3/(\text{kgmol.h})$ |
| $\rho_w = 1000kg/m^3$       | $A_{tc} = 3.8223 \times 10^{10} \text{ m}^3/(\text{kgmol.h})$ |
| $C_p = 2.0kJ/(kg.K)$        | $A_{td} = 3.1457 \times 10^{11} \text{ m}^3/(\text{kgmol.h})$ |
| $C_{pw} = 4.2kJ/(kg.K)$     | $A_{td} = 3.1457 \times 10^{11} \text{ m}^3/(\text{kgmol.h})$ |

$$\frac{dT}{dt} = \frac{(-\Delta H)k_p C_m P_0}{\rho C_p} - \frac{UA}{\rho C_p V}(T - T_j) + \frac{F(T_{in} - T)}{V} \quad (3.3)$$

$$\frac{dD_0}{dt} = (0.5k_{tc} + k_{td})P_0^2 + k_{fm}C_m P_0 - \frac{FD_0}{V} \quad (3.4)$$

$$\frac{dD_1}{dt} = Mm(k_p + k_{fm})C_m P_0 - \frac{FD_1}{V} \quad (3.5)$$

$$\frac{dT_j}{dt} = \frac{F_{cw}(T_{w0} - T_j)}{V_0} + \frac{UA}{\rho_w C_{pw} V_0}(T - T_j) \quad (3.6)$$

$$P_0 = \sqrt{\frac{2f^* C_I k_I}{k_{td} + k_{tc}}} \quad (3.7)$$

The temperatures are measured using standard thermocouples. Table 3.1 lists the design and operating parameters.  $f^*$  is the initiator efficiency.

### 3.3.3 Estimation framework

The temperatures ( $T_j, T$ ) are the measured states, while the reactor concentrations ( $C_m, C_I$ ) are considered as the hidden states (to be estimated). Polymer moments ( $D_0, D_1$ ) are not included in the estimator model as they are not observable states. Parameter estimation can be considered for any of the kinetic parameters ( $k_i, k_p, k_{fm}, k_{tc}, k_{td}$ ).

### 3.3.4 Observability

Linear observability analysis reveals that only 4 of the states are observable when the temperatures are the measured variables. The temperatures and the concentrations are the observable variables, and the moments are not observable. Observability has been checked based on the rank of the observability matrix obtained from the linearized system equations (the Jacobian).

## 3.4 Filter performance under different noise statistics

The model is tested for various scenarios of Gaussian and non-Gaussian state and measurement noise sequences. Using these case studies, we establish cases in which significant difference in the performance of various filters is exhibited. Measurement noise is considered on the reactor and coolant temperatures. State noise is added to the system dynamic equations of the monomer and initiator concentrations. The estimates of polymer moments are not used to compare filter performance as they are unobservable states.

### 3.4.1 Case studies

#### Case 1

This case assumes Gaussian noise on the measurements (temperatures). Fig. 3.2 indicates that the EKF works extremely well when the estimator is used to filter the measurement noise. It also tracks the concentrations (hidden states). It is important to note that there is an exact match of plant and model in this case. In this case, the Kalman gain goes to zero, and the estimator trusts the model estimates completely. This shows the importance of good process models in estimation.

#### Case 2

In this case, in addition to Gaussian measurement noise on the temperatures, Gaussian state noise is introduced in the dynamic estimation for the concentrations. Fig. 3.3 demonstrates the superiority of the performance of the PF and UKF over the EKF. The Kalman gain is adjusted using the noise covariance matrices and it is a finite non-zero value, thus weighting the measurement innovations and the

estimates. The soft-sensing ability of the EKF is limited as it diverges completely in concentration estimation.

### Case 3

In this case, non-Gaussian measurement and non-Gaussian state noise is introduced into the system. Fig. 3.4 indicates that the results are similar to that of Case 2. Note that the step tests performed in case 2 and 3 are different. In case 2, the input disturbance was a 10% change in cold water flow rate, while in case 3, it is a 10% change in monomer inlet flow rate. The EKF again diverges, while the PF and UKF estimates match the true state closely.

### Case 4

In this case, non-Gaussian measurement noise is introduced, but there is no state noise. It is seen that the EKF works extremely well in tracking the true measurement (Fig. 3.5). This reiterates what was concluded in case 1, that for reasonable measurement noise and exact plant-model match, the EKF gives good estimates.

## 3.4.2 Analysis of case studies

Table 3.2 summarizes the case studies described above. When there is no plant-model mismatch, the model captures the system dynamics including the state noise sequences. For perfect plant-model match, the EKF is capable of providing good estimates if the state noise to measurement noise covariance ratio is adjusted such that Kalman gain goes to zero. When the Kalman gain approaches zero, it indicates that there is complete trust in the model and full disregard of the correction due to the measured states (Cases 1 & 4) and no measurement correction takes place. It is important to note that if plant-model mismatch exists, the effect will be seen in poor estimation in the unmeasured states. The ratio of state noise to measurement noise is a tuning parameter that decides the value of the Kalman gain. The study of effect of the noise ratios is described in the subsequent section.

The UKF and PF seem to be similar in performance behavior; however, for extreme non-Gaussian behavior, a difference in estimator performance can be seen. The level of estimator performance varies based on the degree of non-linearity of the system dynamics, state and measurement noise, and the degree of plant-model mismatch. Three important conclusions can be drawn from the above case studies : (1) The EKF is unable to capture the true dynamics of the unmeasured states under

high nonlinearity. It can be seen in fig 3.3 that the EKF estimates seem to be biased. This is because the linearization approximation of the EKF does not capture highly nonlinear process dynamics accurately. This is called the linearization error.

(2) The performances of UKF and PF are very similar in all these cases. This indicates that the PF will show a superior performance over the UKF when the posterior density is non-Gaussian, and not necessarily when the noise distributions are non-Gaussian. Gaussian noise sequences may also cause the posterior to be non-Gaussian in some cases. This depends on the degree of nonlinearity of system dynamics.

(3) Though not explained in the case studies, the tuning of Kalman update based filters is different from tuning of Monte Carlo based particle filters.

Table 3.2: Summary of case studies ( $G = Gaussian$  ;  $NG = Non-Gaussian$ )

| Case | Measurement Noise | State Noise | Plant-Model Mismatch | Conclusion (choice of filter) |
|------|-------------------|-------------|----------------------|-------------------------------|
| 1    | G                 | None        | None                 | EKF, UKF, PF                  |
| 2    | G                 | G           | None                 | UKF,PF                        |
| 3    | NG                | NG          | None                 | UKF,PF                        |
| 4    | NG                | None        | None                 | EKF UKF, PF                   |

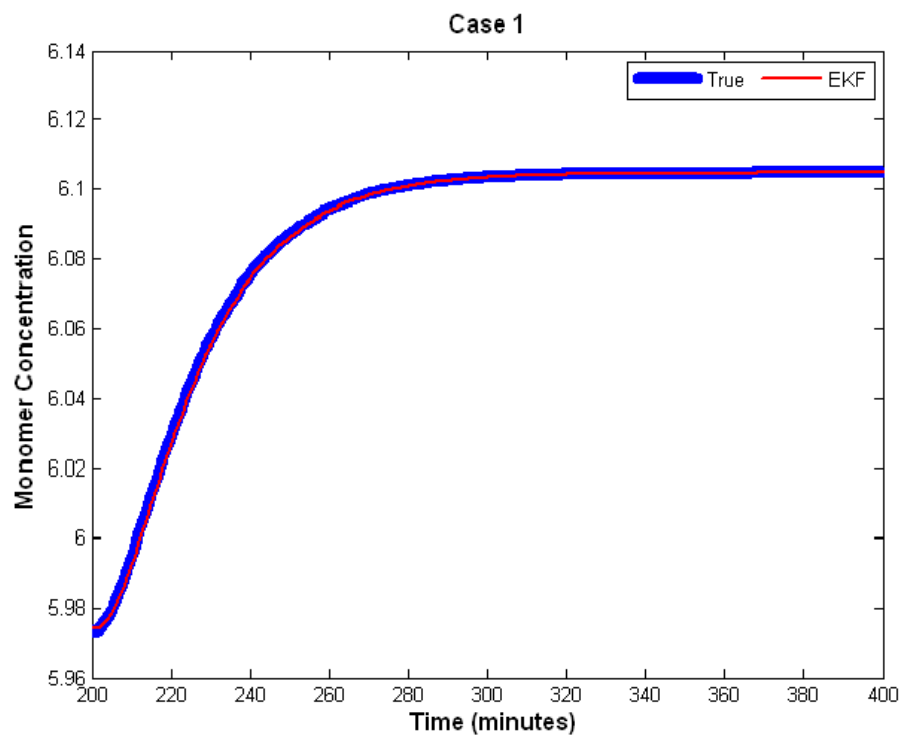
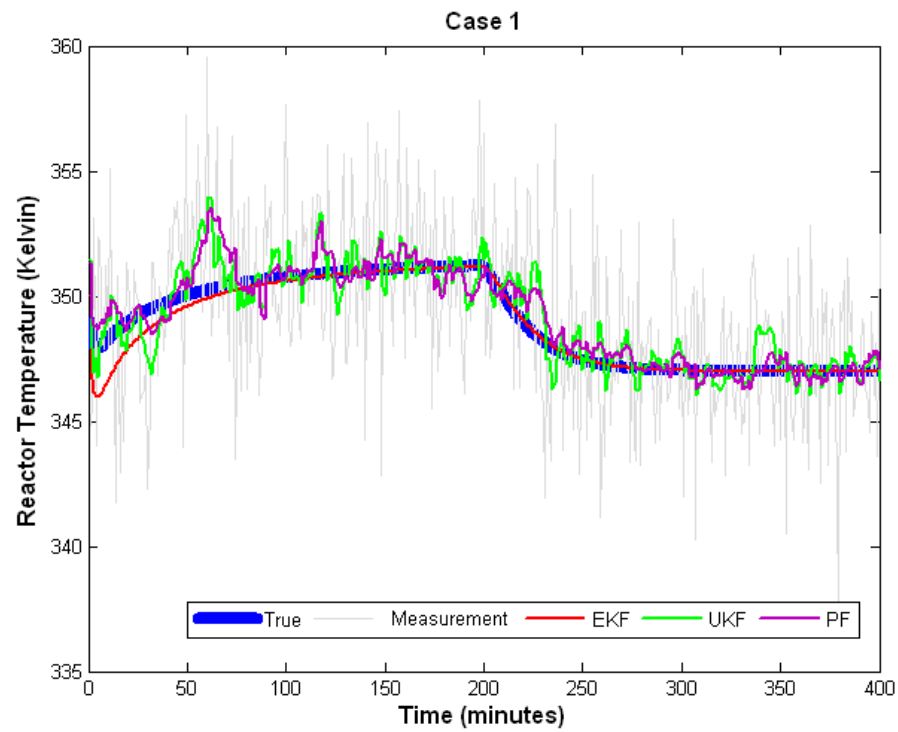


Figure 3.2: State estimation in the presence of zero process noise, Gaussian measurement noise (standard deviation (std) of 0.01), and a 10% positive step in cold water flow rate.

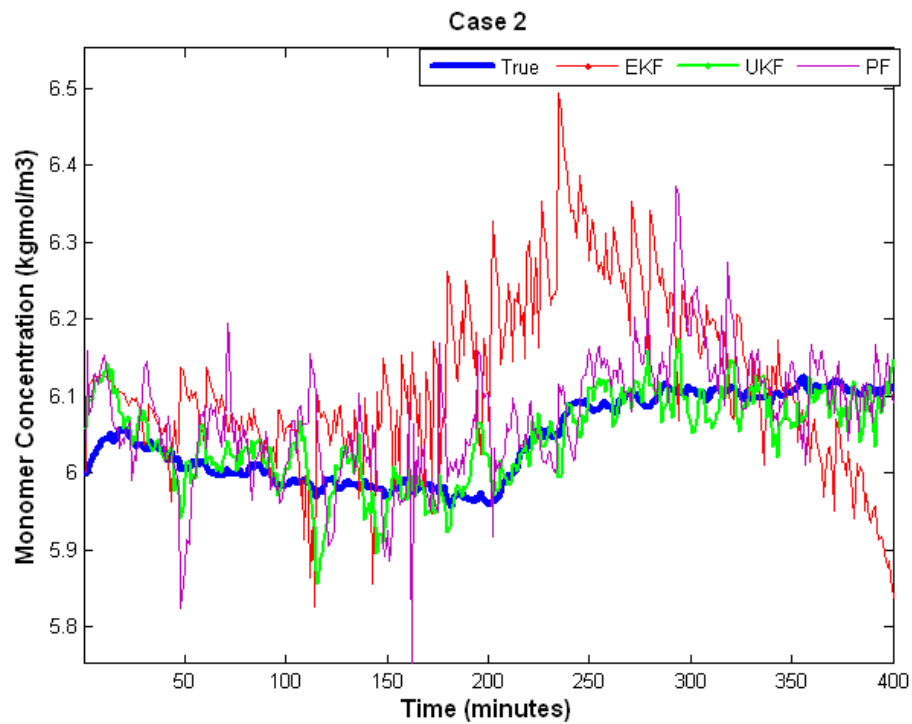
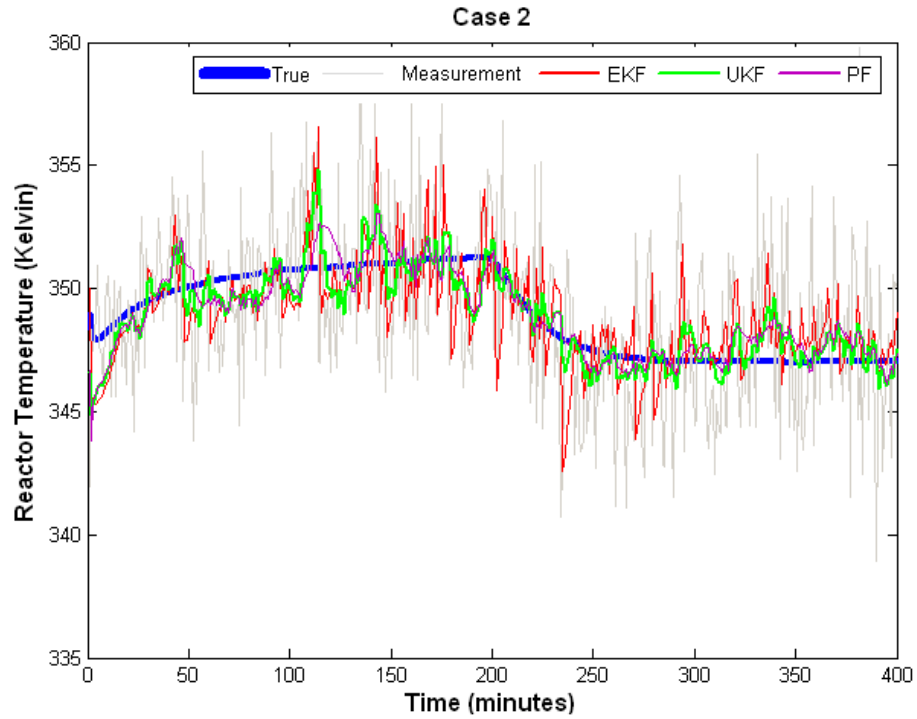


Figure 3.3: State estimation in the presence of Gaussian state noise (std of 1 and 0.01 on the monomer and initiator concentrations respectively), Gaussian measurement noise (std of 0.01 on the temperatures), and a 10% positive step in cold water flow rate.

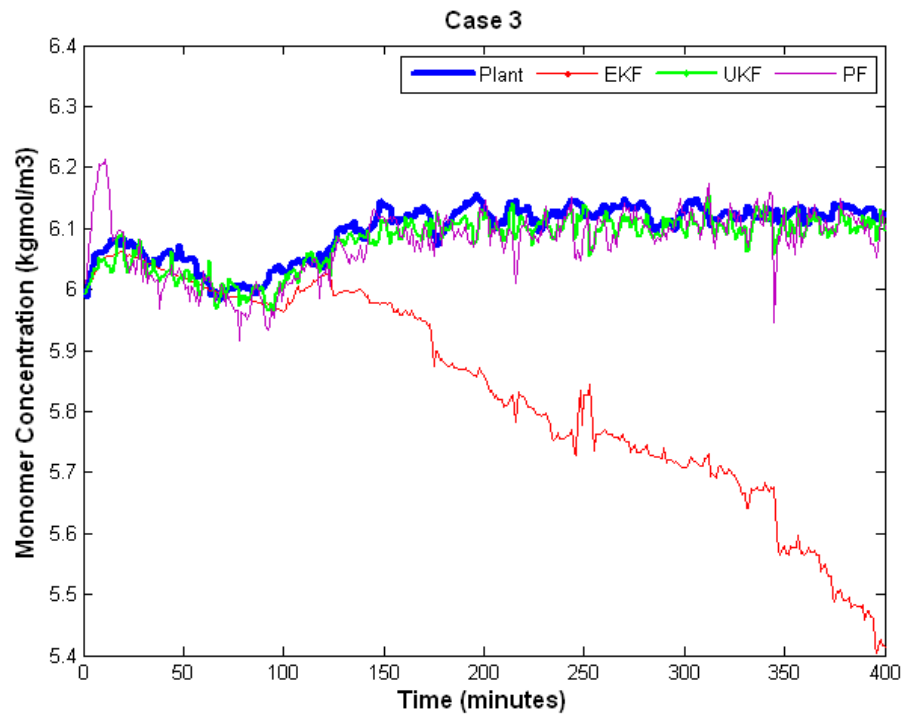
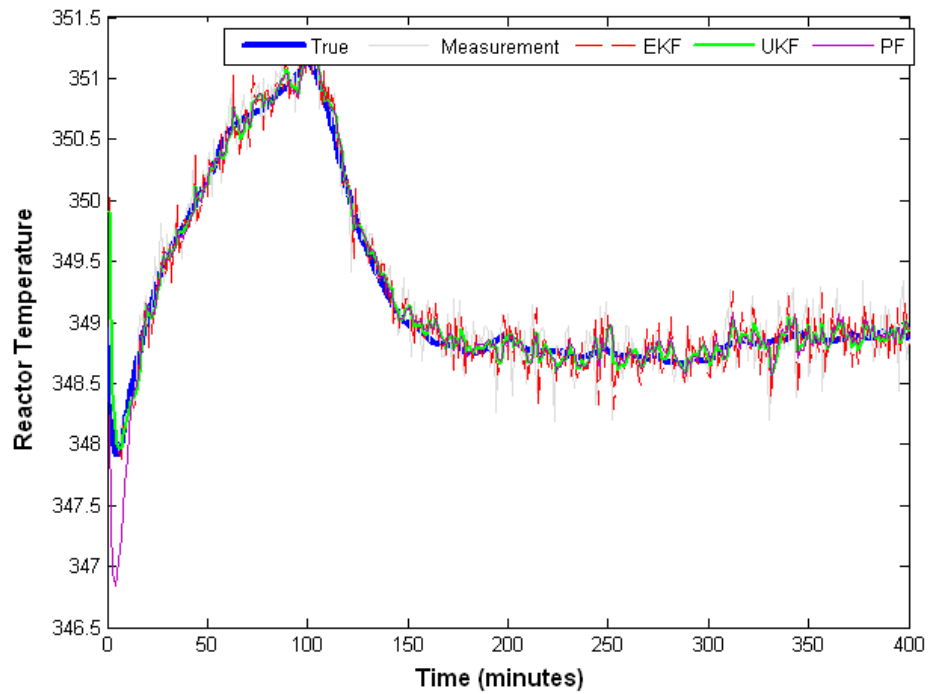


Figure 3.4: State estimation in the presence of non-Gaussian state (multimodal with std of 1 and 0.01 on the monomer and initiator concentrations respectively), non-Gaussian measurement noise (multimodal with std of 0.01 on the temperatures) and a 10 % positive step in monomer flow rate.

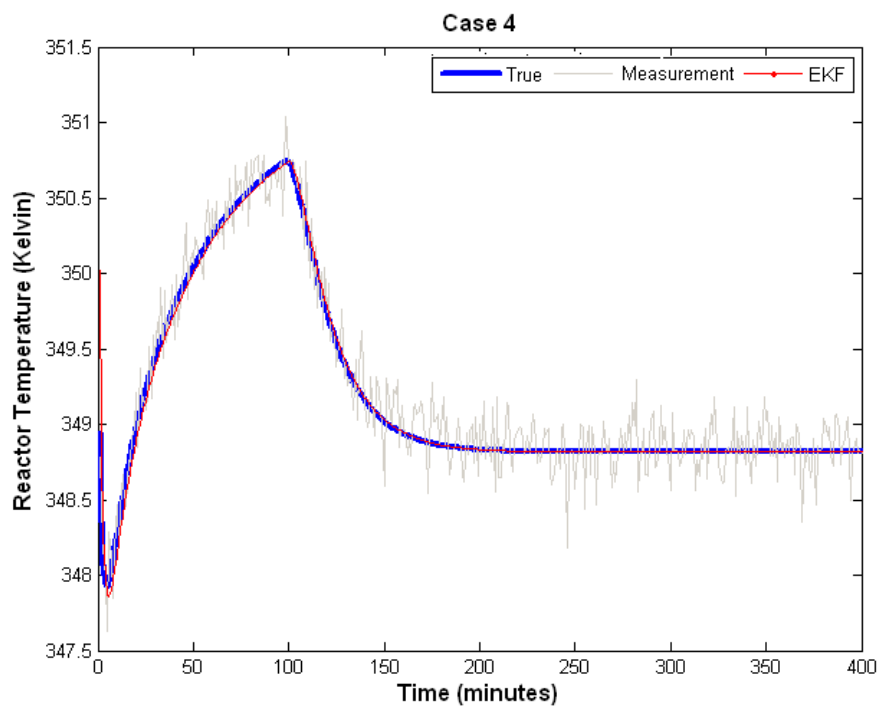


Figure 3.5: State estimation in the presence of non-Gaussian measurement noise (multimodal with std of 0.01 on the temperatures) and a 10 % positive step in monomer flow rate.

### 3.5 EKF versus UKF : Effect of process noise to measurement noise covariance ratios (Q/R) ratio on filter performance

The EKF and the UKF are based on the Kalman update. In the previous section, it was established that the ratio of assumed noise covariances are tuning parameters to change the value of Kalman gain, which in turn affects the weighting of the model estimate and the residual error. In this section, the performance of the EKF and UKF are compared for different ratios of noise covariances using three case studies. Particle filters are excluded from this study, as they are not based on the Kalman update. The tuning of particle filters is discussed in the subsequent section.

#### 3.5.1 Noise statistics and tuning parameters

Additive Gaussian noise was added to the system. Fig. 3.6 represents the noise distribution used.

Covariance of measurement noise added to temperatures (jacket temperature and coolant temperature in order) is given by:

$$\begin{pmatrix} 1.0e-06 & 0 \\ 0 & 1.0e-06 \end{pmatrix}$$

Covariance of process noise added to concentrations (monomer concentration and initiator concentration in order) is given by:

$$\begin{pmatrix} 1 & 0 \\ 0 & 1.0e-04 \end{pmatrix}$$

Covariance of process noise for estimator model:

$$\begin{pmatrix} 1.0 & 0 & 0 & 0 \\ 0 & 1.0e-04 & 0 & 0 \\ 0 & 0 & 1.0e-06 & 0 \\ 0 & 0 & 0 & 1.0e-06 \end{pmatrix}$$

Covariance of measurement noise considered in the estimation process:

$$\begin{pmatrix} 1.0e-06 & 0 \\ 0 & 1.0e-06 \end{pmatrix}$$

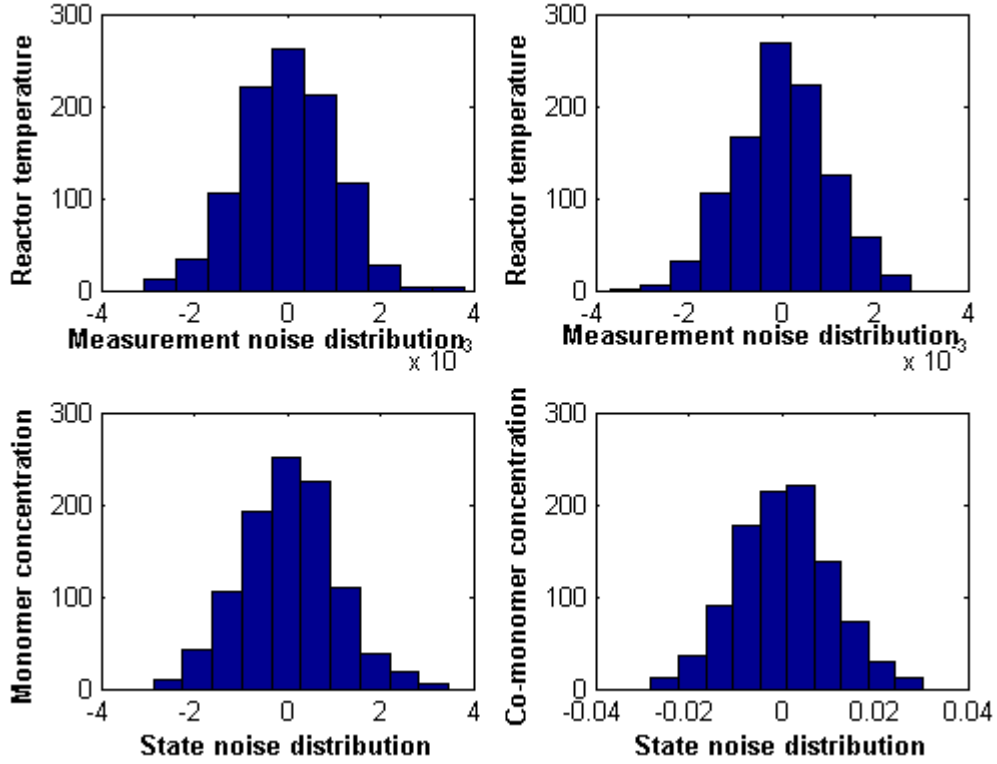


Figure 3.6: Distribution of noise sequences used in the simulation studies that follow.

Initial state noise covariance matrix:

$$\begin{pmatrix} 1.2e-03 & 0 & 0 & 0 \\ 0 & 7.5e-07 & 0 & 0 \\ 0 & 0 & 6.5e-06 & 0 \\ 0 & 0 & 0 & 2.5e-05 \end{pmatrix}$$

### 3.5.2 Case 1 - Low Q/R ratio

In this case, the process (state) noise covariance is chosen to be much smaller than the measurement noise covariance. This forces the Kalman gain (K) to approach zero. When the Kalman gain is zero, and the state estimates are the model estimates. This can be seen from equation. 3.8, which reduces to equation. 3.9 when K is zero.

$$\hat{x}_{k|k} = \hat{x}_{k|k-1} + K(y_k - H_k \hat{x}_{k|k-1}) \quad (3.8)$$

$$\hat{x}_{k|k} = \hat{x}_{k|k-1} \quad (3.9)$$

The estimator performance now depends entirely on the model. All estimators based on the Kalman update will perform similarly in this case. Fig. 3.7 shows the state estimation results for this case study. However, a slight difference can be observed between the EKF and UKF estimates. The difference in estimation is simply due to the method in which the *a priori* estimates are calculated. In the EKF, it is directly the model estimates, but in the UKF, sigma points are propagated through system dynamics, and the statistics of model estimates are obtained from these propagated sigma points. The small difference in performance can be removed by changing the several tuning parameters used to select sigma points in the UKF algorithm. It must be noted that this case study is conducted under no plant model-mismatch. Fig. 3.8 shows the propagation of noise covariances, and fig. 3.9 shows that the Kalman gain tends to zero in this case.

The assumed covariance of process noise for estimator model:

$$\begin{pmatrix} 1.0 & 0 & 0 & 0 \\ 0 & 1.0e-04 & 0 & 0 \\ 0 & 0 & 1.0e-06 & 0 \\ 0 & 0 & 0 & 1.0e-06 \end{pmatrix}$$

The assumed covariance of measurement noise added to estimators:

$$\begin{pmatrix} 1.0 & 0 \\ 0 & 1.0 \end{pmatrix}$$

### 3.5.3 Case 2 - Q and R ratios are comparable

In case study 2, the process and measurement noise covariances are chosen such that the Kalman gain considers both the state estimate and the measurement residuals. Fig 3.10 represents the Kalman gain at each time instant. Clearly, the Kalman gain lies between 0 and 1 indicating that estimation is taking place. Fig 3.11 demonstrates the difference in estimation performance between the EKF and UKF. From table. 3.3, it can be seen that under similar tuning rules, the UKF performs better than the EKF for case study 2. The difference between the EKF and the UKF algorithms lies in the methodology used to calculate the statistics of a variable undergoing a nonlinear transformation. The EKF simply linearizes the system, unlike the UKF where sigma points are used to represent nonlinear transformations.

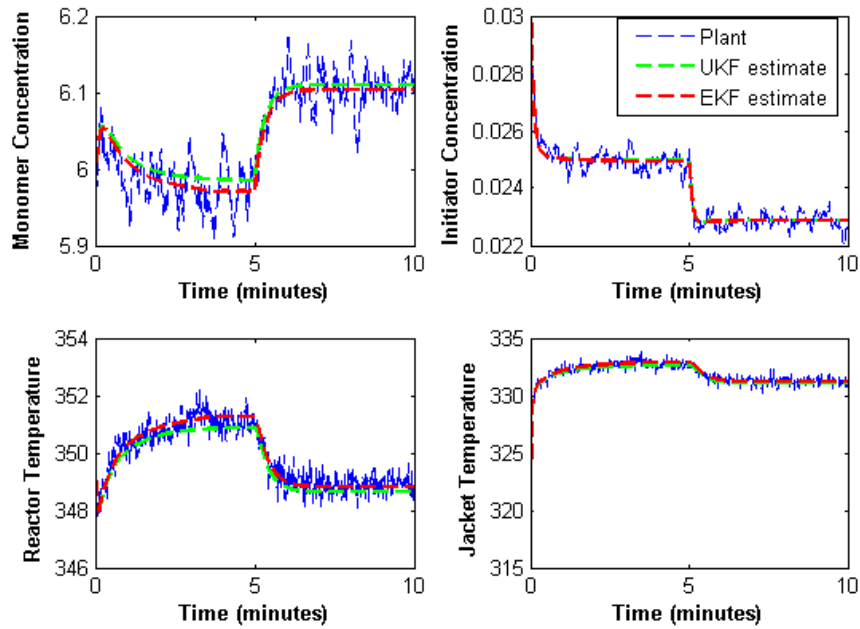


Figure 3.7: Case 1 - Estimation under low process-measurement noise ratio.

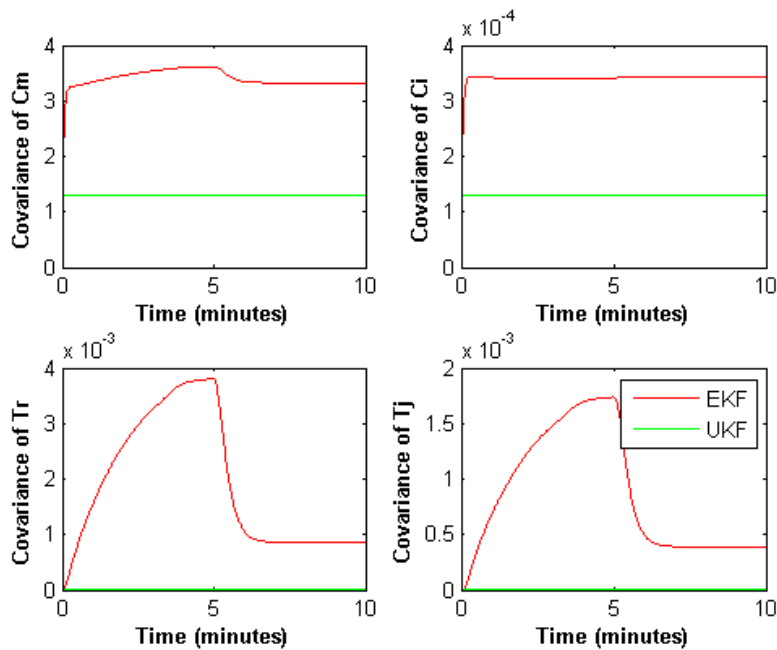


Figure 3.8: Case 1 - Covariance propagation under low process-measurement noise ratio.

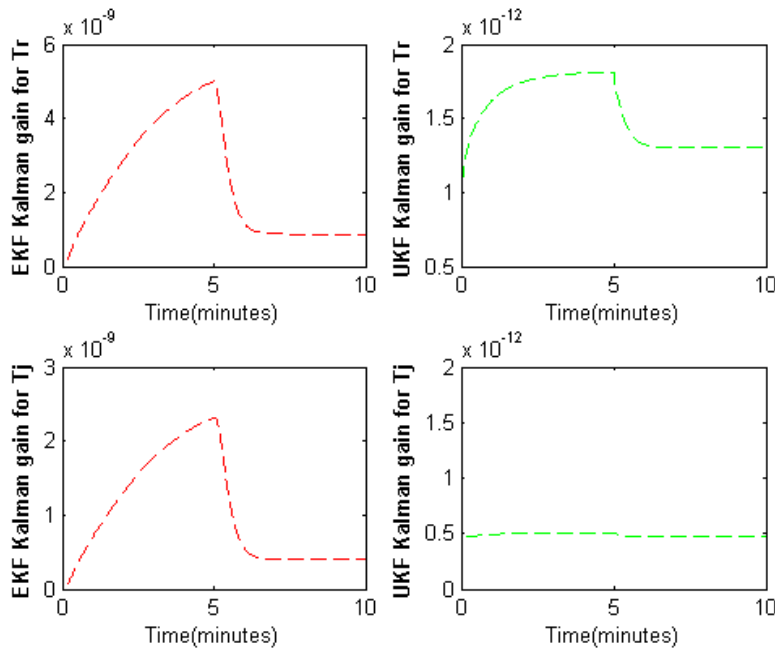


Figure 3.9: Case 1 - Kalman gain propagation of measured states under low process-measurement noise ratio. The figure shows the Kalman gains tend to zero.

Fig 3.12 shows how the linearization causes a bias (linearization error) in estimating unmeasured states. It can also be noticed that the Kalman update seems to overestimate the covariance matrices associated with these unmeasured states (for both EKF and UKF). It must be noted that the exact noise statistics are known in this ideal case study, and these noise covariance matrices are used in the estimator algorithms.

The assumed covariance of process noise for estimator model:

$$\begin{pmatrix} 1.0 & 0 & 0 & 0 \\ 0 & 1.0e-04 & 0 & 0 \\ 0 & 0 & 1.0e-06 & 0 \\ 0 & 0 & 0 & 1.0e-06 \end{pmatrix}$$

The assumed covariance of measurement noise added to estimators:

$$\begin{pmatrix} 1.0e-06 & 0 \\ 0 & 1.0e-06 \end{pmatrix}$$

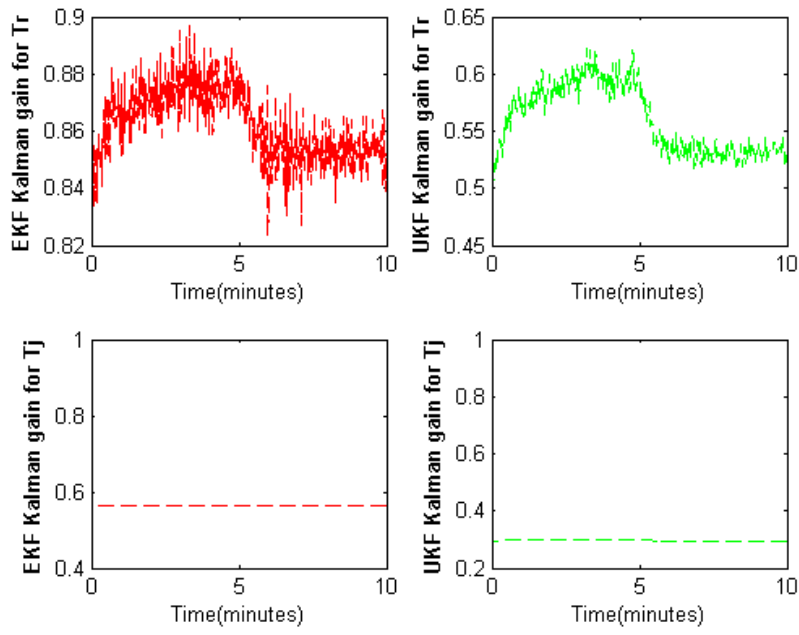


Figure 3.10: Case 2 - Kalman gain propagation of measured states under unit process-measurement noise ratio. The figure shows the Kalman gain lies between 0 and 1.

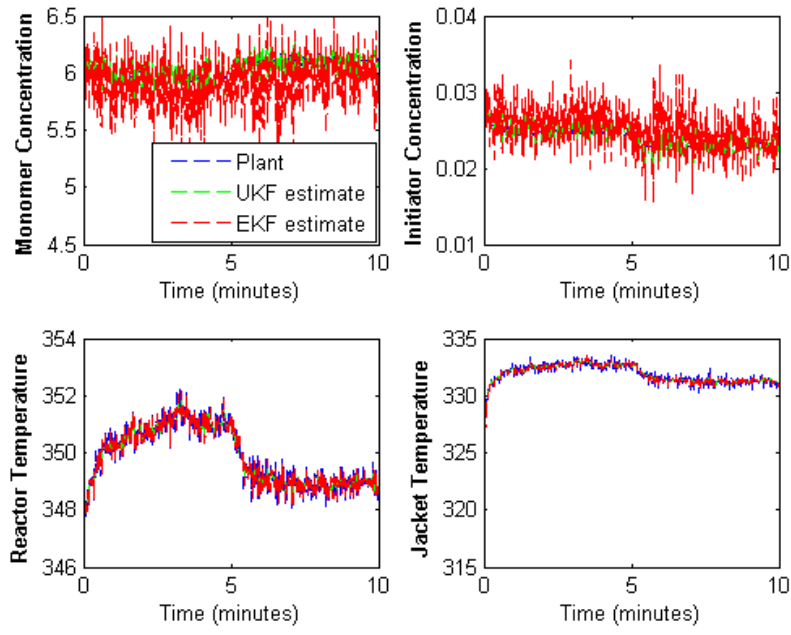


Figure 3.11: Case 2 - Estimation under unit process-measurement noise ratio.

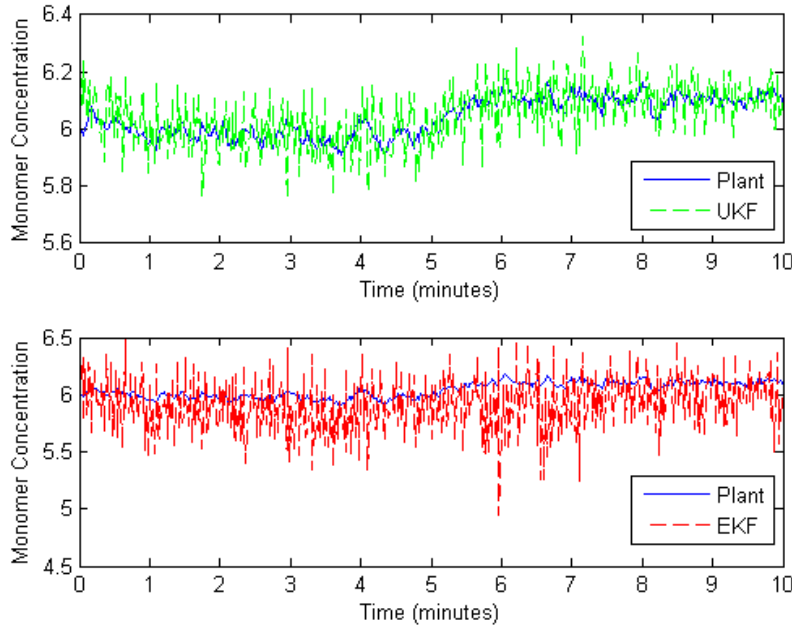


Figure 3.12: Case 2 - Plots to show biased EKF estimates compared to UKF estimates for monomer concentration under unit process-measurement noise ratio. The bias is not more than that seen in case 3.

### 3.5.4 Case 3 - High Q/R ratio

In case study 3, the process noise covariance is much higher than the measurement noise covariance forcing the Kalman gain for the measured state to 1 (fig. 3.14). This indicates that the measurements are now trusted completely, and play a major role in the state estimate. Fig 3.15 shows the estimation performance under this scenario and table. 3.3 indicates the performance of the estimators. The mean square error (MSE) values for measured states are exactly the same (unlike case study 2), while for the unmeasured states, the MSE values are clearly smaller for the UKF. Fig. 3.16 indicates the reason for the higher MSE values for the unmeasured states with the EKF. The estimation bias caused by linearization of the system dynamics is clearly evident in these plots. The bias seems to be much higher for case 3 (fig. 3.16) than that of case 2 (fig. 3.7). This is because the weighting caused by the Kalman gain in case 2 was able to correct the bias to a certain extent. The EKF covariance for measured states is smaller than the UKF covariance for case study 3 (fig. 3.17). This is in contradiction to the covariance propagation of measured states in case 2 (fig. 3.13).

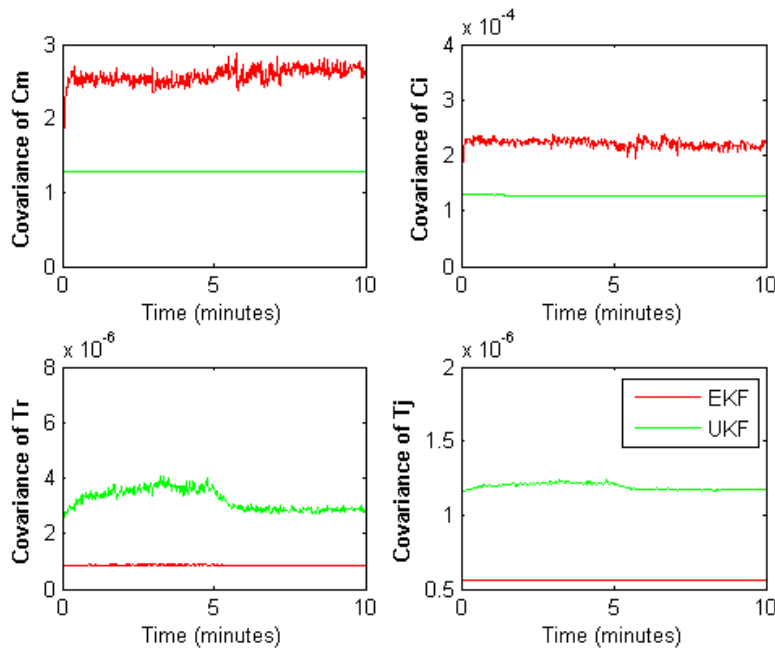


Figure 3.13: Case 2 - Covariance propagation under unit process-measurement noise ratio.

Covariance of process noise for estimator model:

$$\begin{pmatrix} 1.0 & 0 & 0 & 0 \\ 0 & 1.0e-04 & 0 & 0 \\ 0 & 0 & 1.0e-06 & 0 \\ 0 & 0 & 0 & 1.0e-06 \end{pmatrix}$$

Covariance of measurement noise added to estimators:

$$\begin{pmatrix} 1.0e-12 & 0 \\ 0 & 1.0e-12 \end{pmatrix}$$

### 3.5.5 Analysis and Concluding remarks - EKF versus UKF

When the Kalman gain is non-zero, plant measurements are trusted, i.e., estimation actually begins to take place. If the ratio of process to measurement noise is low, the estimates are the *a priori* estimates (model predictions). If the process model is good enough to capture the true process dynamics accurately, then the estimator is dispensable, or a low value of noise covariance ratios may be used (Q/R). When

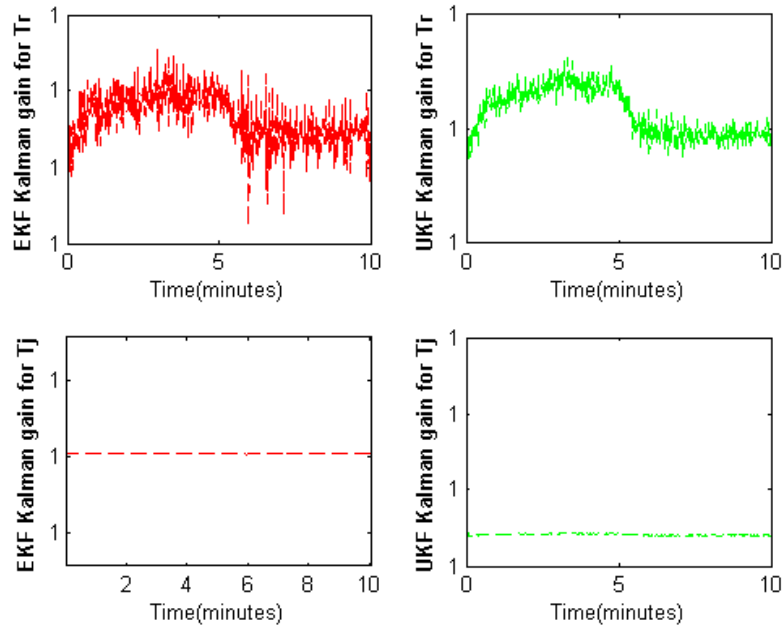


Figure 3.14: Case 3 - Kalman gain propagation of measured states under high process-measurement noise ratio. The figure shows the Kalman gain approaches 1.

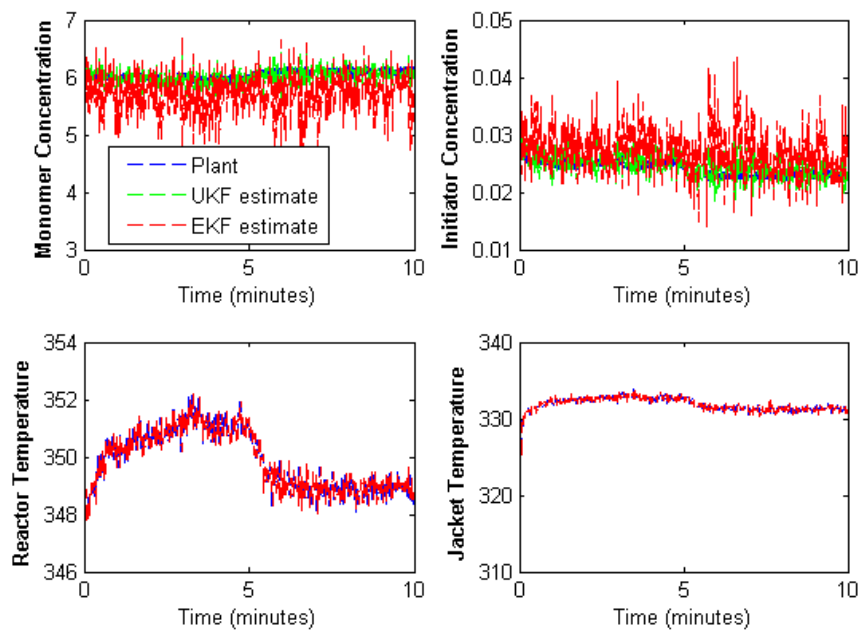


Figure 3.15: Case 3 - Estimation under high process-measurement noise ratio.

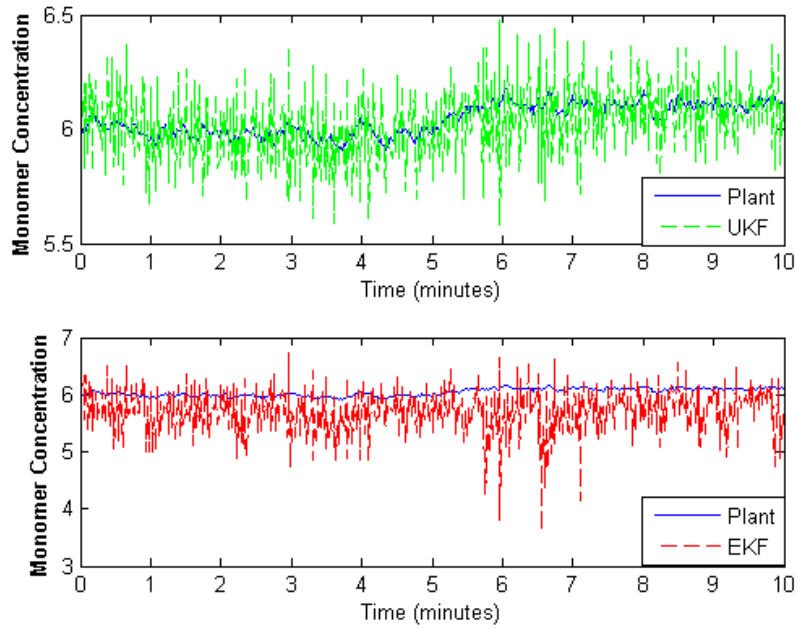


Figure 3.16: Case 3 - Plots to show biased EKF estimates compared to UKF estimates for monomer concentration under high process-measurement noise ratio.

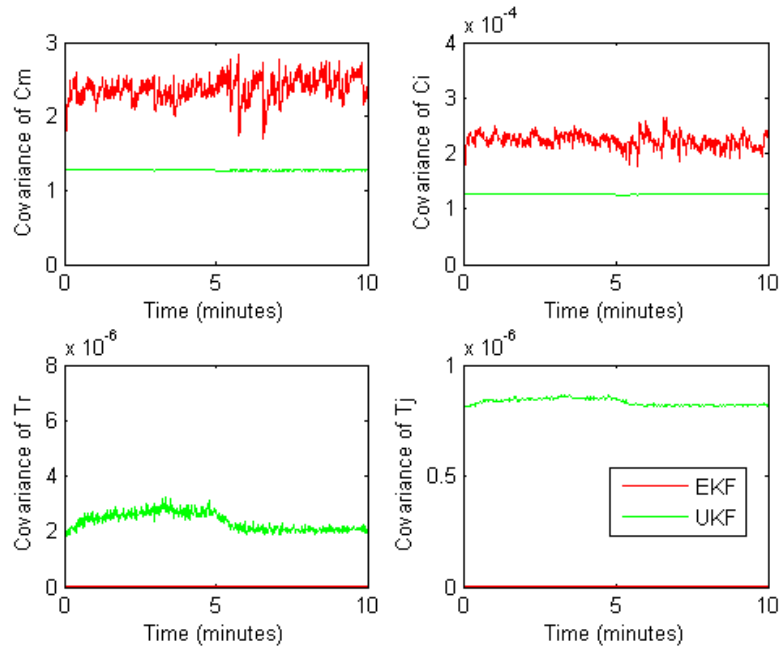


Figure 3.17: Case 3 - Covariance propagation under high process-measurement noise ratio.

the model estimates are not trusted entirely, the Q/R ratio is adjusted such that the Kalman gain lies between 0 and 1 and thus considers a weighted sum of the measurement residual and model prediction. If the model is not good, then the Q/R ratio is set close to 1, thus trusting the measurements almost completely.

In this system, the EKF estimates for unmeasured states (concentrations) are biased owing to the linearization error. We believe that the linearization error is caused due to the imperfect linearization of  $C_m P_0 \sim C_m \sqrt{C_i}$  in equation. 3.1. Fig. 3.18 represents the results for 1000 Monte-Carlo simulations of the temperature estimates when Q/R is equal (approximately) to 1 (i.e. Kalman gain lies between 0 and 1). Both the EKF and UKF are able to smooth the estimates. In fig. 3.19, the linearization error in the EKF estimate of concentrations is clearly visible. The estimates seem to be biased towards one direction. The box plots in fig. 3.20 provide a good summary of estimation results for the PMMA system. The estimators successfully smooth the measured states, while the EKF provides biased estimates (unlike the UKF) for the unmeasured states.

Table 3.3 lists the EKF to UKF mean squared error values for the three different case studies. In case 1, the MSE values should be close to 1, as there is no estimation taking place. The difference in performance seen here was explained earlier in the first case study for low Q/R ratios. When Q/R equals (approximately) 1, the UKF provides better estimates than the EKF, especially in the case of unmeasured states. When the Q/R ratio is high, the UKF provides better estimates than the EKF for the unmeasured states while the MSE ratio for measured states is close to 1 (as measurements are trusted).

As reported earlier, Romanenko and Castro (2004) have indicated that the linearization error occurs when Kalman gain is close to zero. However, this is really an approximation error, and should not be referred to as linearization error. Linearization error does not effect the model estimates, it is the covariance matrix and in turn the Kalman gain which are affected. There are two kinds of errors that may occur -

(1) An error can occur due to the approximation made as shown in equation. 3.10. This approximation error would be evident when the Kalman gain is close to zero, and the model represents the state estimates. The greatest advantage of the UKF is the increased accuracy of the mean transformation.

$$E[f(x)] \approx f(E[x]) \tag{3.10}$$

(2) Error due to linearization of nonlinear equations can be propagated through

Table 3.3: EKF versus UKF for varying process-measurement noise ratio

| Variable | Variable Property | (EKF MSE)/(UKF MSE)   |                     |                        |
|----------|-------------------|-----------------------|---------------------|------------------------|
|          |                   | Case 1<br>(Q/R = Low) | Case 2<br>(Q/R = 1) | Case 3<br>(Q/R = High) |
| Tr       | Measured          | 3.61e-001             | 1.87e+000           | 1.00e+000              |
| Tj       | Measured          | 3.41e-001             | 2.167e+000          | 1.00e+000              |
| Cm       | Unmeasured        | 8.99e-001             | 1.06e+001           | 1.22e+001              |
| Ci       | Unmeasured        | 9.91e-001             | 7.84e+000           | 7.36e+000              |

the covariance matrix and in turn the Kalman gain. This is the linearization error that has been exhibited in the case studies above. It is shown here that bias/error of EKF estimates can occur due to covariance approximation and not just mean transformations.

It is important to note that these errors are system specific and depend on the dynamics of the system or process.

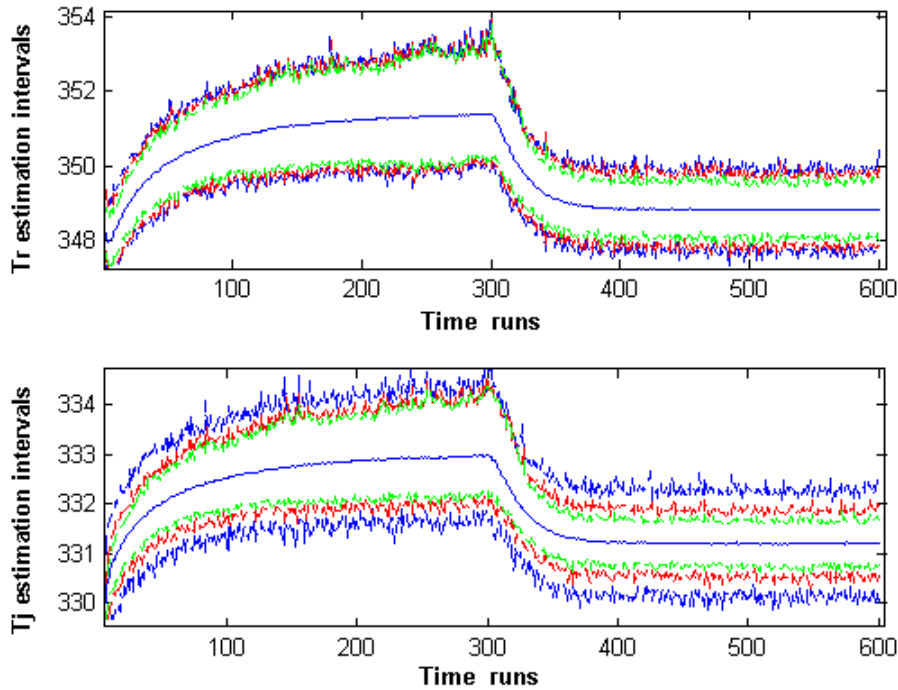


Figure 3.18: Estimation intervals for temperatures (measured states). Intervals obtained as maximum and minimum values at each time instant for 1000 Monte Carlo simulations. Plant (blue), EKF (Red) and UKF (green). The solid blue line that runs through the center is the average of plant values.  $Q/R \sim 1$ .

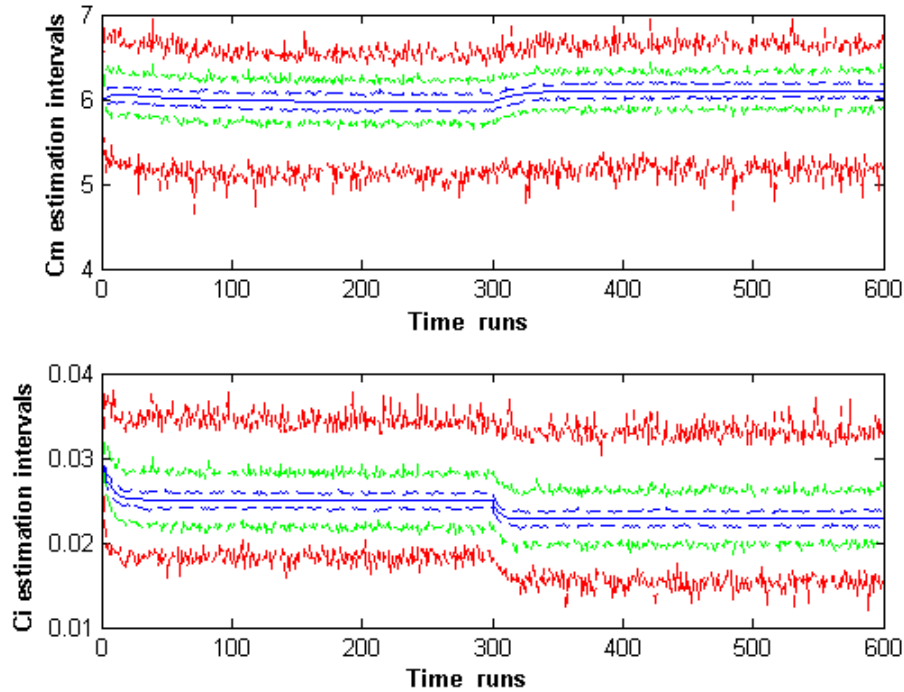


Figure 3.19: Estimation intervals for concentrations (unmeasured states). Intervals obtained as maximum and minimum values at each time instant for 1000 Monte Carlo simulations. Plant (blue), EKF (Red) and UKF (green). The solid blue line that runs through the center is the average of plant values.  $Q/R \sim 1$ .

### 3.5.6 Heuristic tuning of Kalman update based filters

In this section, we provide a heuristic way of tuning the Kalman update based filters. It is assumed that the value of measurement noise ( $R$ ) can be accurately obtained. Once  $R$  is known, the  $Q/R$  ratio is set be low and decreased until the Kalman gain is close to zero. This case provides a method to study the model estimation accuracy. If the estimates are good, then the model is accurate and hence the  $Q/R$  ratio can be set to a low value. If not, the  $Q/R$  ratio is increased until the Kalman gain lies between 0 and 1. If the measurements can be trusted completely (i.e. sensors are trusted to be good), then the  $Q/R$  ratio can be set close to 1. Note that all comparison of estimator performance here is being done using measured quantities alone and not the hidden states. A proportional integral based Kalman filter framework maybe used as described in the later part of the thesis.

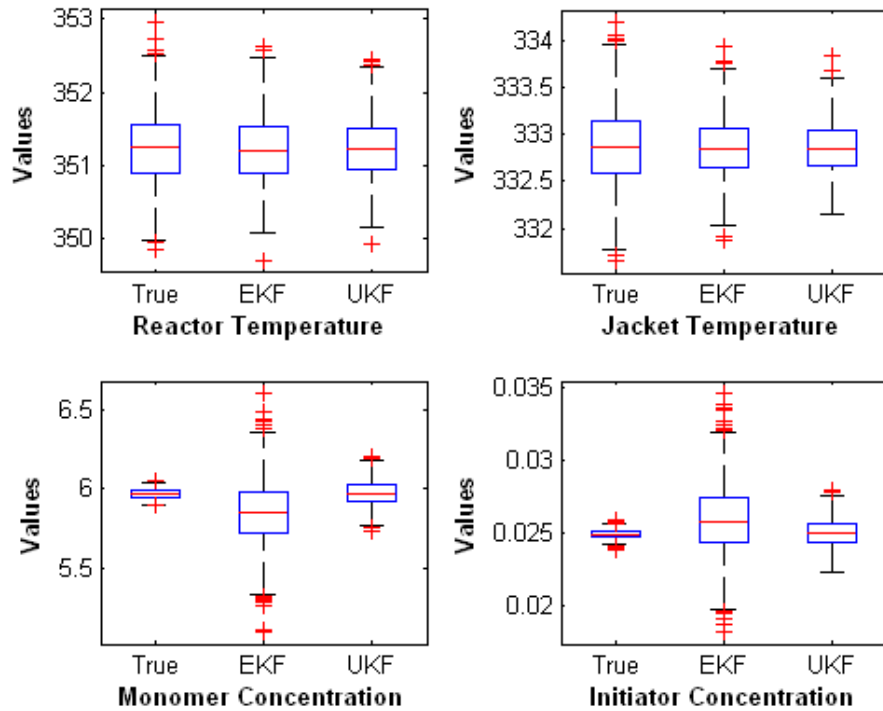


Figure 3.20: Box plots for 100 Monte Carlo simulations for the case where Q/R ratio  $\sim 1$ .

### 3.6 Ensemble Kalman filter for state estimation

In this section, the results for the application of the EnKF to the PMMA reactor are described. As explained in the previous chapter, the EnKF is an estimation algorithm that combines the Kalman update with Monte Carlo simulations. The ensemble members that are propagated through time are comparable to particles used in the particle filtering algorithm. However, Kalman update based filters are based on mean and covariance propagation, i.e., the first and the second moment alone. Thus, only Gaussian distributions are represented accurately by the EnKF. However, under this assumption, it outperforms other estimators. In the following section, the advantages and disadvantages of the EnKF are discussed.

#### 3.6.1 Analysis of the application of EnKF to a PMMA reactor

The EnKF and UKF were run for 60 time instants (fig. 3.21) under similar initial conditions. The mean squared error values can be seen in fig. 3.22. As expected, the

EnKF performance is comparable to the UKF performance (MSE of UKF/EnKF close to 1). Both the EnKF and UKF were devised to address the linearization error in the EKF algorithm for highly nonlinear systems. In this case, the UKF seems to have a slight edge in performance over the EnKF. This may be due to the tuning of the initial covariance matrix of the EnKF. Tuning the initial state covariance matrix in the EnKF is very important, as the ensemble is not resampled and the algorithm relies completely on the propagation of initial ensemble chosen. A small initial covariance may lead to computation of a low value of sample covariance. Higher initial covariance with a larger ensemble may lead to good estimates of the covariance matrix. However, the calculation of a point estimate from a larger ensemble is difficult, as the mean of the ensemble is affected by points that may lie far from the value of the state estimate. However, with progress in time, the ensemble members will converge, hence eliminating this problem. It is important to choose the right number of ensembles and good value of the initial covariance matrix. In this example, deterministic sampling (UKF) seems to be helpful in providing good estimates. The computation time is much higher for the EnKF than the UKF (fig. 3.23). EnKF is used mainly in large scale systems such as reservoir simulations and weather forecasting. This is due to the following advantages over the UKF:

- 1) The size of the ensemble required for large state systems may be less than the number of sigma points required by the UKF algorithm ( $2 \times \text{number of states} + 1$ )
- 2) Moreover, the EnKF does not use a square root operator which is used by the UKF in calculation of the sigma points. This requires the covariance matrix to be positive definite at all instants of time. This criteria need not be fulfilled in the EnKF.
- 3) Also, in the EnKF, the ensemble is updated by the Kalman update. No resampling takes place at each instant. In the UKF, sigma points need to be computed at each instant of time. This may prove to be computationally cumbersome for large scale systems.
- 4) Covariance update is not required in the EnKF. It simply uses the members of the ensemble to calculate the sample covariance. The sample covariance is not required in any calculations in the EnKF algorithm; it is merely the second moment of the Gaussian random variable estimate.

The main advantage of both the EnKF and the UKF is that they do not need

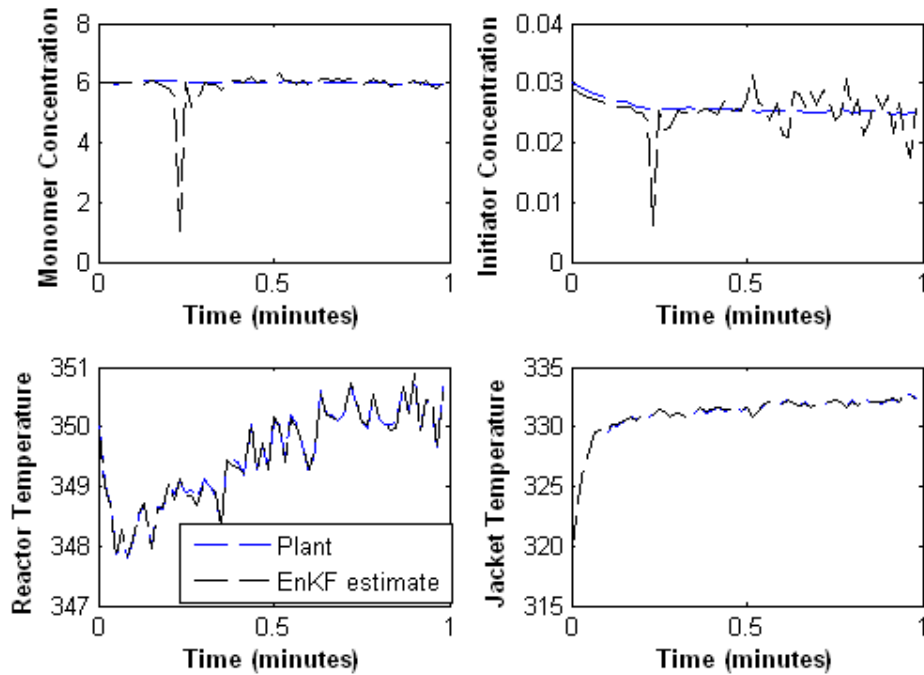


Figure 3.21: EnKF estimation plots for 1 minute of time run

computation of the Jacobian, unlike the EKF. The use of the EnKF over UKF and vice versa comes down to computational power required by each estimator for the system under consideration. Usually, for small systems, the UKF is the preferred algorithm owing to lower computational time. For large scale systems, the EnKF is the choice owing to its simplicity (no square root and resampling) and lower computational time as the size of the ensemble becomes smaller than the number of sigma points. Hence, the choice of estimator between EnKF and UKF may be based solely on the dimension of the state space and the computational time required for the estimation algorithm to run. However, it is important to note that both the EnKF and the UKF are based on the Kalman update and hence only represent Gaussian random variables.

### 3.7 State estimation in case of non-Gaussian posterior

When the dynamics of a process are highly nonlinear, it is likely that any Gaussian or non-Gaussian noise sequences will cause the posterior distribution to be non-

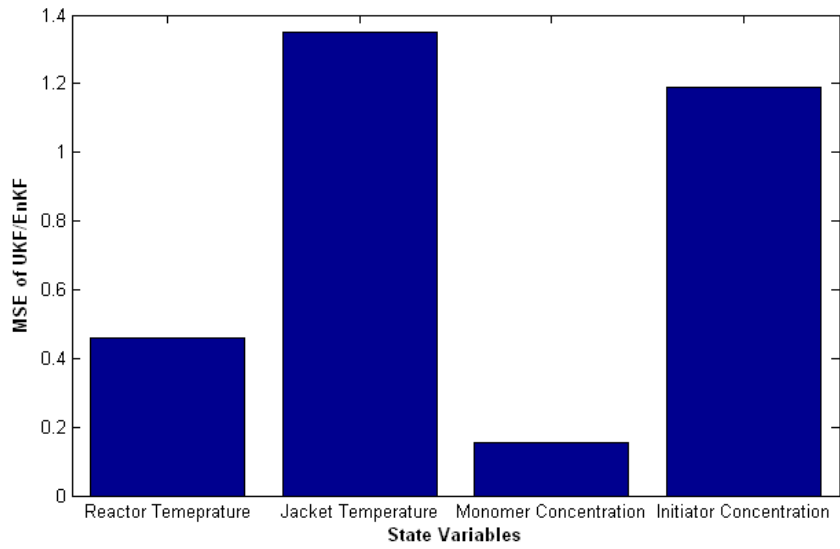


Figure 3.22: MSE values of UKF/EnKF for the case study on comparison of UKF and EnKF performances on a PMMA reactor.

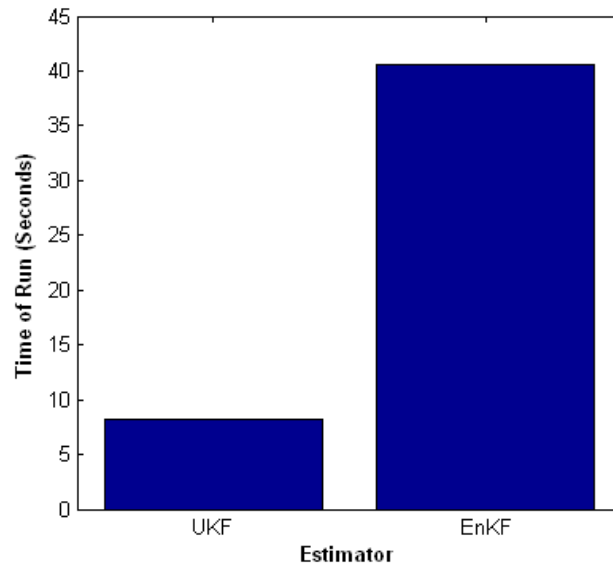


Figure 3.23: CPU run times of UKF and EnKF for the case study on comparison of UKF and EnKF performances on a PMMA reactor.

Gaussian. The extent of non-Gaussian behavior depends on the system dynamics and the distribution of the noise sequences affecting the system. Figures. 3.24 to 3.26 shows the non-Gaussian posterior distributions that occur for the PMMA reactor under simple Gaussian noise sequences. The solid line in these figures depicts the best possible Gaussian fits to these distributions. In most cases here, the mean of the best Gaussian fit may represent the true estimate. However, if the extent of non-Gaussian behavior were to be increased, Gaussian approximation of these skewed/multi-modal distributions would lead to significant errors. In this section, we introduce the application of particle filters for full state distributions.

### **3.7.1 Application of particle filters**

The Kalman update based filters are based on representation of random variables using Gaussian statistics (i.e. mean and covariance). As discussed earlier, in case of highly non-Gaussian distributions, these GRV (Gaussian random variable) based estimators may give significant error. Hence, one needs an alternate solution. Particle filters are based on full state distributions (not just the mean and the covariance of the estimate) and are capable of representing multi-modal and skewed distributions. Fig 3.27 represents the plots for the application of particle filter onto the PMMA reactor under high process noise covariance. Effective tuning of the filter is described in the subsequent section.

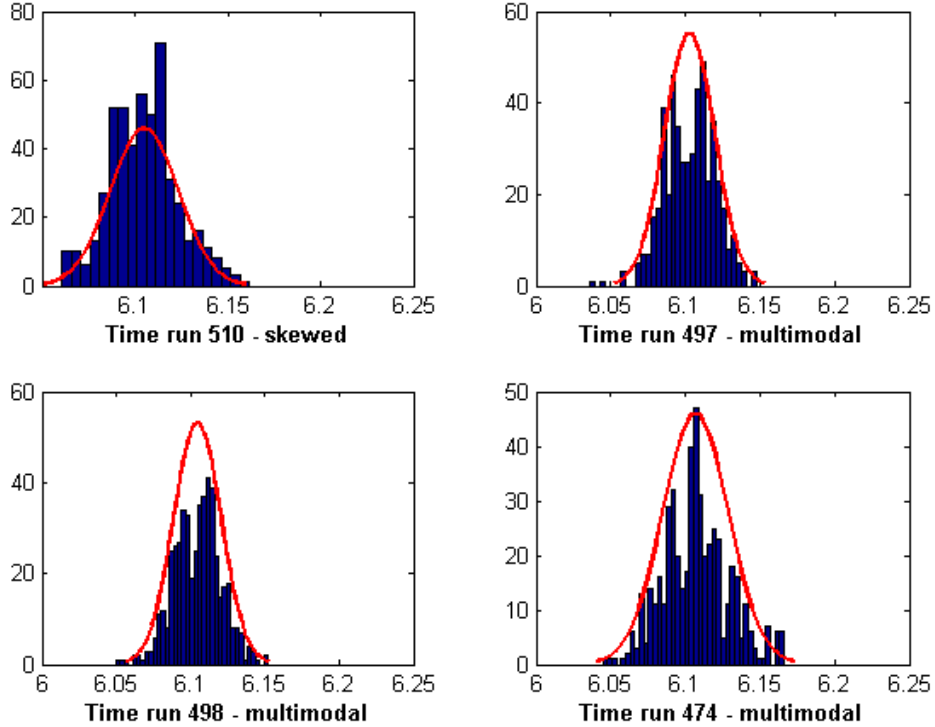


Figure 3.24: Evolution of posterior for  $C_m$ . The posterior is either skewed or multimodal. The overlying Gaussian distribution fails to describe the histogram accurately.

### 3.7.2 Filter tuning and performance

The algorithm given by Imtiaz et al. (2006) was used to tune the particle filter. The process noise was chosen to be higher (one order higher) than the actual process noise. This helps to make the prior wide and hence to cover the actual states of the system. Fig. 3.27 represents the simulation results for this case (Case 1). Large oscillations were observed in the unmeasured state variables, indicating that the selected process noise is very high. A series of simulations were used to select a suitable process noise covariance matrix. The process noise covariance was selected such that the estimation of unmeasured states was jittery, but not oscillatory. Figures. 3.28 and 3.29 represent the simulation study for this case (Case 2). The distribution of weights to *a priori* states shows that the weighting between model estimates and plant measurements was uneven. Keeping the process noise covariance constant, the measurement noise covariance was increased until the distribution of weights to *a priori* states indicated that both measurements and model estimates were shaping the prior and in turn affecting estimation. Figures. 3.30 and 3.31

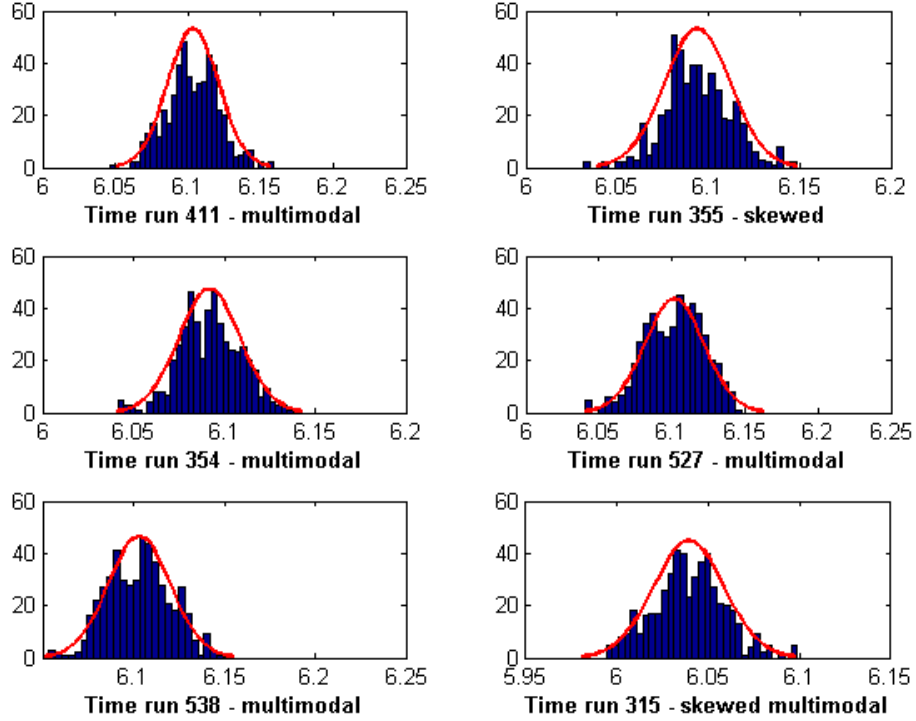


Figure 3.25: Evolution of posterior for  $C_m$ . The posterior is either skewed or multimodal. The overlying Gaussian distribution fails to describe the histogram accurately.

indicate the tuning based on distribution of weights to *a priori* states. Table. 3.4 gives the MSE values for each of these cases.

### 3.7.3 Concluding remarks for the particle filter

The particle filter holds a clear advantage to the EKF and UKF when the posterior distributions are highly non-Gaussian. Table 3.5 represents the mean squared error values, in case one were to heuristically tune all the estimators. Tuning of Kalman update based filters (based on ratios of noise covariances) is different from tuning of particle filters (distribution of weights). It can be shown that as the number of particles approaches infinity, the posterior approaches the true posterior represented by the information (measured output) at any instant of time. The use of particles and weights to represent the posterior ensures that non-Gaussian distributions are represented accurately, i.e., multi-modal or skewed distributions are represented. It is important to note that the particle filter algorithm deals with full state distributions alone, and not point estimates. The extraction of a point estimate from

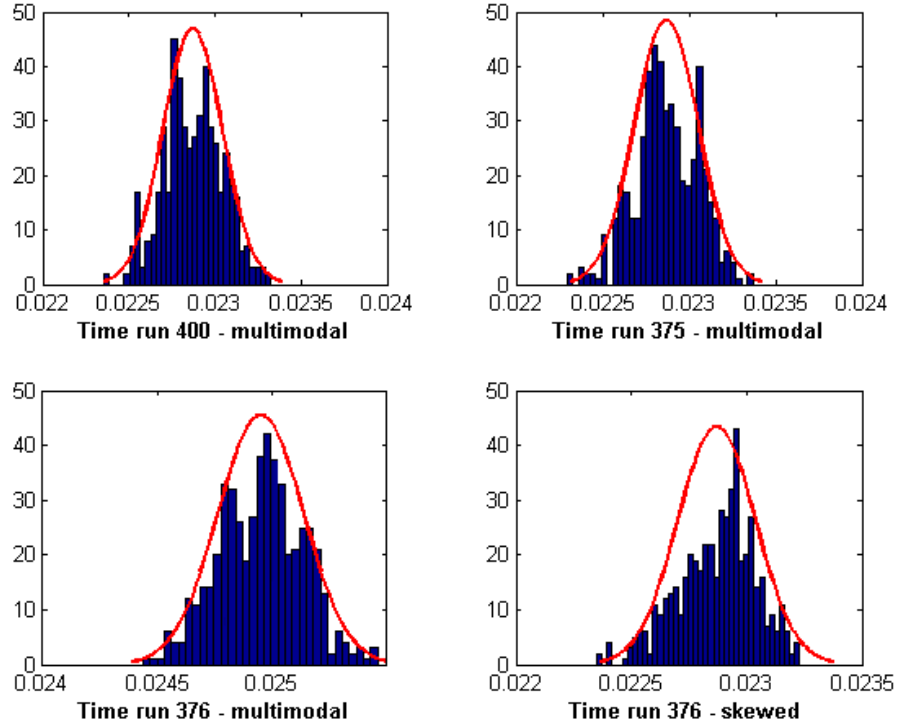


Figure 3.26: Evolution of posterior for  $C_i$ . The posterior is either skewed or multimodal. The overlying Gaussian distribution fails to describe the histogram accurately.

full state distributions is an open problem, and is discussed later in this chapter. Unlike the particle filter, the generic EKF or UKF are able to calculate only the first two moments of the posterior (mean and variance). Calculation of additional moments may require additional computation. Hence, the particle filter is clearly a better filter when the posterior estimates are highly non-Gaussian. It is, however, important to note that in cases when the assumptions of the EKF or UKF hold, they may perform comparable to the particle filter.

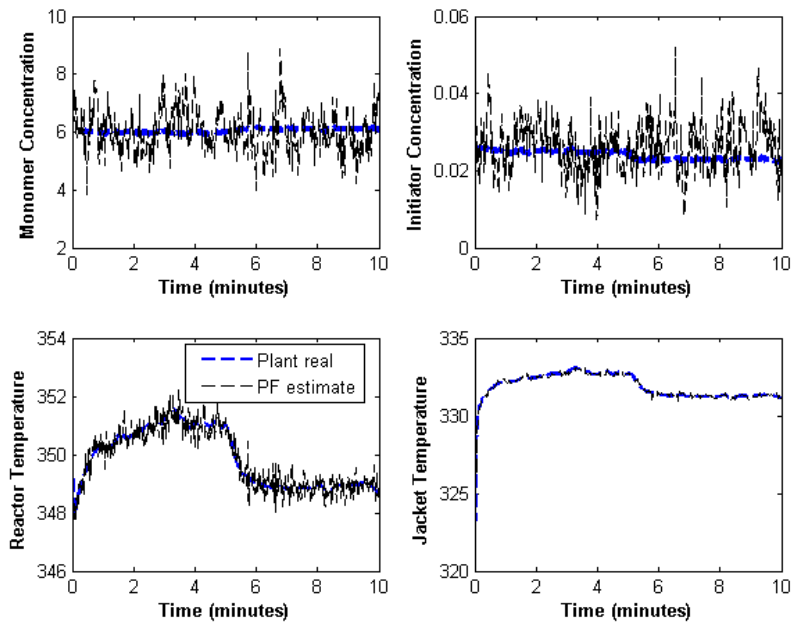


Figure 3.27: Particle filter performance for Case 1 under high process covariance.

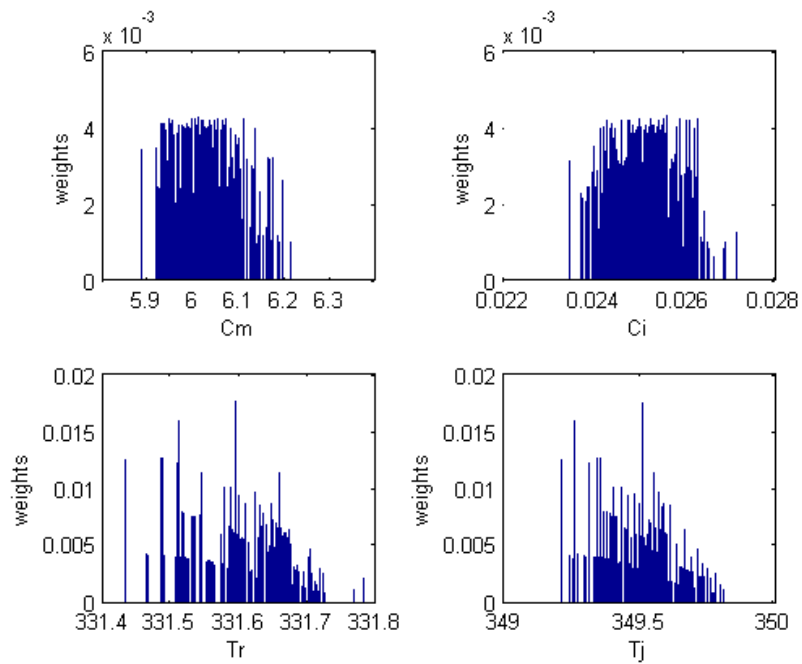


Figure 3.28: Distribution of weights for particle filter application for Case 2 (under reduced process covariance).

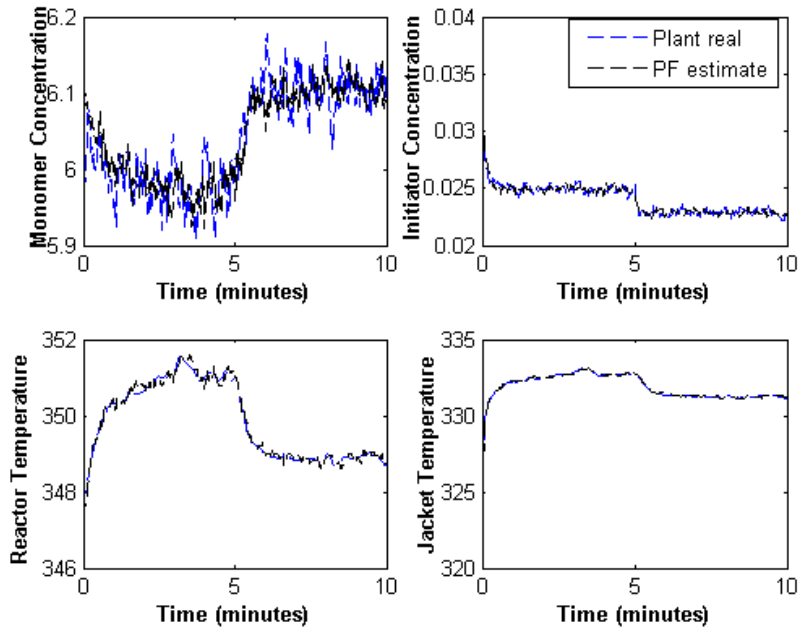


Figure 3.29: Particle filter performance for Case 2 (under reduced process noise covariance).

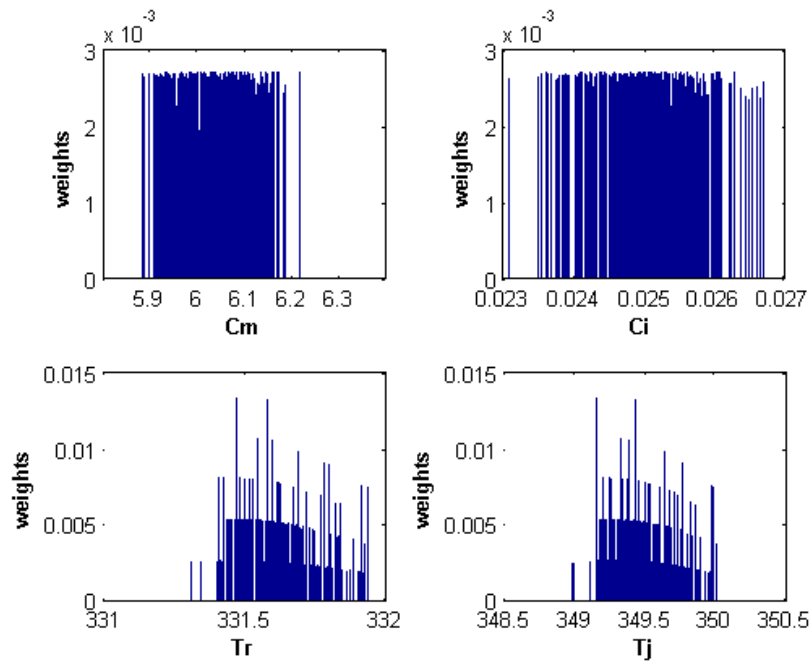


Figure 3.30: Distribution of weights for particle filter application for Case 3 (under increased measurement noise covariance).

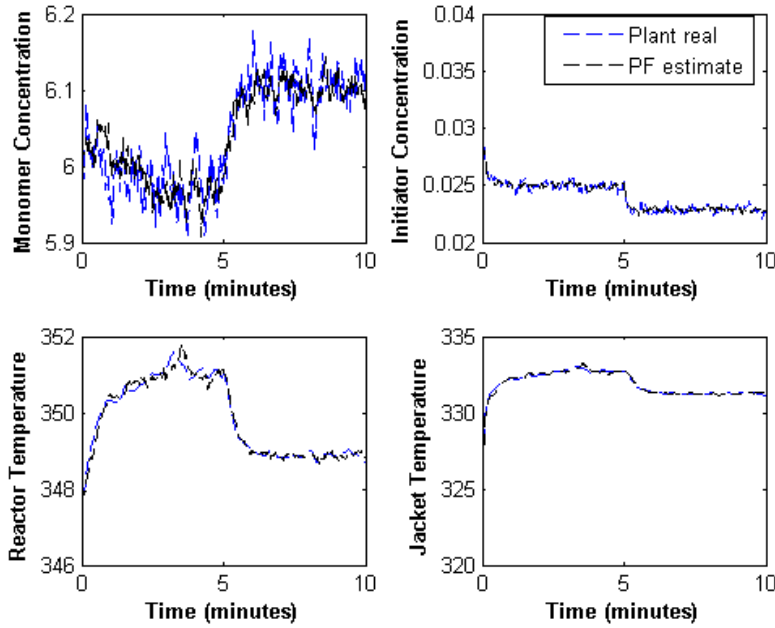


Figure 3.31: Particle filter performance for Case 3 (under increased measurement noise covariance).

Table 3.4: MSE values for tuning of particle filter

| Variable | Variable Property | Case 1  | Case 2  | Case 3  |
|----------|-------------------|---------|---------|---------|
| Tr       | Measured          | 5.97e-4 | 9.37e-5 | 1.44e-4 |
| Tj       | Measured          | 1.19e-4 | 7.49e-5 | 9.66e-5 |
| Cm       | Unmeasured        | 3.33e+2 | 6.54e-1 | 5.22e-1 |
| Ci       | Unmeasured        | 2.91e-2 | 9.83e-5 | 5.94e-5 |

Table 3.5: Comparison of EKF , UKF and PF MSE values

| Variable | Variable Property | EKF     | UKF     | PF      |
|----------|-------------------|---------|---------|---------|
| Tr       | Measured          | 4.83e-4 | 2.58e-4 | 1.44e-4 |
| Tj       | Measured          | 4.21e-4 | 1.94e-4 | 0.97e-4 |
| Cm       | Unmeasured        | 4.12e+1 | 0.39e+1 | 0.05e-1 |
| Ci       | Unmeasured        | 5.09e-3 | 0.65e-3 | 0.06e-3 |

## 3.8 Proportional-integral based Kalman filters

Integral action is used in control loops to remove constant bias that may occur during proportional control. It is due to this reason that most controllers in industry are based on proportional-integral action. In the previous section, it was shown that the EKF provided biased estimates due to linearization error. Biased estimates may also be obtained due to parameter mismatch in the plant and model. In this section, we discuss the introduction of integral action in Kalman filtering, to remove bias. The Kalman update equation contains the Kalman gain term, which is comparable to the proportional gain in a PID controller. The Kalman filter may give a bias due to gain or time constant mismatch between the plant and the model. We try to eliminate this bias by incorporating the integral action with common fundamentals as that in PID controllers.

### 3.8.1 PI-KF algorithm

In the proposed algorithm, the accumulated error is calculated and added to the model prediction as uncertainty. Two tuning parameters are used.  $\gamma$  is the tuning parameter that is used to regulate the addition of the integral error to the model prediction.  $\gamma$  is a square matrix with same number of rows as the state transition matrix. If all the values in  $\gamma$  are set to zero, the filter reduces to the traditional Kalman filter, and there is no integral action taking place. Integral gain ( $K_{integral}$ ) is comparable to a forgetting factor that weights the effect of past accumulated error on the current state variables. For ease of tuning,  $\gamma$  is restricted to values of 0 or 1 on the diagonal (off diagonal elements are 0) and only  $K_{integral}$  is used as a tuning parameter. Tuning of these terms is discussed for the two tank system given in the next sub-section. Eq. 3.11 is the prediction step of the Kalman filter algorithm. Eq. 3.12 is the new step introduced after calculation of the Kalman gain.  $v$  represents the integral/accumulated error.

$$\hat{x}_{k|k-1} = F\hat{x}_{k-1|k-1} + Bu_k + \gamma v \quad (3.11)$$

$$v = v + K_{integral}(z_k - H_k\hat{x}_{k|k-1}) \quad (3.12)$$

### 3.8.2 PI-KF algorithm on two tank system

The proposed algorithm was tested on a simulated two tank system. Fig. 3.32 shows the system under consideration. The model dynamics and parameters may

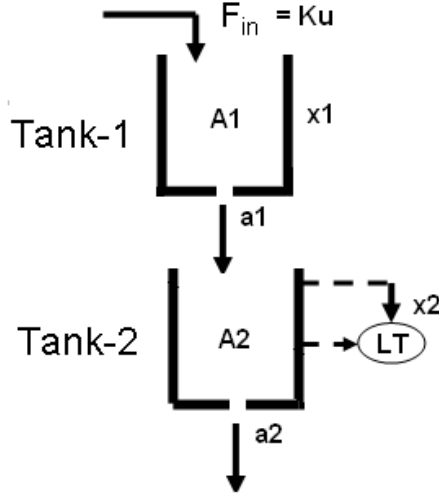


Figure 3.32: Schematic of two tank system used to study the PF-KF problem

be obtained from the MATLAB tutorial files on system identification. Eq 3.13 and 3.14 describe the nonlinear dynamics of this process. However, a linearized version of this system is used for this study (both plant and estimator model). Eq 3.15 and 3.16 describe the linearized continuous time state space model. Table. 3.6 gives the values parameters and variables associated with this system.  $x_1$  and  $x_2$  are the water levels in tank 1 and tank 2 respectively.

$$\frac{dx_1(t)}{dt} = \frac{1}{A_1}(Ku(t) - a_1\sqrt{2gx_1(t)}) \quad (3.13)$$

$$\frac{dx_2(t)}{dt} = \frac{1}{A_2}(a_1\sqrt{2gx_1(t)} - a_2\sqrt{2gx_2(t)}) \quad (3.14)$$

$$\dot{x} = Ax + Bu \quad (3.15)$$

$$y = Cx + Du \quad (3.16)$$

$$A = \begin{bmatrix} -\sqrt{\frac{g}{2x_{1ss}}} \frac{a_1}{A_1} & 0 \\ \sqrt{\frac{g}{2x_{1ss}}} \frac{a_1}{A_2} & -\sqrt{\frac{g}{2x_{2ss}}} \frac{a_2}{A_2} \end{bmatrix}$$

$$B = \begin{bmatrix} \frac{K}{A_1} \\ 0 \end{bmatrix}$$

$$C = [ 0 \quad 1 ]$$

$$D = [ 0 ]$$

$x1_{ss}$  and  $x2_{ss}$  are steady state values that can be obtained by equating eq 3.13 and 3.14 to 0.

Table 3.6: Tabulation of variables for two tank system

| Variable | Description                 | Units    | Plant value | Model Value |
|----------|-----------------------------|----------|-------------|-------------|
| A1       | Area of tank 1              | $m^2$    | 0.500       | 1.000       |
| A2       | Area of tank 2              | $m^2$    | 0.250       | 0.125       |
| a1       | Tank 1 outlet area          | $m^2$    | 0.020       | 0.010       |
| a2       | Tank 2 outlet area          | $m^2$    | 0.015       | 0.0075      |
| g        | Acceleration due to gravity | $m/s^2$  | 9.810       | 9.810       |
| K        | Pump constant               | $m^3/sV$ | 0.005       | 0.005       |
| u        | Voltage to pump             | $V$      | 10.000      | 10.000      |

Fig 3.33 shows the estimation performance using the Kalman filter. In fig 3.34, the bias is removed by the integral action.  $\gamma$  is set to diagonal[1 0], as this drives  $x1$  to a value which tries to correct  $x2$  (i.e true value of  $x2$ ). If one were to choose  $\gamma$  to be diagonal[1 1], the state  $x1$  would not be corrected entirely. If there exists a parameter such that it effects the dynamics of  $x2$  alone, then one could do a two step correction which would include correcting  $x2$  using  $x1$  initially ( $\gamma = \text{diagonal}[1 0]$ ) and then correcting  $x2$  after a delay ( $\gamma = \text{diagonal}[0 1]$ ). Tuning  $K_{integral}$  is done in a manner similar to tuning integral action in PID controllers, i.e., starting with a low value of  $K_{integral}$  and increasing it until a good integral action response is seen (similar to figure. 3.34). If the value of  $K_{integral}$  is increased by a large amount, the estimate would be highly oscillatory or unstable. The value of  $K_{integral}$  used in these simulations is 0.2.

However, for the two tank system, if only  $a1$  were changed, this would not work. This is because we would change the steady state of the system if the ratio of  $a1$  to  $a2$  is not maintained. Hence, experiments need to be performed to get the accurate value of  $a1/a2$ , while  $a1$  and  $a2$  can individually take be any value. Hence, the two tank system problem needs to be considered under a constrained framework (in this case constant value) for  $a1/a2$ .

The process transfer function is given by Eq 3.17

$$\frac{X_2(s)}{U(s)} = \frac{K \frac{a1}{a2} \sqrt{\frac{2x1_{ss}}{g}}}{(A2 \frac{a1}{a2} \sqrt{\frac{2x2_{ss}}{g}} s + 1)(A1 \sqrt{\frac{2x1_{ss}}{g}} s + 1)} \quad (3.17)$$

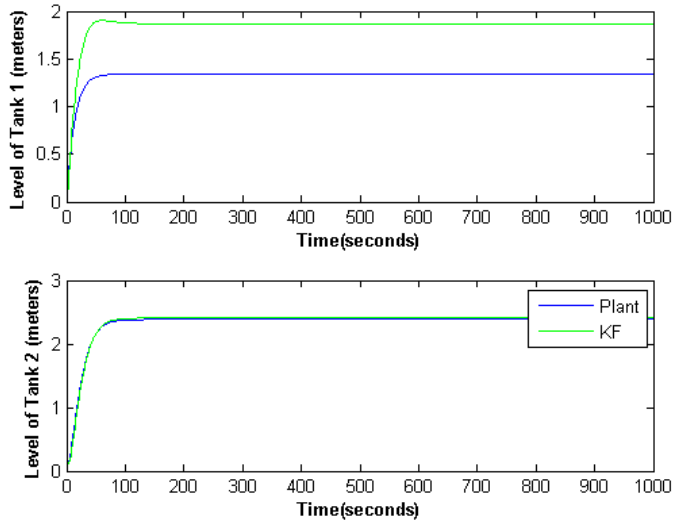


Figure 3.33: State estimates for the two tank system with Kalman filter

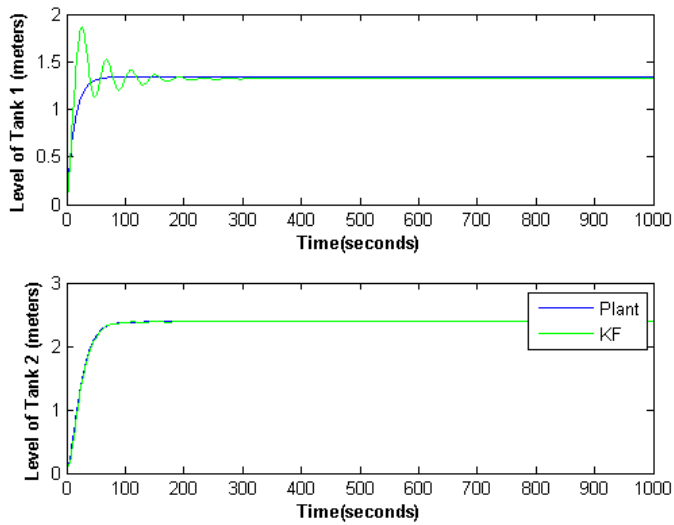


Figure 3.34: State estimates for the two tank system response with proportional integral Kalman filter

Under constraints ( $a1/a2$ ), the PI based Kalman filter will handle gain mismatch and mismatch in time constants (i.e. mismatch in variables  $K, A1, A2, a1, a2, g$ ).

### 3.8.3 Similarity between integral action and state augmentation

It was later found that this method is similar to the state augmentation method used by Lee and Ricker (1994) (in turn inherited from Goodwin and Sin (1984)). Here the entire uncertainty is clubbed into an additive noise model. The PI action shown above condenses to this state augmentation methodology. The above case study demonstrates the importance of considering state augmentation in state estimation. A noise model needs to be augmented to the dynamic state equations with appropriate values of  $\gamma$  (to control the position of the term to club the uncertainty) and  $K_{integral}$  (as a forgetting factor). The use of this algorithm will remove any uncertainty that occurs due to observable parameters. Hence, under a stochastic framework, it is good to consider a noise model or a PI based Kalman filter. Note that the integral states that are added are not being estimated, i.e., the integral terms that are added to the state equation do not undergo any actual estimation.

### 3.8.4 Concluding remarks

When accurate/true parameter values are not important, and only good state estimates are required, PI based Kalman filter can be used. However, it should be noted that any bias caused by an unobservable parameter cannot be corrected. It should be noted that the structure of noise model and hence tuning of  $\gamma$  and  $K_{integral}$  are important with respect to PI based Kalman filtering. Non-zero off diagonal elements in  $\gamma$  might help in reducing estimator bias when parameters are jointly (and highly) correlated to two or more states. The proportional integral framework may be extended to other Kalman update based estimation algorithms (EKF, UKF).

## 3.9 Point estimate extraction from full state distributions

Estimators provide state estimates at every time instant. The Kalman update based estimators like the EKF or UKF provide point estimates which can then be used by a controller for good control of processes. In the previous section, it was demonstrated that particle filters, provide a full distribution of the posterior states. However, it is important to obtain point estimates from these distributions which need to be passed on to the controller. In most cases, the mean of the distribution is used as the point estimate. The mean however does not represent the expected value of the distribution. Fig. 3.35 indicates how the mode and mean differ in the case of non-Gaussian distributions. In this section, the issue of extracting a point estimate from a full state posterior distribution is addressed.

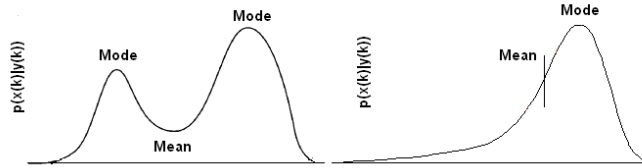


Figure 3.35: Importance of point estimate extraction from non-Gaussian posteriors. Notice that the mode and mean do not match for non-gaussian distributions.

### 3.9.1 Non-stationary growth model

A non-stationary growth model is used to illustrate the importance of full state information, and the extraction of an appropriate point estimate from the full state distribution. This example has been used to show the evolution of non-Gaussian posteriors in many studies such as Gordon et al. (1993) and Chen et al. (2004). The dynamic system consists of one state equation (equation. 3.18) and the measured output is a derivative of the state (equation. 3.19).  $w$  and  $v$  represent the noise statistics.

$$x(k) = 0.5x(k-1) + \frac{25x(k-1)}{(1+x(k-1)^2)} + 8\cos(1.2(k-1)) + w(k) \quad (3.18)$$

$$y(k) = \frac{x(k)^2}{20} + v(k) \quad (3.19)$$

$$w = N(0, 10)$$

$$v = N(0, 1)$$

The estimator tuning parameters were:

Process noise covariance:  $Q = N(0, 10)$

Measurement noise covariance:  $R = N(0, 1)$

Initial covariance matrix:  $P = N(0.1, 1)$

### 3.9.2 Non-Gaussian posteriors

The evolution of non-Gaussian posteriors is represented in Fig. 3.36. As concluded earlier, the EKF is supposed to exhibit poor performance when posteriors are non-Gaussian. Fig. 3.37 confirms the poor performance of the EKF.

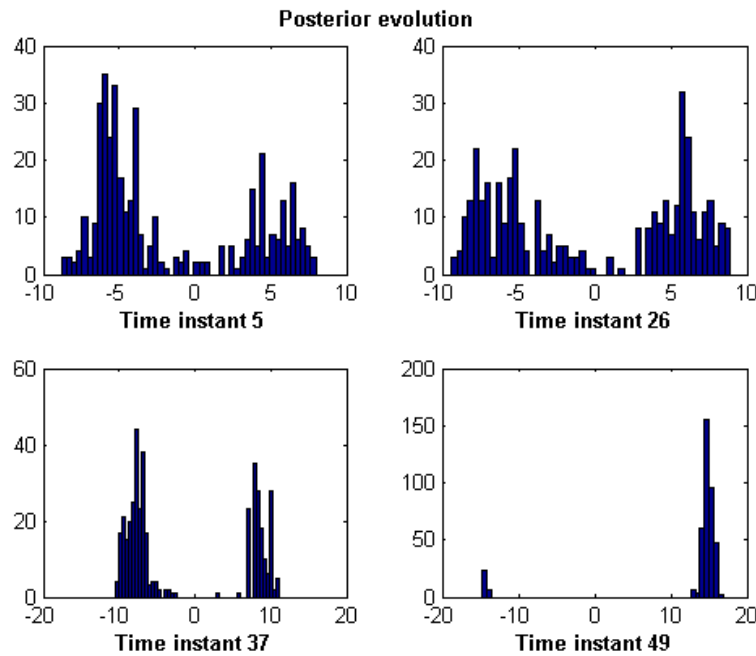


Figure 3.36: Evolution of non-Gaussian posteriors at specific time instants for non-stationary growth model.

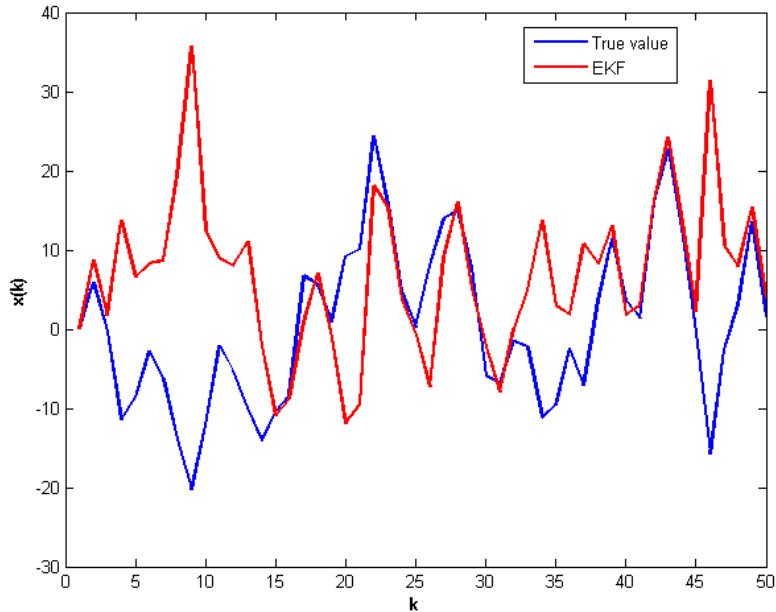


Figure 3.37: Poor performance of EKF for non-stationary growth model.

The best known method to handle multi-modal distributions is to use a particle filter that provides full state information. The superior performance of the particle filter in comparison to the EKF is shown in Fig. 3.38.

It can be seen that at most time instants (fig. 3.38), the particle filter does not represent the true value exactly. Particle filters provide full state information in the form of a posterior distribution. The method to extract a point estimate from this full state distribution for each time instant is an open problem. This is often a problem with particle filters and has been highlighted by several publications such as Rawlings and Bakshi (2006). Most applications of the particle filter use the mean of the full state distribution (as in fig. 3.38). As demonstrated in fig 3.35, the mean is not the correct point estimate. The next section describes the different methods of point estimate extraction from full state distributions.

### 3.9.3 Methods of information extraction

#### Mean

One way is to take the mean of the distribution. However, this yields the true state only for symmetric unimodal distributions where the expected value is equal to both the mean and median.

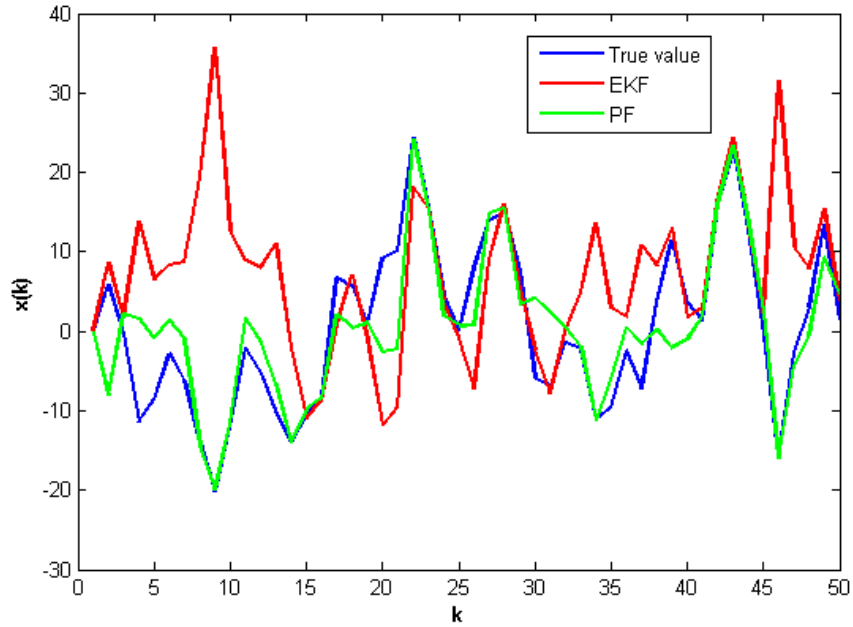


Figure 3.38: Superior performance of PF in comparison to EKF for non-stationary growth model.

### Mode

Another option is to take the mode of the distribution as the point estimate. This may work for skewed distributions, but for multi-modal distributions, it may select the tallest peak, which may still not represent the actual solution. Also, for multivariate systems, the simple mode may have to be selected for each of the states separately. The collection of modes then obtained for each state might not belong to the multivariate distribution. Fig. 3.39 shows the performance of using the mode as the point estimate in a particle filter. Even though this method works well at many time instants compared to the mean (time instant 17), it fails at other instants (time instant 20). The failure is illustrated in fig. 3.40. To understand this failure, one must understand evolution of such a multi-modal distribution. The measurement equation is such that at certain time instants, two roots can exist for a given value of measurement ( $y$ ). For the equation  $y = x * x$  and measurement of  $y = 1$ ,  $x$  can take both values of  $+1$  and  $-1$ . Though the particle filter correctly indicates the two solutions of  $x$  that exist for the measurement  $y$ , the particle filter does not automatically indicate the correct value of  $x$ . In fig. 3.40, if one were to believe the particle filter and choose the mode with highest concentration of the particle cloud,

the estimate would not be correct.

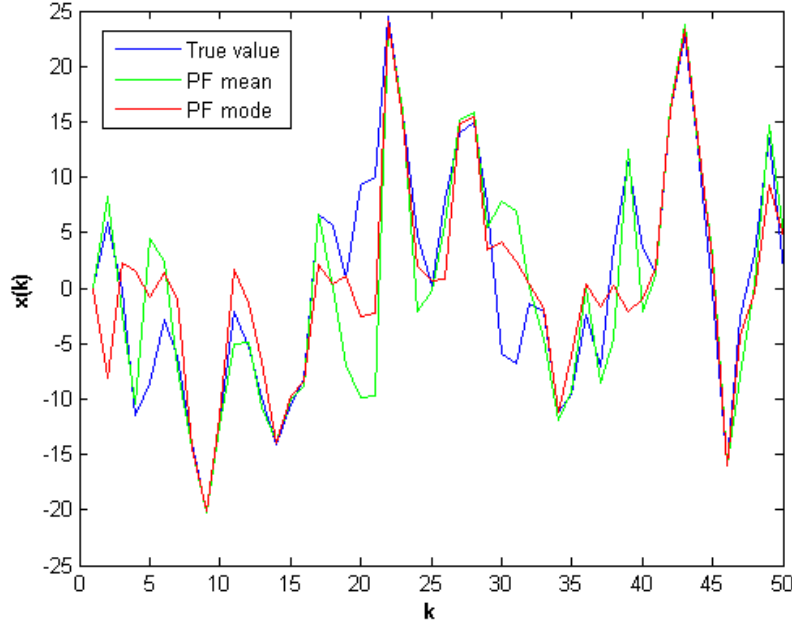


Figure 3.39: PF with mean and mode as point estimates for non-stationary growth model.

### Mode detection using k-means clustering

The proposed method in this section is to identify a point estimate for multimodal distributions using clustering, followed by the application of process knowledge to select a particular cluster and its centroid as the point estimate. k-means is a data classification technique that is used to cluster the particles based on Euclidean distance. In this case, the k-means method is used to extract all possible modes from a non-Gaussian distribution. Initially, we start with a high number of clusters, and the distance between the clusters is compared with that of a threshold value. The threshold can be defined by inverting the measurement equation at each time instant, i.e  $x = \sqrt{(20y - E[v])}$ . If the distance between any two clusters is less than the threshold, then the k-means technique is applied again by reducing the number of clusters. The centroid of each cluster is assumed to be a mode of the posterior distribution. In case that only one cluster occurs, the mode of all the particles is selected as the posterior point estimate.

Fig 3.41 indicates how the modes are captured using k-means clustering.

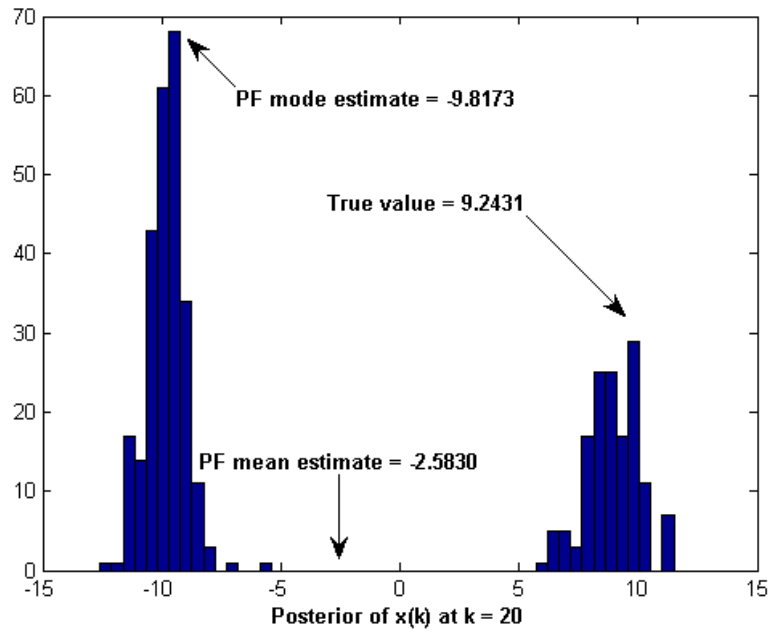


Figure 3.40: Failure in information extraction from full state distribution provided by particle filter.

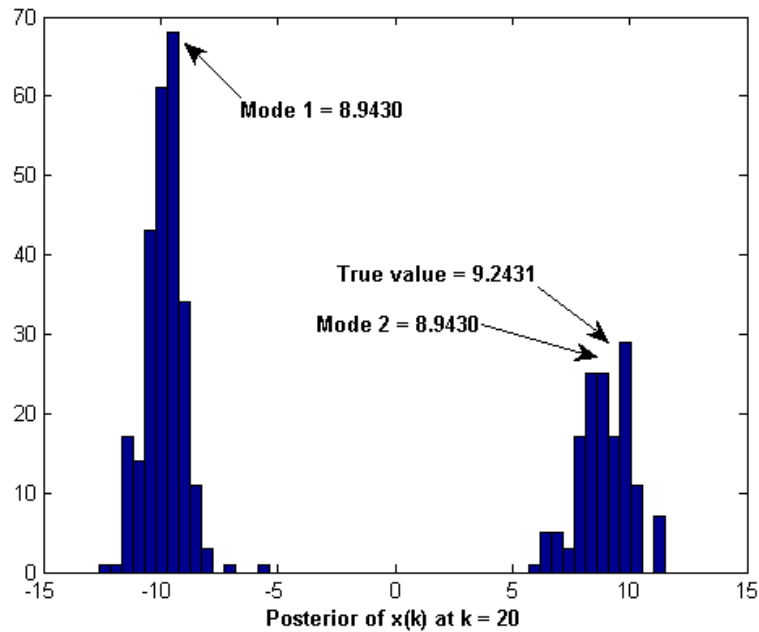


Figure 3.41: Information extraction using k-means clustering from full state distribution provided by particle filter.

The next step is to incorporate process knowledge to select one mode as the point estimate. One way to do so is to use constraints on physical quantities. For example, the height of a tank may never go negative or the temperature of the reactor may not go beyond a certain value, and this can be used to eliminate some modes. In certain cases, however, no previous (process) knowledge of the state is known. In this case, the only way would be to present all possible modes to an operator who can then infer the right mode based on his or her knowledge. Fig. 3.42 indicates how the state is captured at each time instant. At certain time instants (e.g.: 8, 10, 14), a single mode is captured indicating a unimodal distribution (maybe Gaussian or skewed) and at certain instants (e.g.: 3, 13, 26), two modes are captured indicating a multi-modal distribution. In this example it is assumed that a maximum of two modes occur.

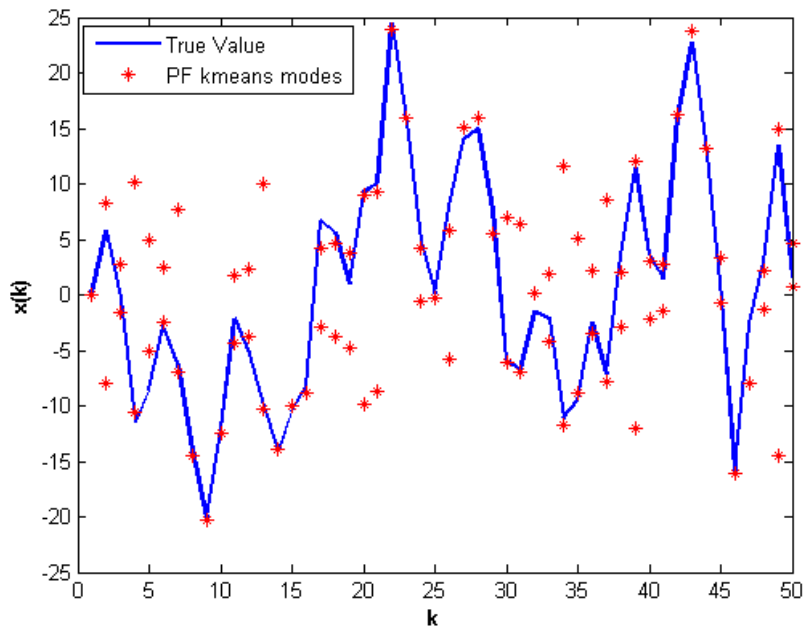


Figure 3.42: 'K-means' clustering from full state distributions provided by particle filter.

### 3.9.4 Summary on point estimate extraction from full state distributions

The non-stationary growth model has been widely used in literature to compare performance of different estimators (Chen et al. (2004), Mukherjee and Sengupta

(2010)). Gordon et al. (1993) introduced the resampling step in particle filters and used this example to compare their results with the extended Kalman filter. In the literature, the mean or the mode has been used as the point estimate and the mean square error has been computed using this point estimate. For the non-stationary growth example, k-means clustering of the posterior distribution (provided by particle filter), solves the state estimation, as one of the modes always lies on the true state at each time instant. It has been shown that the mean square error value is zero when information can be extracted exactly from the full state distribution that is provided by the particle filter. In the case of non-Gaussian posteriors, the Kalman update based filters might choose one of the Gaussian peaks from the many peaks as the true estimate. Particle filters, however, will use the entire non-Gaussian distribution. Using k-means, one could separate the data into peaks and clusters. Once this information is extracted, process knowledge in the form of constraints may be used to eliminate certain modes.

# Chapter 4

## State and parameter estimation of a gas phase polyethylene reactor using particle filters

In the previous chapter, we compared various unconstrained estimators, and highlighted the properties of the particle filter. In this chapter, we explore the application of the particle filter to a realistic large scale chemical process. Many control applications require on-line estimation of states and parameters simultaneously. In a mathematical sense, the nonlinear dynamic system with time varying parameters can be represented by equations. 4.1 and 4.2, where  $\theta(k)$  represents the time varying parameters.

$$x(k) = F(x(k-1), u(k), \Theta(k)) + w(k) \quad (4.1)$$

$$y(k) = H(x(k), \Theta(k)) + v(k) \quad (4.2)$$

In estimation, the parameters to be estimated are treated as augmented states with their dynamics assumed to be random walk models ( $d(\theta)/dt = 0$ ). Thus, the new state is a combination of system states and parameters ( $x^* = [\frac{x}{\theta}]$ ).

This chapter is concerned with the simultaneous state and parameter estimation of a high dimensional gas phase polyethylene reactor. Two main concepts have been addressed:

- (1) Application of estimation techniques (PF, UKF, UPF) to the gas phase polyethylene fluidized bed reactor process (FBR)
- (2) Control of high dimensional reactors with reduced order models using particle filters

Section 4.1 contains a survey of the literature on modeling and control of the gas phase process. Section 4.2 provides a description of the process along with the reactor model and the estimation framework. Application of particle filters to this system is analyzed in section 4.3. Section 4.4 introduces the unscented particle filter (UPF) and the analysis of its application to the gas phase FBR.

## 4.1 Literature review

The need for monitoring of processes has led to the development of process models to represent complex process dynamics. The UNIPOL process (gas phase FBR technology licensed by Univation Technologies) is a very complicated process to control owing to its complex reaction mechanism with multiple catalyst sites and reactor instability. For the gas phase FBR process, good process models are required to monitor process variables (such as gas phase concentrations), polymer properties (such melt index and polymer density), molecular weight distributions and particle size distributions to avoid segregation of polymer particles. Models are also needed to build effective control strategies, and develop grade transition strategies to optimize consumption of resources and economic benefits.

In one of the first attempts to model the gas phase polyethylene process for quantitative understanding of its dynamic behavior and knowledge for process control, Choi and Ray (1985) present a combination of mass transfer mechanisms, flow characteristics and kinetic polymerization models. Later, Carvalho et al. (1989) presented a complex kinetic model with pseudo kinetic rates accounting for the large molecular weight distributions using multiple catalyst site models to describe the kinetic mechanism. In one of the most cited papers in modeling of industrial gas phase reactors, McAuley et al. (1990) developed a model that could predict copolymer composition and molecular weight properties in an industrial-scale fluidized-bed reactor under good temperature regulation. The model was an attempt to provide a simulation platform to test on-line quality control schemes and predict the effects of grade transition policies on molecular weight and compositional distributions. A collection of the early work in the field with a comparison of different models developed in the early 1990's is documented by Hatzantonis et al. (2000).

Most of the early work aimed at developing homogenous reactor models (constant temperature and composition through out the reactor) which could provide molecular weight distributions. Successful homogenous reactor modeling lead to increased research in developing models that could account for heterogeneity and

provide distributions of molecular weights and particle sizes. In one of the early works, Hutchinson et al. (1992) developed a model to study particle growth. In an attempt to model the particle related (growth, attrition, agglomeration and elutriation) phenomena in a fluidized bed reactor, Hatzantonis et al. (1998) presented a population balance model. Yiannoulakis et al. (2001) provided a review of the literature involving estimation of particle size distributions (PSD) and the effect of many reactor variables on the PSD. Kanellopoulos et al. (2004) developed a random pore polymeric flow model to analyze the growth of a single particle in a FBR.

Taking into account heterogeneity in the reactor, Fernandes and Lona (2001) developed a model taking into account interactions between three different phases. In more recent work, Dompazis et al. (2005) developed a multiscale model that incorporates a combination of molecular level (kinetic mechanism) and reactor level (PSD) phenomenon to predict both the MWD and the PSD. In more recent efforts on modeling of gas phase polymerization reactors, Dompazis et al. (2008) have presented a complex multiscale multiphase and multicompartment dynamic model that takes into account different phases, mechanisms and varying property gradients (such as temperature variations along the height of the reactor).

With respect to control and grade transition, McAuley and MacGregor (1991) first developed inferential schemes to predict polymer properties (melt index and polymer density) online. It must be noted that these polymer properties cannot be directly measured online. Later, McAuley and MacGregor (1992) used these inference schemes and designed optimal grade transition strategies. In this contribution, it was highlighted that grade transitions should not be carried out without feedback control. Disturbances and model mismatch could lead to transition trajectories that deviate from optimal trajectories. In a separate contribution, McAuley and MacGregor (1993) used an EKF based estimation scheme to estimate disturbances and reduce plant-model mismatch and incorporate nonlinear feedback control. Hydrogen and butene flow rates were then manipulated to design optimal grade transition strategies. More recently, Chatzidoukasa et al. (2003) provided alternate methods to optimal grade transition by designing an objective function that took into account controller pairings in the optimality criteria. Grade transition, nonlinear control, study of development and effect of catalysts on MWD and PSD, and study of unstable operating conditions are still open areas of research with respect to gas-phase polymerization.

In this work, we use a model adapted from McAuley et al. (1990) and McAuley

(1991), and use it as a basis for estimation studies using particle filters. A description of the model follows:

## 4.2 Gas phase polyethylene reactor

### 4.2.1 Process description

The gas-phase solid catalyzed polymerization process has long been recognized as being very efficient for producing polyolefins. Fig. 4.1 provides a schematic of the polymerization process. In the fluidized bed reactor (FBR), catalyst particles are continuously fed into the reactor, and they react with the incoming fluidizing reaction medium to produce a broad distribution of polymer particles. The gas mixture in the case of polyethylene production contains ethylene (monomer), butene (comonomer), hydrogen and some inert gasses (e.g.: nitrogen). The catalyst usually requires an initiator in the form of aluminium alkyl. Polymer is removed from the bottom of the reactor in the form of pellets. Industrial polyolefin FBR, typically operate at temperatures of 75-110<sup>0</sup>C and pressures of 20-40 bar (Xie et al. (1994)). The recycle stream consists of a heat exchanger to continuously remove the heat generated by exothermic reactions. A small amount of the recycle stream is removed in the form of bleed flow rate. This helps to regulate pressure and composition in the reactor and recycle stream. The recycle stream consists of a large volume of the gases. This accounts for the fluidizing mechanism wherein the catalyst particles are kept suspended by the incoming recycle stream from the bottom of the fluidized bed. The reactor system usually consists of three basic regulatory controllers. The temperature is controlled using the coolant flow in the heat exchanger. Pressure is controlled using the flow of inert gasses in the reactor. The polymer outflow is used to regulate the level of components in the fluidized bed. Shenoy et al. (2008) provide a review of the process along with some basic regulatory control strategies.

### 4.2.2 Reactor modeling

The reactor model has been adapted from McAuley (1991). Simulating the reactor involves kinetic expressions, pseudo kinetic expressions, mass and energy balance equations, and PID controller equations. The following section documents the kinetic and reactor models used in the case study presented in this chapter.

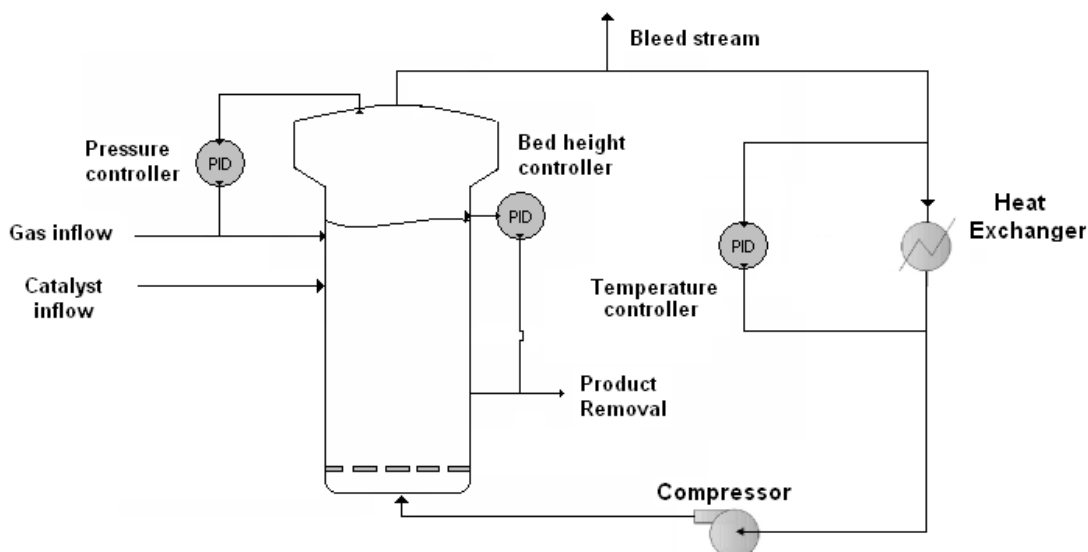


Figure 4.1: Schematic of a gas phase fluidized bed reactor for polyethylene production

## Kinetic model

The kinetic model consists of consumption rates of species, which are functions of kinetic parameters, and mass/mole balance equations for kinetic species (e.g.: active catalyst sites). The type of reactions that take place in the reactor include:

### (1) Formation and initiation of active sites

Potential active sites undergo a formation reaction with the cocatalyst (aluminium alkyl) to give active catalyst which is now ready to undergo reaction with other species in the reactor. The active sites undergo an initiation reaction when they react with the monomer.

### (2) Propagation reactions

Living polymer chains refer to catalyst with chains of monomers and comonomers attached that are ready to undergo further reaction. Here, the live polymer chains grow by the addition of a monomer or a comonomer. It is important to note the kinetic rates for the propagation differ with - the type of molecule (monomer or comonomer) joining the living polymer chain, the end molecule in the living polymer chain and the type of catalyst site to which the living polymer chain is bound. This reaction gives rise to 8 different kinetic expressions for a 2 site reaction with a single monomer and comonomer.

### (3) Chain transfer reactions

Live polymer chains undergo chain transfer reactions to give dead polymer chains. Dead polymer chains do not undergo any further reactions while the liberated catalyst site might undergo further reactions. Chain transfer agents include the monomer itself, hydrogen and the cocatalyst. Spontaneous chain transfer can also take place where in no chain transfer agent is required.

### (4) Additional reactions

In addition to the above reactions, side deactivation reactions due to presence of poisons such as carbon monoxide or impurities can take place.

In this model, it has been assumed that the catalyst has two different types of active sites. The two active sites differ from each other on the basis that their reaction constants are different. For example, the first type of active site may undergo formation reactions more readily than the second active site. This gives rise to pseudo kinetic expressions, i.e., if one were to represent the rate of propagation, the difference in propagation rate constant values of the two sites must be taken into account. Hence, a pseudo kinetic expression that combines both the propagation rates needs to be defined. This has to be done for each of the kinetic expressions listed above. Pseudo kinetic expressions can be obtained from McAuley (1991) and Carvalho et al. (1989). Usually, the kinetics of different active sites are combined using two terms:

(1) Mole fraction of monomer of type  $i = \frac{[M_i]}{[M_1]+[M_2]}$ .  $[M_1]$  and  $[M_2]$  refer to the concentration of monomer and comonomer respectively.

(2)  $\Phi_i(j)$ , the fraction of active sites of type  $j$  having terminal monomer  $M_i$ .

Using the above two variables, pseudo kinetic expressions for formation, initiation, propagation and chain transfer reactions are obtained.

Following the rate expressions, mass balance equations (equation. 4.3) are used to represent the dynamic nature of the concentration of kinetic species in the reactor. Kinetic species include potential active sites, initiation sites, sites with a single monomer attached to them, and finally polymer moments for live and dead polymer chains. In the reactor, polymer chains (both dead and alive) are of varying length based on the number of monomers and comonomers that they are made up off. Thus, polymer chains in the reactor can be represented as distributions of two forms - chain length distributions and molecular weight distributions. Representation of mass balance equations for polymer chains is done in the form of moments of

these distributions (usually the zeroth, first and second moments). Thus, mass balance expressions for 3 moments for live and 3 moments for dead polymer moments can be written.

$$Accumulation = Inflow + Generation - Consumption - Outflow \quad (4.3)$$

Temperature effects are included in the kinetic rate constants in the form of equation. 4.4.  $k(T)$  is the kinetic constant as a function of temperature,  $A$  is the Arrhenius constant,  $E$  the activation energy,  $T$  the temperature and  $R$  the universal gas constant.

$$k(T) = A \exp\left(\frac{-E}{RT}\right) \quad (4.4)$$

The concentration of gaseous entities (monomer, comonomer, hydrogen, inert) is different from their concentrations in the amorphous phase (the phase in which kinetic reactions take place). Henry's constant ( $K_p$ ) is used to account for difference in gas phase and amorphous phase concentrations (as shown in eq. 4.5)

$$[M_i]_{polymer} = K_p(M_i, T)[M_i]_{gas} \quad (4.5)$$

The kinetic model is simplified by assuming that some of the intermediate species such as active sites and sites with a single monomer attached have fast dynamics. Thus the mass balance expressions for these species reduce to algebraic expressions. Molecular weight properties (weight average molecule weight, number average molecular weight and polydispersity index) are used to describe the molecular weight distributions of the polymer product. The values for these properties can be calculated using the live and dead polymer moments. To calculate the melt index and polymer density, inference schemes are developed.

Given the concentration of reactants in the gas phase and the reactor temperature, the kinetic model can predict the polymer production rate and polymer quality.

## Reactor model

If a model of the process needs to be used for controller design, development and testing, dynamic mass balances of the reactants are required to predict the gas compositions in the reactor. This is due to the fact that the reactor feeds/inputs rather than gas phase concentrations are the manipulated variables. Thus, the model must predict the effect of feed flow changes on reactor operation. For this purpose a model of the reactor is combined with the kinetic model. Dynamic mass balances

of the form represented by eq. 4.3 need to be written for inert, hydrogen, monomer, comonomer, cocatalyst and impurity, respectively.

A dynamic energy balance for the species accounts for the temperature in the reactor. It is assumed that the turbulent mixing in the FBR causes the temperature throughout the bed to be uniform. The energy balance equation for the reactor is represented by eq. 4.6.

$$(M_w C_{pw} + V_p \rho C_{ppol}) \frac{dT}{dt} = H_f + H_{gi} - H_{g0} - H_r - R_v \rho C_{ppol} \quad (4.6)$$

$M_w$  and  $C_{pw}$  are the mass and heat capacity of the reactor wall respectively.  $C_{ppol}$ ,  $V_p$  and  $\rho$  are the heat capacity, volume and density of the polymer in the reactor.  $H_f$  and  $H_{gi}$  are inflow enthalpies of feed inlet and recycle gas respectively.  $H_{g0}$  and  $R_v \rho C_{ppol}$  represent the enthalpy outflows due to recycle gas outflow and polymer product outflow.  $-H_r$  accounts for heat liberated by the polymerization reactions. Energy balance equations are also required to represent the energy regulation by the heat exchanger on the recycle stream. The reactor model also consists of the regulatory PID controller equations. An algebraic expression is used to calculate the pressure in the reactor, and a controller equation regulates the pressure using the inert inflow into the reactor. Temperature control is achieved by regulating the inflow of coolant to the heat exchanger. Bed level control is achieved using the product discharge line at the bottom of the reactor. To illustrate the controller equation, the bed level control equations are represented in eq. 4.7 as:  $b_w$  is the bed level,  $b_{wsp}$  the bed level set point and  $\tau_{bw}$  is the time constant of the closed loop response (chosen to 1 here).

$$\frac{db_w}{dt} = \frac{b_{wsp} - b_w}{\tau_{bw}} \quad (4.7)$$

Thus, a set of 35 nonlinear differential equations (35 state system) combined with numerous algebraic rate expressions and fast dynamics mass and energy balances are used to represent the dynamic behavior of the gas phase polymerization process. This model can be used to study the effect of temperature on reactor conditions, design of controllers, grade transition strategies and so on.

### 4.2.3 Estimation framework

This section discusses the estimation framework for the polyethylene reactor. Using sensitivity analysis, the variables that most affect reactor properties have been identified. These variables need to be modified as manipulated variables for nonlinear product property control and grade transition. Using the identified sensitive

variables, reduced order models are built to aid in reactor control. In this case study, the reduced order model has been adapted from McAuley (1991). The reduced order model used in this case is represented by equations. 4.8 to 4.11. The model is capable of predicting the effect of hydrogen and butene feed rates on melt index and density. It also accounts for the effect of reactor temperature, vent flow rate, catalyst feed rate, and bed level on product properties; these variables change quickly during grade transition.

$$V_g \frac{d[H_2]}{dt} = \frac{F_H}{mw(H)} - khY[H_2] - \frac{[H_2]b_T}{[C_T]} - gl[H_2] \quad (4.8)$$

$$(V_g + V_s) \frac{d[M_2]}{dt} = \frac{F_{M_2}}{mw(M_2)} - kp_2Y[M_2] - \frac{[M_2]b_T}{[C_T]} - S(M_2)[M_2]O_p \quad (4.9)$$

$$\frac{dY}{dt} = F_{cat}a_{cat} - \frac{YO_p}{B_w} - kdY \quad (4.10)$$

$$\frac{dB_w}{dt} = Ykp_1[M_1]mw(M_1) + kp_2[M_2]mw(M_2) - O_p \quad (4.11)$$

In the reduced order model,  $[H_2]$ ,  $[M_2]$ ,  $[M_1]$  represent the concentrations of hydrogen, comonomer and monomer, respectively.  $F_x$  represents the inflow rate of  $x$ .  $V_g$  is the volume of the gas in reactor and can be calculated from known and estimated quantities as  $V_{Total} - \frac{B_w}{\rho_c}$ .  $kh$ ,  $kp_1$  and  $kp_2$  are the respective pseudo-rate constants for consumption of hydrogen, ethylene and butene, and  $kd$  is the deactivation constant.  $Y$  is the total number of moles of active catalyst in the reactor.  $b_T$  is the total gas bleed rate and  $C_t$  is the total gas phase concentration.  $V_s$  is the equivalent gas volume of butene dissolved in the polymer bed and can be calculated from known quantities,  $S$  is the solubility coefficient for butene sorption.  $O_p$  is the outflow rate of polymer from the reactor and  $a_{cat}$  is the number of moles of active sites per unit mass of catalyst in the catalyst feed stream.

Estimation schemes are used to filter the disturbances and reduce the plant model mismatch by incorporating measurements in the reduced order model. Moreover, the nonlinear controller uses values of states and parameters that are estimated by the estimation scheme. Fig. 4.2 describes the estimation schematic under consideration. The estimated states are  $[H_2]$ ,  $[M_2]$ ,  $Y$  and  $B_w$ . Parameters estimated include  $kp_2$ ,  $gl$ ,  $kd$  and  $O_p$ . The measurements used from the plant are shown in the schematic. Under this scheme, the system is full state observable (McAuley (1991)). For this study, the plant is represented by simulation of the 35 state higher dimensional

model. This kind of a high plant - low model order representation brings in plant model mismatch, specifically structural as well as parametric mismatch. Hence, an estimator is a must in order to incorporate measurement feedback into the dynamic model. It is important to note that there is structured plant-model mismatch, and some of the parameters represented by the lower order model may not correspond to parameters in the higher dimensional model. For example, the termination rate constant in the low-dimension model does not represent any termination constant of the higher dimensional model.

The model used by the estimation scheme is given by :

$$\begin{pmatrix} \dot{x} \\ \dot{\Theta} \end{pmatrix} = \begin{pmatrix} f(x, \Theta, u) \\ 0 \end{pmatrix}$$

, where  $x^T = \{[H_2] [M_2] Y B_w\}$  and  $\Theta^T = \{kp2 gl kd O_p\}$ .

The measurement equation is given by  $y = \begin{pmatrix} [H_2] \\ [M_2] \\ P_R \\ B_w \end{pmatrix} = \begin{pmatrix} [H_2] \\ [M_2] \\ Y(kp1[M_1]mw_1 + kp2[M_2]mw_2) \\ B_w \end{pmatrix}$

Apart from the above measurement matrix, other raw measurements from the large dimensional plant are used in the estimation model (such as pressure, temperature,  $[M_1]$ , etc).

The tuning parameters include:

Measurement noise covariance :  $R = diag[1e-8, 1e-8, 1e-4, 0.04]$

Process noise covariance :  $Q = diag[1e-10, 2.5e-7, 1e-2, 0.25, 0.01, 1e-4, 1e-12, 9]$

State covariance :  $P = diag[1e-4, 1e-4, 1e-2, 25, 1, 4, 1e-6, 2500]$

The melt index (MI) and polymer density ( $\rho$ ) can be inferred from equations. 4.12 and 4.13.  $k_0, k_1, k_3, k_7, p_0, p_1, p_2$  and  $p_4$  are constants that are updated at irregular intervals by a multirate estimator when lab readings of MI and polymer density become available.  $T_0$  is the reference temperature , while  $T$  is the temperature measured in the reactor. It is important to note that these soft sensing inference schemes provide estimates of melt index and polymer density at each sampling instant. The only other way to measure these polymer properties is through off-line laboratory measurements, which have significant delay and cannot be obtained at every instant

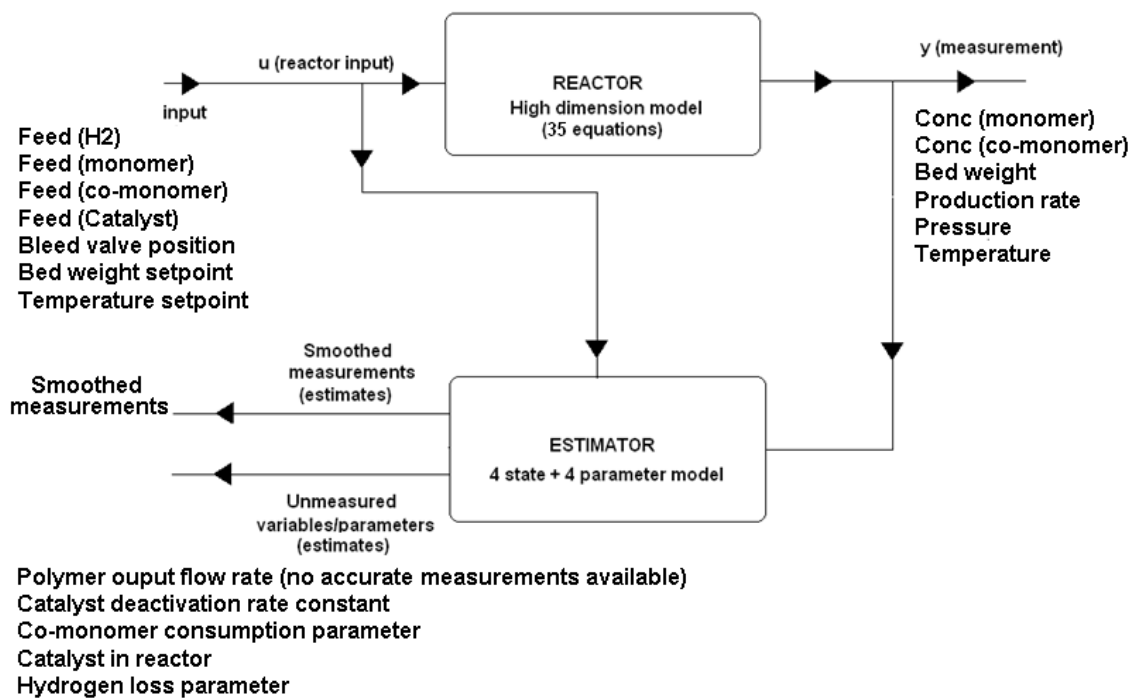


Figure 4.2: Estimation framework for the gas phase fluidized bed reactor for polyethylene production

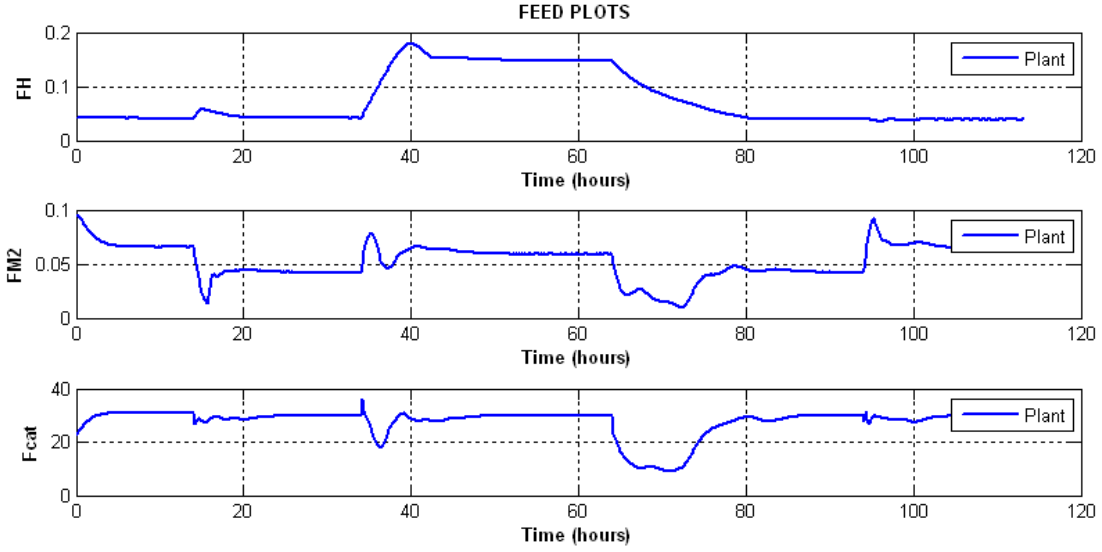


Figure 4.3: Plot of inlet feeds for gas phase FBR for polyethylene production (plots have been scaled due to the proprietary nature of the data)

of time.

$$\ln(MI) = k_7 \left( \frac{1}{T} - \frac{1}{T_0} \right) + 3.5 \ln \left( k_0 + k_1 \frac{[M_2]}{[M_1]} + k_3 \frac{[H_2]}{[M_1]} \right) \quad (4.12)$$

$$\rho = p_0 + p_1 \ln(MI) - \left\{ p_2 \frac{[M_2]}{[M_1]} \right\}^{p_4} \quad (4.13)$$

Fig. 4.3 represents the manipulation of some of the input variables for the case studies below.

### 4.3 Application of particle filters

In the earlier work , McAuley and MacGregor (1993) used two EKF's to update the MI and polymer density inference schemes and eliminate disturbances and reduce plant-model mismatch in the reduced order model. According to our studies in the previous chapter, an EKF might not be the right choice of estimator owing to the linearization and approximation errors as well as its inability to handle non-gaussian disturbances. A particle filter on the other hand is able to handle non-Gaussian distributions, and this motivates the use of a particle filter. In this section, we analyze the results of applying a particle filter with the lower dimensional model.

The tuning parameters, estimation framework and input sequences for the application of the PF were provided in the previous section. Figs. 4.4 to 4.7 represent the

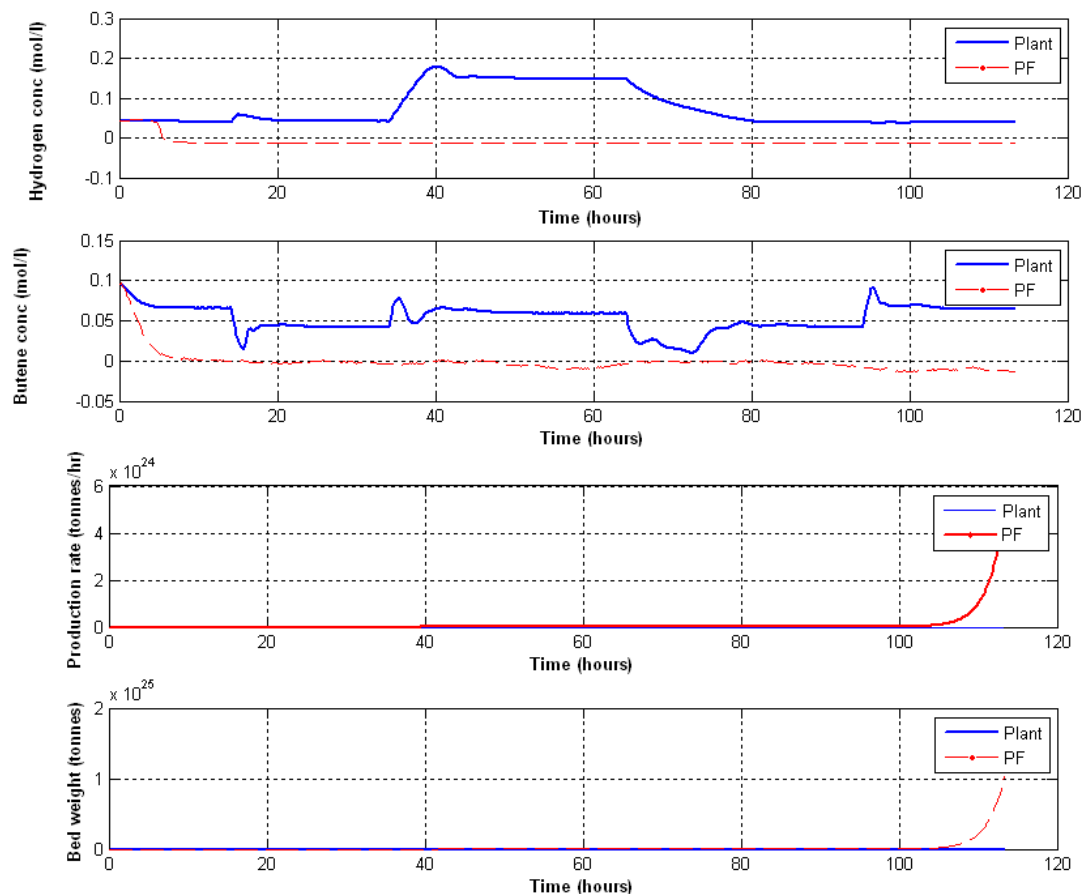


Figure 4.4: Measurement smoothing using particle filters for gas phase FBR for polyethylene production (plots have been scaled due to the proprietary nature of the data)

plots for the application of the generic (SIR) PF to this system. It is seen that the PF tracks the true state up to a certain time instant, after which it fails to estimate the states and parameters. An investigation into the cause of this behavior leads to the fact that the weights of all particles tends to zero after a certain time instant. The reason for this is that the predicted states (particles) lie near the tail of the likelihood or far away from the likelihood (no overlap). In this case the weights of the particles would initially be very low and finally decay to zero. Thus, none of the particles would lie in the region of the true state. Fig. 4.8 highlights this problem.

There are two solutions to this problem:

- (1) To give a very large (overestimated) estimate of measurement noise covariance.

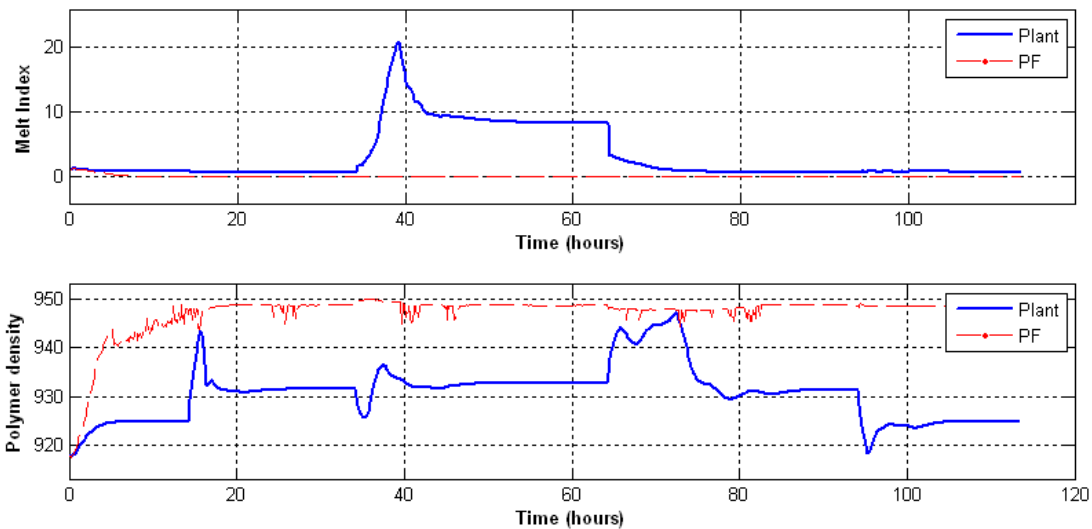


Figure 4.5: Estimation of polymer product properties using particle filters for gas phase FBR for polyethylene production (plots have been scaled due to the proprietary nature of the data)

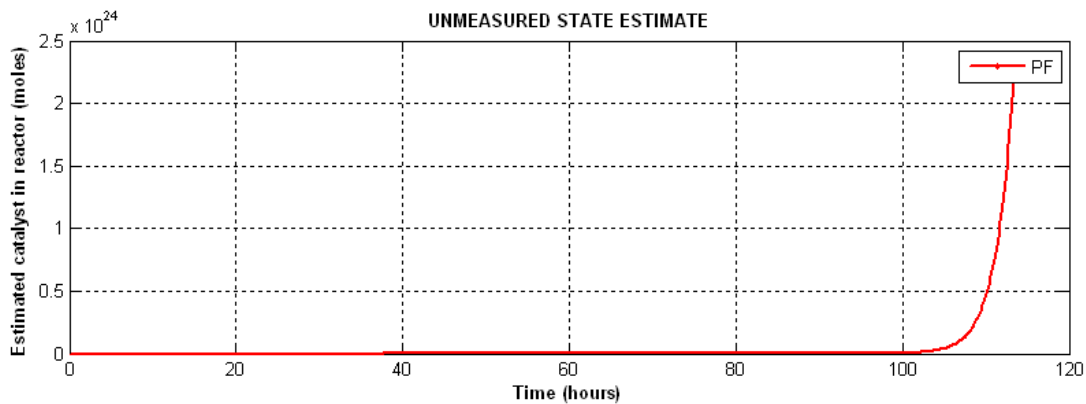


Figure 4.6: Estimation of unmeasured state using particle filters for gas phase FBR for polyethylene production (plots have been scaled due to the proprietary nature of the data)

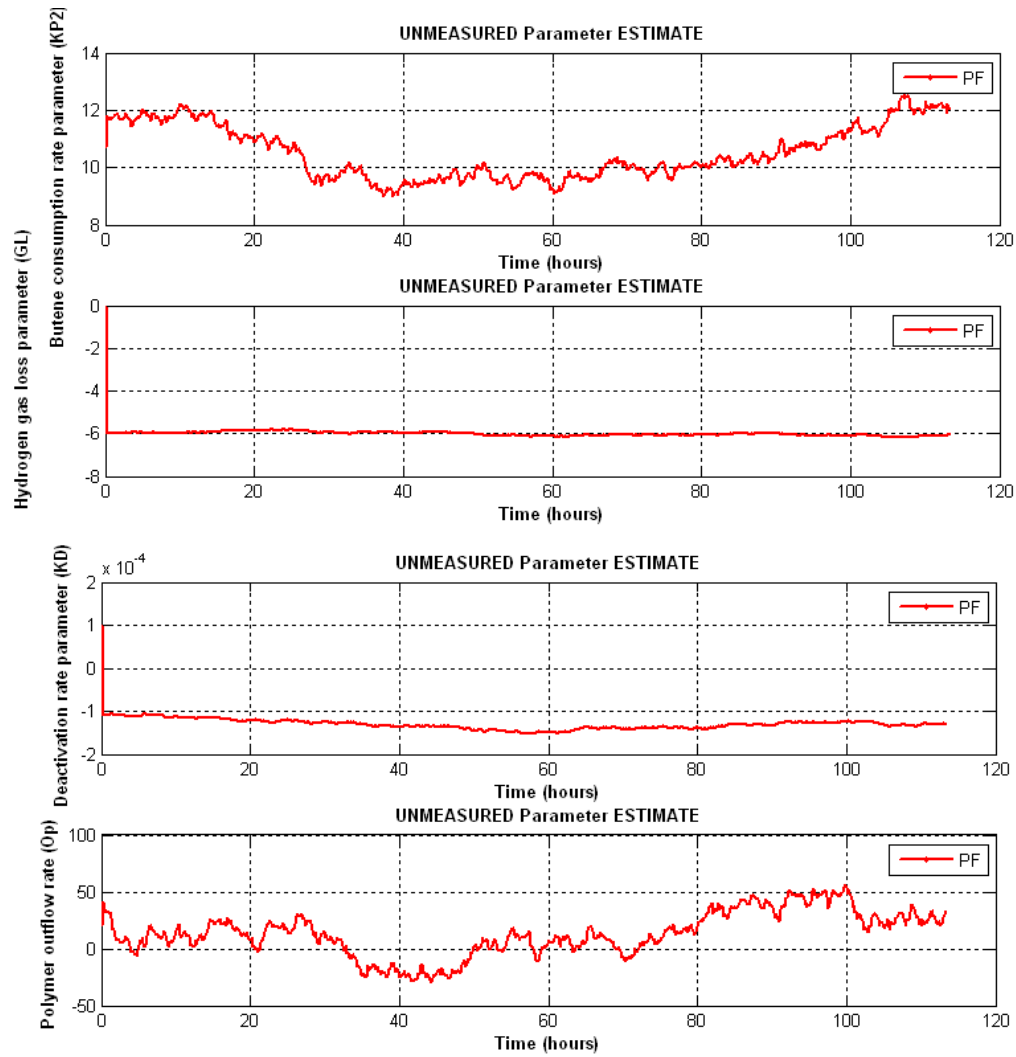


Figure 4.7: Parameter estimation using particle filters for gas phase FBR for polyethylene production (plots have been scaled due to the proprietary nature of the data)

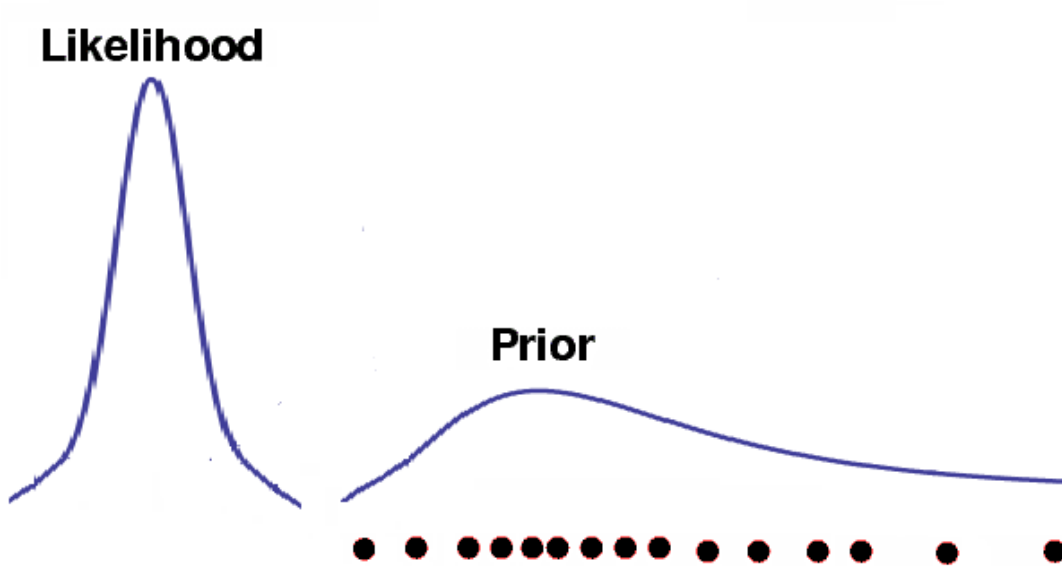
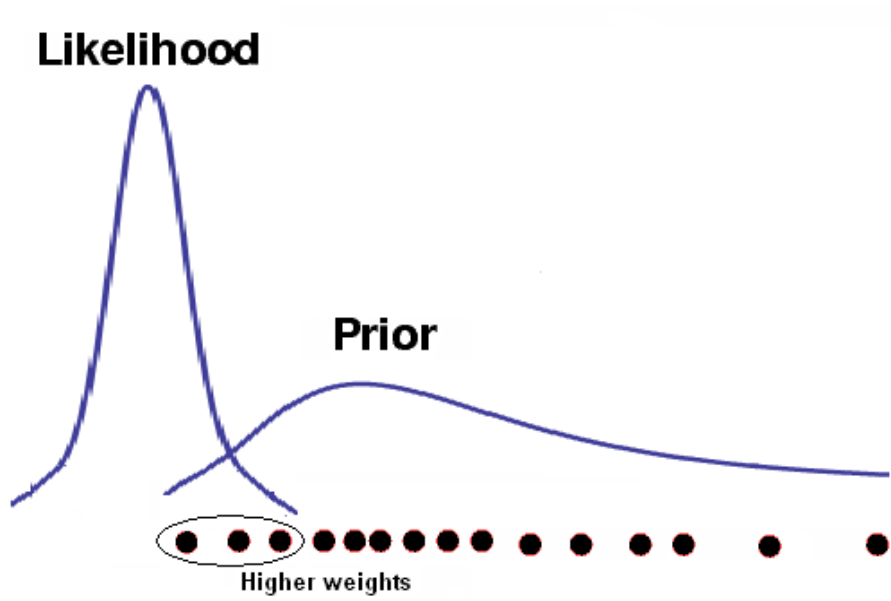


Figure 4.8: Problem of particle degeneracy due to overlap of likelihood and prior near tail of likelihood or no overlap at all. (idea for figures adapted from der Merwe et al. (2000))

This would make the likelihood spread to be very large (large variance in likelihood), and hence the state estimates would lie within the likelihood region. However, a trial of this method on this system leads to the finding that a very large covariance (of the order  $10^{10}$  times the true measurement covariance) is required for successful estimation using a generic PF. Such a value of measurement noise covariance is not physically realizable. Moreover, owing to the large spread of the measurement likelihood, a large number of particles are required so as to avoid degeneracy of particles (i.e., particles with zero weights). This is computationally cumbersome.

(2) The other method is to introduce feedback into the one step ahead prediction of particle locations (fig. 4.9). This is done by effective generation of the proposal distribution, using a bootstrap method. For example, using a Kalman update based filter to generate the proposal moves the particles towards regions of high likelihood. This brings in feedback correction into the proposal, thus helping the stability of the particle filter. Such a formulation, using UKF to generate proposal is called the unscented particle filter (UPF) and has been tested on this system, as described in the next section.

## 4.4 Unscented particle filters for high plant-model mismatch

In this section, the problem of particle weights going to zero in a generic particle filter under the large-plant lower dimensional model case is resolved. A Kalman update based filter, in this case the UKF is applied to this system. the estimation problem formulation and tuning parameters are same as that used in the case study provided in the previous section. Fig. 4.10 is the plot of the polymer quality variables (melt index and polymer density) for this case study. The UKF is able to track the polymer quality variables accurately. This establishes that the stability of a Kalman update based filter, compared to the PF, for such formulations of plant-model mismatch. Thus, in case of structural mismatch between plant and model, a Kalman update based estimator is the appropriate choice of estimator. However, as highlighted by Ning and Fang (2008), if non-Gaussian noise sequences are present, the choice of estimator has to be a sequential Monte Carlo estimator that deals with estimation of full state distributions, without making assumptions for variables to be Gaussian. Hence, the PF with a Kalman update based filter to generate the

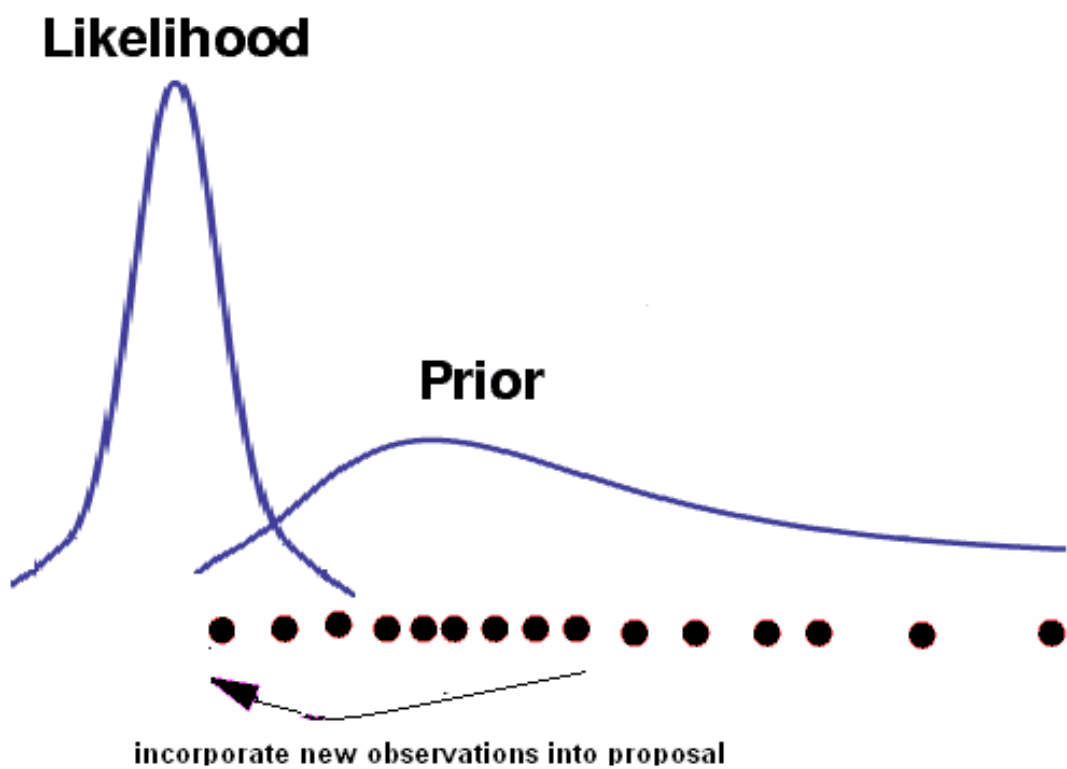


Figure 4.9: Incorporating feedback into prior particles using Kalman update based filters for proposal generation. (figure adapted from der Merwe et al. (2000))

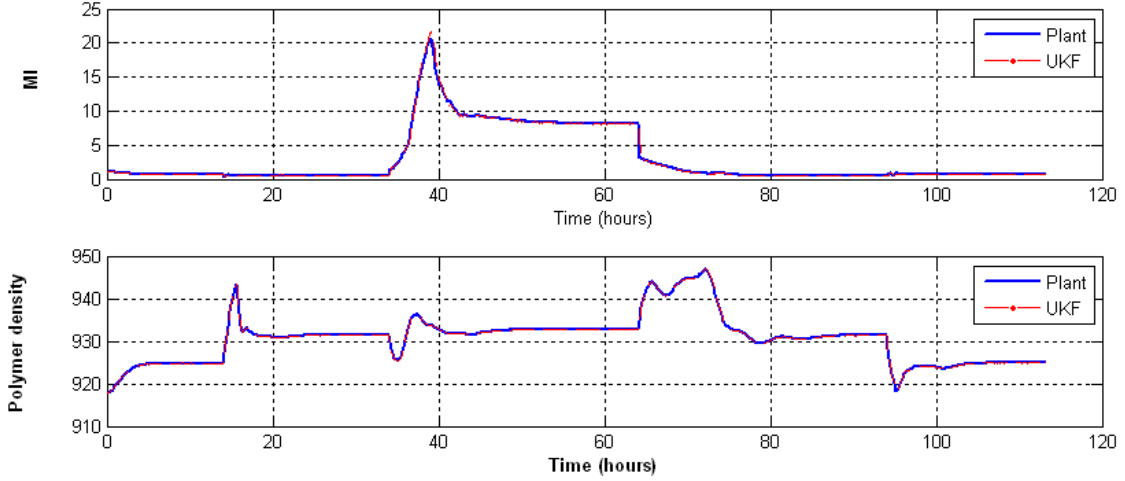


Figure 4.10: Estimation of polymer product properties using unscented Kalman filters for gas phase FBR for polyethylene production (plots have been scaled due to the proprietary nature of the data)

proposal needs to be used. The UPF would be a very powerful tool, as it provides robustness to the PF. der Merwe et al. (2000) , Rui and Chen (2001), Daum (2005), Prakash et al. (2008) have all highlighted the importance of proposal generation. The algorithm for the UPF has been highlighted below.

In the generic formulation of the PF using Bayes rule, the weights of the particles are

$$w_k^i \propto w_{k-1} p(y_k | x_k) p(x_k | x_{k-1}) q(x_k | X_{k-1}, Y_k)$$

In the SIR PF, which is the easiest form of the particle filter in terms of implementation, the proposal distribution ( $q(x_k | X_{k-1}, Y_k)$ ) was chosen to be the transition prior ( $p(x_k | x_{k-1})$ ).

In the UPF, the proposal is generated by a UKF, i.e.,  $q(x_k | X_{k-1}, Y_k) = p(x_k | X_{k-1}, Y_k)$  where  $p(x_k | X_{k-1}, Y_k)$  is the posterior distribution generated by the UKF. The UKF being a Kalman update based filter, represents the posterior probability distribution ( $p(x_k | X_{k-1}, Y_k)$ ) in the form of a Gaussian distribution represented by its means and covariance ( $N(\hat{x}_k, cov[x_k])$ ).

Thus,  $q(x_k | X_{k-1}, Y_k) = N(\hat{x}_k, cov[x_k])$ .

The use of UKF to generate proposal in PF provides measurement feedback to the importance particles, as measurements are used in the UKF algorithm. Thus, particles remain in regions of high measurement likelihood.

#### 4.4.1 Analysis of application of UPF to gas phase polyethylene FBR

The Unscented particle filter was applied to the polyethylene FBR. The formulation of the problem is similar to the high dimensional plant and low dimensional model used in the previous case study of the particle filter. The tuning parameters also remain the same. Fig. 4.11 to 4.14 shows plots of the successful implementation of the UPF for this system with this type of plant-model mismatch (high dimensional plant represented by a low dimension model for estimation purposes). It is seen that the use of the UKF to generate the proposal distribution, provides feedback to the prior particles. Thus, prior particles always remain within the region of high measurement likelihood. As shown in the previous case study, a Kalman update based estimator is stable under such formulations of plant-model mismatch. Thus, estimation in case of non-Gaussian distributions under such problem formulations will require a Kalman update based estimator to be coupled with a PF to provide stability to the PF algorithm. It is important to note that, such a formulation is true for most cases of online implementation where the order of the true process is unknown. Even though a Gaussian distribution is used in the proposal, it serves to bring the particles closer to the true value of the state, thus providing a tighter region for the spread of the particles. This improves the performance of the PF.

### 4.5 Concluding remarks

Through a case study on a realistic system, we have shown that with high plant model mismatch it is important to incorporate feedback in the proposal distribution. It is important to note that high-plant model mismatch is inevitable in real time implementation of estimation algorithms on large-scale chemical processes. It has been shown that Kalman update based filters are more stable than generic formulations of the particle filter (e.g.: SIR-PF), which use the transition prior as the proposal distribution. In order to address the problem of non-Gaussian distributions in such cases of high plant-model mismatch, particle filters which use Kalman update based filters to generate proposal distributions are required. The UPF is more robust to plant-model mismatch than the PF, and it retains its ability to estimate non-Gaussian distributions.

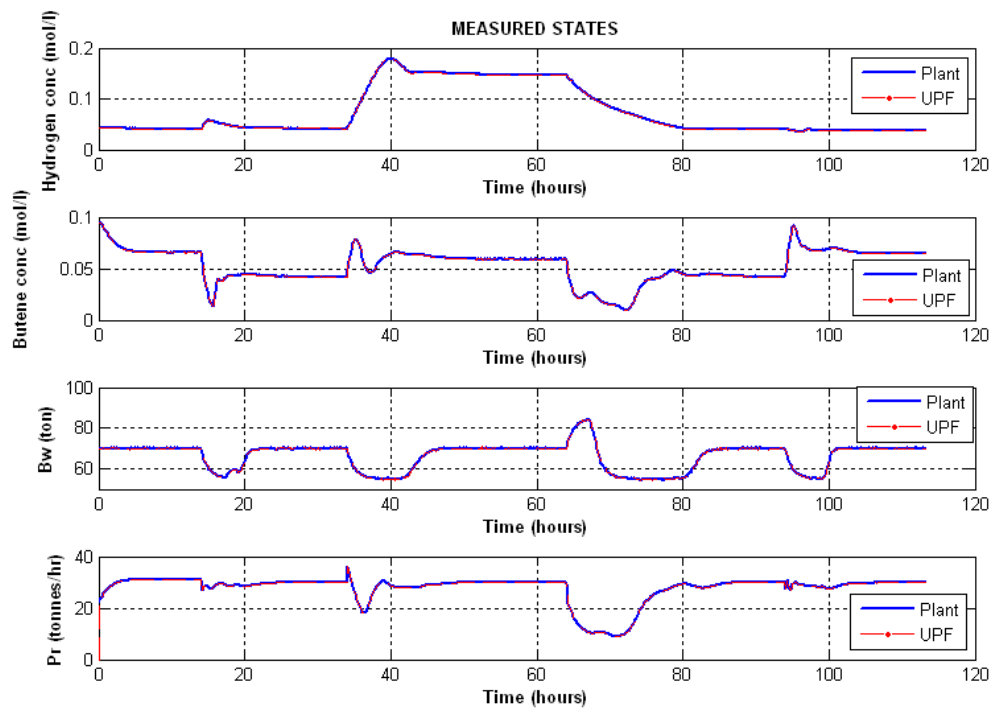


Figure 4.11: Measurement smoothing using unscented particle filters for gas phase FBR for polyethylene production (plots have been scaled due to the proprietary nature of the data)

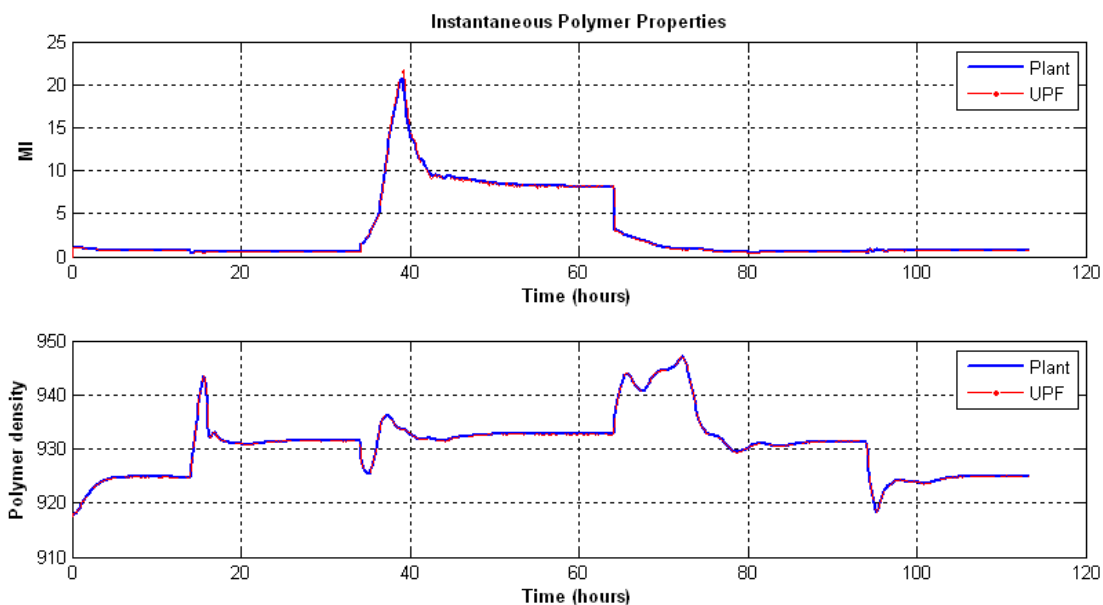


Figure 4.12: Estimation of polymer product properties using unscented particle filters for gas phase FBR for polyethylene production (plots have been scaled due to the proprietary nature of the data)

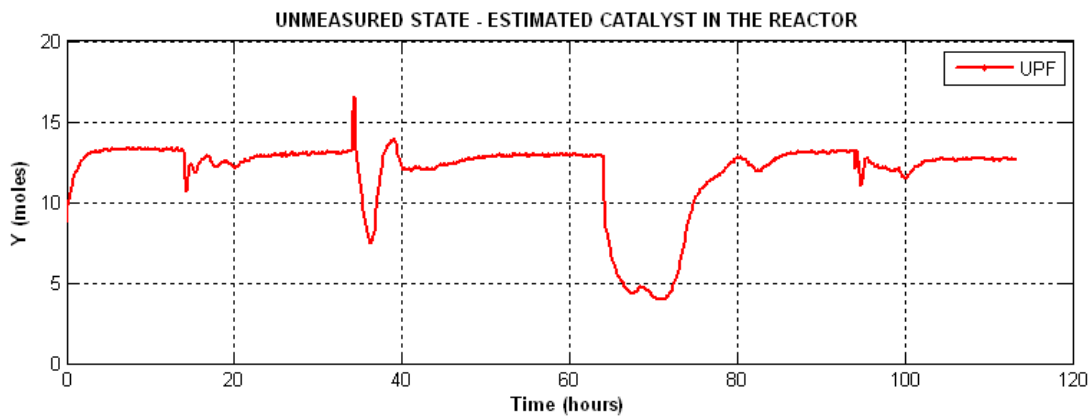


Figure 4.13: Estimation of unmeasured state using unscented particle filters for gas phase FBR for polyethylene production (plots have been scaled due to the proprietary nature of the data)

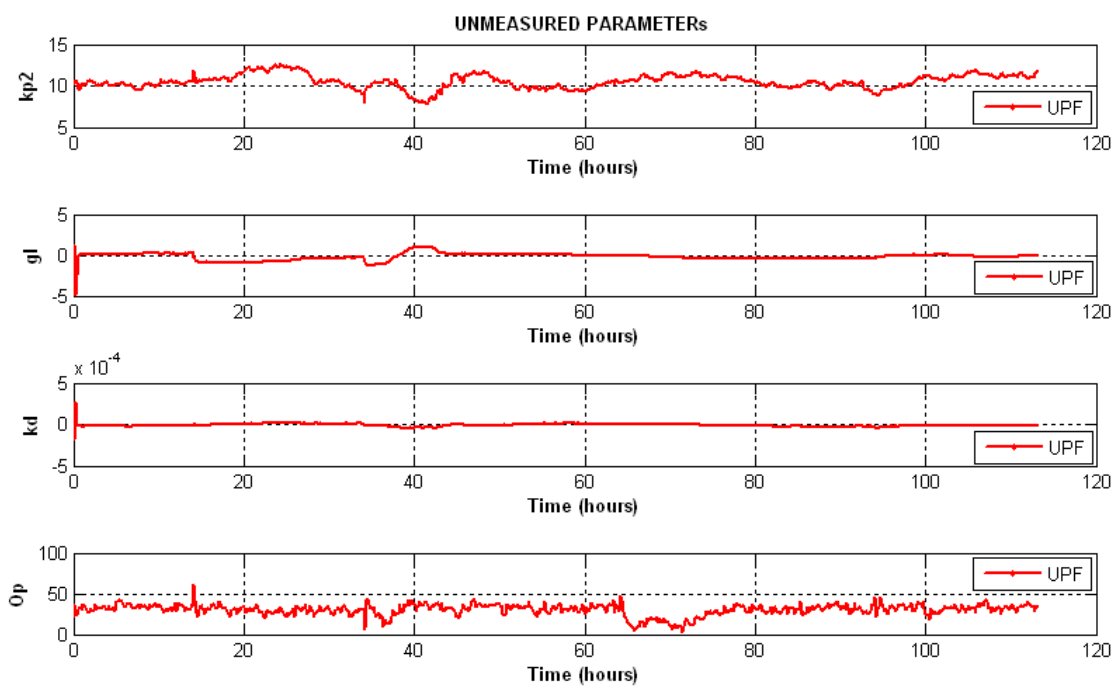


Figure 4.14: Parameter estimation using unscented particle filters for gas phase FBR for polyethylene production (plots have been scaled due to the proprietary nature of the data)

# Chapter 5

## Concluding remarks and future work

### 5.1 Concluding remarks

Fig. 5.1 summarizes the approach to estimation developed and investigated in this thesis. While this work focuses on chemical process systems, the results are applicable to all fields of science and engineering that may make use of unconstrained estimation techniques. The KF is the optimal solution to linear systems. In the case of nonlinear systems, the EKF is the most widely used filter. In this thesis, it was shown that the EKF is prone to approximation and linearization errors depending on the nonlinear dynamics of the system under consideration. In this case, the UKF and EnKF provide improved solutions to the estimation problem. However, the choice between the EnKF and UKF depends on the computational power of the two algorithms. This varies with the system under consideration. Most process dynamics are highly nonlinear and this leads to non-Gaussian distributions of states and parameters. To handle this, a filter that does not approximate distributions to be Gaussian must be used. The particle filter was shown to be an effective solution for non-Gaussian distributions. However, the PF is not robust to plant-model mismatch. In chapter 4, the effectiveness of the UPF for estimation in the case of high plant-model mismatch was clearly demonstrated. The UPF is a filter that handles non-Gaussian random variables, full state distributions and is stable enough to be used in cases of high plant-model mismatch. The only drawback of the UPF, compared to the PF, is the added computational requirement.

In this thesis, various estimation techniques were compared. Some of the robustness issues of estimators were also addressed. One of them was the bias that

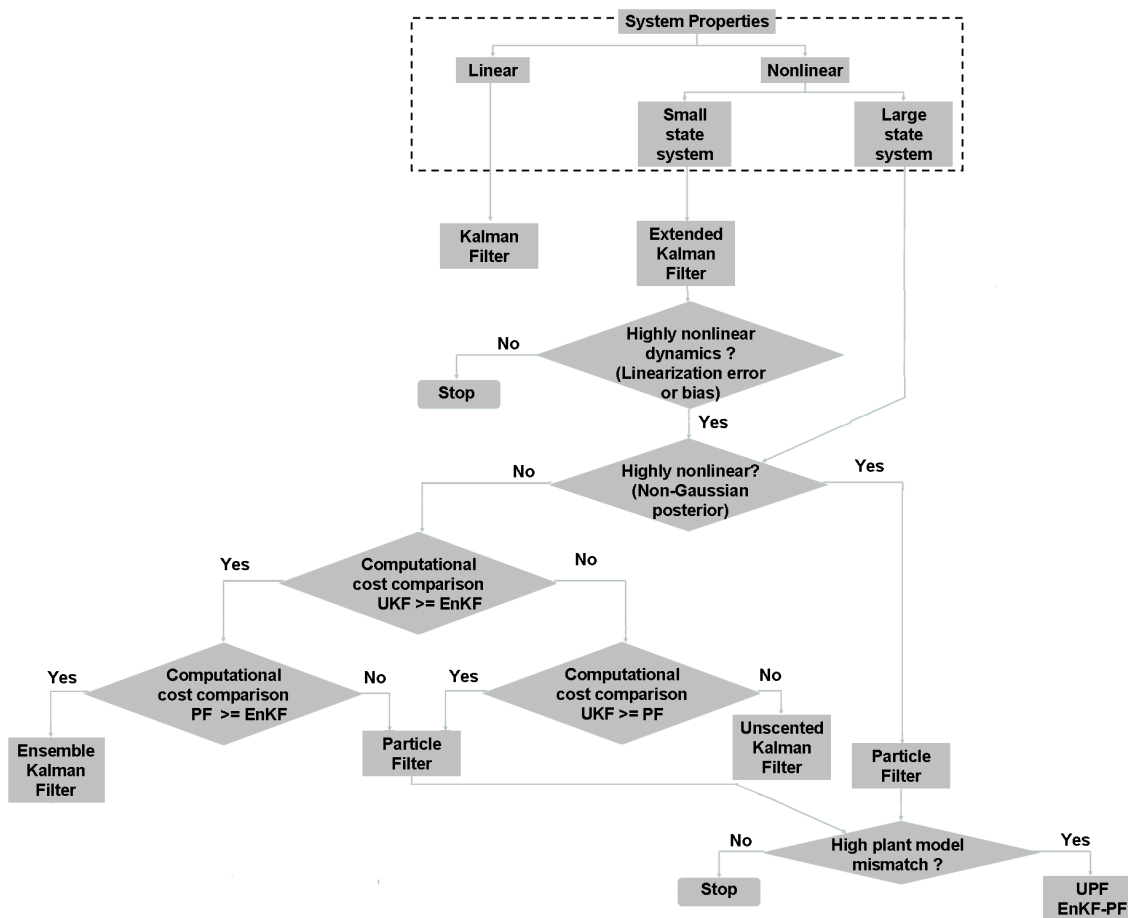


Figure 5.1: Flowchart to help in the decision for choice of state estimation technique

occurred between the state estimate and the true state. Bias in state estimates can occur due to parametric mismatches between the model and true parameters or due to linearization errors. Bias can be eliminated using methods of state augmentation or parameter estimation. In chapter 3, integral action, similar to that of PID controllers, was used to eliminate bias. Another issue that was addressed, was the extraction of a point estimate from the full state distributions obtained using PFs. k-means clustering was used to extract the modes from the posterior distributions obtained using the PF.

Nonlinear estimation is an open area of study. However, it is important to note that there may not exist a general solution to the nonlinear state estimation problem. But the application of estimation theory is system specific and depends on the dynamics and stability of the system under consideration.

To elucidate the novelty of our work: This thesis provides detailed guidelines for the selection of appropriate unconstrained estimators for chemical processes. In chapter 2, first, a systems approach of state estimation was analyzed using a PMMA reactor under different noise distribution sequences. Later, the linearization error of the EKF was exhibited. A comparison of the EnKF and UKF, followed by the advantage of the PF in estimating non-Gaussian distributions was demonstrated. The robustness of the UPF, in comparison to the PF, in the case of high plant-model mismatch was demonstrated in chapter 4. To account for estimation bias due to model-plant mismatches, integral action was introduced in state estimation algorithms. k-means clustering was used to extract a point estimate from full state posterior distributions.

## **5.2 Future work**

### **5.2.1 Nonlinear observability**

As explained in the introduction of this thesis, observability is a very important criteria, that defines which states can be estimated. For linear systems, the rank of the observability matrix defines the number of states that can be estimated. In the case of EKF, the same procedure holds good, as the equations representing system dynamics are linearized at each instant in time. However, in the case of the other nonlinear estimators (UKF, PF, EnKF), the nonlinear equations are directly used (no linearization) by the estimation algorithms. Finding the observability of a nonlinear system is an open problem. Research needs to be conducted, to

demonstrate the advantages or disadvantages of using estimation techniques that use linear or nonlinear observability. It is important to note that a systems observability may change based on it being linearized or not. However, examples pertaining to change in observability have not been discovered yet and need to be demonstrated.

### **5.2.2 Issues with particle filters**

#### **Effective handling of non-Gaussian measurement noise**

Though a lot of literature aims at generation of proposal distributions, not much information exists about the design of likelihood functions based on measurement noise statistics. In most examples, the likelihood is represented by a Gaussian probability density function. However, in the case of non-Gaussian measurement noise sequence, models of measurement noise can be identified and the distribution can be represented in the form of sum of Gaussian distributions. A recent study in this area has been done by Mukherjee and Sengupta (2010). This would provide better state estimates, as the assumption of Gaussian measurement likelihood is eliminated.

#### **Multivariate methods for mode detection in case of non-Gaussian posteriors**

In this thesis, the importance of extraction of a point estimate from full state distributions obtained using particle filters was demonstrated. However, the method developed was easy to implement for the example used, as distributions were distinctly bimodal or unimodal. Generalized methods in the form of constraints or multivariate methods need to be designed in order to resolve the problem of point estimate extraction from full state distributions. If the correct point estimate is extracted, the particle filter can be considered as the optimal solution for the nonlinear state estimation problem.

### **5.2.3 Subspace identification for state estimation**

Subspace identification is able to provide all the necessary information for implementing Kalman filters for linear systems. This would solve two major issues - (1) The physical models that are required by the estimator may be eliminated (2) Noise covariance matrices obtained through subspace identification are actually tuning parameters when the estimators are implemented using first principles models. The

use of subspace identification for state estimation and tuning needs to be attempted. Obtaining a physically meaningful state transition matrix from input - output data using subspace identification needs to be investigated. These methods must then be extended to nonlinear estimators. This would add to the robustness of using estimators online, as identification models may represent system dynamics more accurately than first principles models.

#### **5.2.4 Proportional integral based estimators**

Integral action is a very powerful tool in PID controllers due to the fact that it eliminates bias. The basis for introduction integral action into estimation algorithms has been outlined in this thesis. The introduction of integral action to various linear and nonlinear estimation algorithms by choosing appropriate noise models needs to be investigated. This would be particularly useful as model-plant mismatch are inevitable.

#### **5.2.5 Polyethylene FBR : future work**

A lot of work is currently being conducted on the polyethylene reactor. The reduced order model is being studied for stability and estimation techniques were being applied under the ideal case of no plant-model mismatch. Estimation techniques under different realistic disturbances that may be experienced in the plant are being used to simulate case studies to study the use of different estimation techniques. On a further scale, the propagation of full state distributions through nonlinear controller is being studied. It is important to note that a full order model should be used for simulation of the plant, and a lower order model for the estimation. This represents a realistic scenario for application of state estimation.

#### **5.2.6 Estimation of MWD and PSD**

Techniques for estimation of MWD and PSD in polymerization reactors remains a long term goal of this project. Complex models that can predict MWD and PSD are being developed by many researchers. However, the application of estimators to these models has not yet been attempted. The challenges in this work include the complexity of the model, and the choice of equations and measurements that might make the model observable.

### **5.2.7 Tuning of filters**

During the course of this work, an attempt was made to address optimal tuning of filters. The vastness of the area and the large amount of literature has lead to it being a part of future work.

# Bibliography

- Arulampalam, S., Maskell, S., Gordon, N., and Clapp, T. (2002). A tutorial on particle filters for on-line non-linear/non-gaussian Bayesian tracking. *IEEE Trans. Signal Processing*, 50 (2), 174 – 189.
- Asua, J. (2007). *Polymer reaction engineering*. Blackwell Publishing.
- Baker, L. (2007). Properties of the ensemble Kalman filter.
- Carvalho, A.B.D., Gloor, P.E., and Hamielec, A.E. (1989). A kinetic mathematical model for heterogenous ziegler-natta copolymerization. *POLYMER*, 30, 280 – 296.
- Chatzidoukasa, C., Perkins, J.D., Pistikopoulos, E.N., and Kiparissides, C. (2003). Optimal grade transition and selection of closed-loop controllers in a gas-phase olefin polymerization fluidized bed reactor. *Chemical Engineering Science*, 58(16), 3643 – 3658.
- Chen, T., Morris, J., and Martin, E. (2005). Particle filters for state and parameter estimation in batch processes. *Journal of Process Control*, 15 (6), 665 – 673.
- Chen, W., Bakshi, B., Goel, P.K., and Ungarala, S. (2004). Bayesian estimation via sequential Monte Carlo sampling: unconstrained nonlinear dynamic systems. *Ind. Eng. Chem. Res.*, 43 (14), 4012–4025.
- Choi, K.Y. and Ray, W.H. (1985). The dynamic behaviour of fluidized bed reactors for solid catalysed gas phase olefin polymerization. *Chemical Engineering Science*, 40(12), 2261 – 2279.
- Daum, F. (2005). Nonlinear filters: beyond the Kalman filter. *IEEE A&E Systems Magazine*, 20, 57–69.

- der Merwe, R.V., Doucet, A., de Freitas, N., and Wan, E. (2000). *The unscented particle filter*. Tech. rep. CUED/F-INFENG/TR 380, Cambridge University Engineering Department.
- Dompazis, G., Kanellopoulos, V., and Kiparissides, C. (2005). A multi-scale modeling approach for the prediction of molecular and morphological properties in multi-site catalyst, olefin polymerization reactors. *Macromolecular Materials and Engineering*, 290(6), 525 – 536.
- Dompazis, G., Kanellopoulos, V., Touloupides, V., and Kiparissides, C. (2008). Development of a multi-scale, multi-phase, multi-zone dynamic model for the prediction of particle segregation in catalytic olefin polymerization fbr's. *Chemical Engineering Science*, 63, 4735 – 4753.
- Doucet, A., de Freitas, N., and Gordon, N.J. (2001). *Sequential Monte Carlo methods in practice*. Springer, NewYork.
- Embirucu, M., Lima, E.L., and Pinto, J.C. (1996). A survey of advanced control of polymerization reactors. *In Proc. SPIE*, 36, 433–437.
- Evensen, G. (1994a). The ensemble Kalman filter: theoretical formulations and practical implementations. *Journal of Geophysical Research*, 99, 10,143 – 10,162.
- Evensen, G. (1994b). Sequential data assimilation with a nonlinear quasi-geostrophic model using Monte Carlo methods to forecast error statistics. *JOURNAL OF GEOPHYSICAL RESEARCH*, 99, 10,143 – 10,162.
- Fernandes, F.A.N. and Lona, L.M.F. (2001). Heterogenous modeling for fluidized-bed polymerization reactor. *Chem. Eng. Sci.*, 56, 963 – 969.
- Gelb, A. (1974). *Applied optimal estimation*. M.I.T. Press Cambridge MA.
- Gillijns, S., Mendoza, O.B., Chandrasekar, J., Moor, B.L.R.D., Bernstein, D.S., and Ridley, A. (2006). What is the ensemble Kalman filter and how well does it work? In *Proceedings of the 2006 American Control Conference*. Minneapolis, Minnesota, USA.
- Goodwin, G.C. and Sin, K.S. (1984). *Adaptive filtering, prediction and control*. Prentice-Hall.

- Gordon, N., Salmond, D., and Smith, A.F.M. (1993). Novel approach to nonlinear and non-gaussian Bayesian state estimation. *Proc. Inst. Elect. Eng.*, 40, 107–113.
- Gudi, R., Shah, S.L., and Gray, M. (1994). Multirate state and parameter estimation in an antibiotic fermentation with delayed measurements. *Biotechnology and Bioengineering*, 44, 1271 – 1278.
- Haseltine, E.L. and Rawlings, J.B. (2005). Critical evaluation of extended Kalman filtering and moving-horizon estimation. *Ind. Eng. Chem. Res.*, 44 (8), 2451 – 2460.
- Hatzantonis, H., Goulas, A., and Kiparissides, C. (1998). A comprehensive model for the prediction of particle-size distribution in catalyzed olefin polymerization fluidized-bed reactors. *Chem. Eng. Sci.*, 53(18), 3251 – 3267.
- Hatzantonis, H., Yiannoulakis, H., Yiagopoulos, A., and Kiparissides, C. (2000). Recent developments in modeling gas-phase catalyzed olefin polymerization fluidized-bed reactors: The effect of bubble size variatio on the reactor’s performance. *Chem. Eng. Sci.*, 55, 3237 – 3259.
- Hutchinson, R.A., Chen, C.M., and Ray, W.H. (1992). Polymerization of olefins through heterogeneous catalysis x: Modeling of particle growth and morphology. *Journal of applied polymer science*, 44, 1389 – 1414.
- Imtiaz, S.A., K.Roy, B.Huang, Shah, S.L., and Jampana, P. (2006). Estimation of states of nonlinear systems using a particle filter. *IEEE International Conference on Industrial Technology*, 1, 2432–2437.
- Jazwinski, A.H. (1970). *Stochastic processes and filtering theory*. Academic Press, New York.
- Jo, J.H. and Bankoff, S.G. (1976). Digital monitoring and estimation of polymerization reactors. *Amer. Inst. Chem. Engrs*, 22 (2), 361 – 368.
- Julier, S.J. and Uhlmann, J.K. (1997). A new extension of the Kalman filter to nonlinear systems. *In Proc. SPIE*, 3068, 182–193.
- Kalman, R.E. (1960). A new approach to linear filtering and prediction problems. *Journal of Basic Engineering (ASME)*, 82D, 35 – 45.

- Kandepu, R., Foss, B., and Imsland, L. (2008). Applying the unscented Kalman filter for nonlinear state estimation. *Journal of Process Control*, 18, 753 – 768.
- Kanellopoulos, V., Dompazis, G., Gustafsson, B., and Kiparissides, C. (2004). Comprehensive analysis of single-particle growth in heterogeneous olefin polymerization: The random-pore polymeric flow model. *Ind. Eng. Chem. Res.*, 43(17), 5166 – 5180.
- Kiparissides, C. and Morris, J. (1996). Intelligent manufacturing of polymers. *Comp. Process Control*, 10, 1637–1659.
- Kolas, S., Foss, B.A., and Schei, T.S. (2009). Constrained nonlinear state estimation based on the UKF approach. *Computers and Chemical Engineering*, 33, 1386 – 1401.
- Kozub, D.J. and MacGregor, J.F. (1992). State estimation for semi-batch polymerization reactors. *Chemical Engineering Science*, 47 (5), 1047 – 1062.
- Lee, J. and Ricker, N. (1994). Extended Kalman filter based nonlinear model predictive control. *Ind. Eng. Chem. Res.*, 33(6), 1530 – 1541.
- Maybeck, P.S. (1979). *Stochastic models, estimation, and control*. Academic Press Inc.
- McAuley, K.B. (1991). *Modelling, estimation and control of product properties in a gas phase polyethylene reactor*. Ph.D. thesis, McMaster University, Canada.
- McAuley, K.B. and MacGregor, J.F. (1991). On-line inference of polymer properties in an industrial polyethylene reactor. *AIChE Journal*, 37(6), 825 – 835.
- McAuley, K.B. and MacGregor, J.F. (1992). Optimal grade transitions in a gas phase polyethylene reactor. *AIChE Journal*, 38(10), 1564 – 1576.
- McAuley, K.B. and MacGregor, J.F. (1993). Nonlinear product property control in industrial gas-phase polyethylene reactors. *AIChE Journal*, 39(5), 855 – 866.
- McAuley, K.B., MacGregor, J.F., and Hamielec, A.E. (1990). A kinetic model for industrial gas-phase ethylene copolymerization. *AIChE Journal*, 36(6), 837 – 850.
- Mukherjee, A. and Sengupta, A. (2010). Likelihood function modeling of particle filter in presence of non-stationary non-gaussian measurement noise. *Signal Processing*, 90, 1873–1885.

- Ning, X. and Fang, J. (2008). Spacecraft autonomous navigation using unscented particle filter-based celestial/doppler information fusion. *Measurement Science and Technology*, 19(9), 1 – 8.
- Ohshima, M. and Tanigaki, M. (2000). Quality control of polymer production processes. *J. Process Control*, 10, 135 – 148.
- P. Vachhani and, S.N. and Rengaswamy, R. (2006). Robust and reliable estimation via unscented recursive nonlinear dynamic data reconciliation. *Journal of Process Control*, 16 (10), 1075 – 1086.
- Prakash, J., Patwardhan, S.C., and Shah, S.L. (2008). Constrained state estimation using particle filter. In *Proceedings of the 17th World Congress The International Federation of Automatic Control*. Seoul, Korea.
- Prakash, J., Patwardhan, S.C., and Shah, S.L. (2010). Constrained nonlinear state estimation using ensemble Kalman filters. *Ind. Eng. Chem. Res.*, 49(5), 2242 – 2253.
- Prasad, V., Schley, M., Russo, L.P., and Bequette, B.W. (2002). Product property and production rate control of styrene polymerization. *Journal of Process Control*, 12(3), 353 – 372.
- Qu, C.C. and Hahn, J. (2009). Process monitoring and parameter estimation via unscented Kalman filtering. *Biotechnology and Bioengineering*, 22, 703 – 709.
- Rawlings, J.B. and Bakshi, B.R. (2006). Particle filtering and moving horizon estimation. *Computers and Chemical Engineering*, 30, 1529 – 1541.
- Ray, W.H. (1981). *Advanced Process Control*. McGraw-Hill, New York.
- Ristic, B., Arulampalam, S., and Gordon, N. (2004). *Beyond the Kalman filter: particle filters for tracking applications*. Artech House, Boston.
- Romanenko, A. and Castro, J.A.A.M. (2004). The unscented filter as an alternative to the EKF for nonlinear state estimation: a simulation case study. *Comp. Chem. Eng.*, 28(3), 347 – 355.
- Rui, Y. and Chen, Y. (2001). Better proposal distributions: Object tracking using unscented particle filter. In *Proc. IEEE Conf. Computer Vision and Pattern Recognition (volume 2)*. Kauai, Hawaii.

- Schmidt, S.F. (1966). Applications of state space methods to navigation problems. In C. T. Leondes, editor, *Advanced Control Systems*, 3, 293 – 340.
- Shao, X., Huang, B., and Lee, J. (2010). Constrained Bayesian state estimation – a comparative study and a new particle filter based approach. *Journal of Process Control*, 20, 143 – 157.
- Shenoy, A.V., Bhat, C., Gundappa, M., and Ravindra, G. (2008). Closed loop regulatory control strategies for a fluidized bed reactor: An industrial case study. In *Proceedings of the 17th World Congress The International Federation of Automatic Control*. Seoul, Korea.
- Simon, D. (2006). *Optimal state estimation*. Wiley-Interscience, New York.
- Sorenson, H.W. (1985). *Kalman filtering: theory and application*. IEEE Press.
- Soroush, M. (1998). State and parameter estimations and their applications in process control. *Comput. Chem. Eng.*, 23(2), 229 – 245.
- Sriniwas, G.R., Arkun, Y., and Schork, F.J. (1994). Estimation and control of an  $\alpha$ -olefin polymerization reactor. *J. Proc. Cont.*, 5(5), 303 – 313.
- Wan, E.A. and van der Merwe, R. (2000). The unscented Kalman filter for nonlinear estimation. *Proc. of IEEE Symposium 2000 (AS-SPCC), Lake Louise, Alberta, Canada*, 153–158.
- Welch, G. and Bishop, G. (2001). An introduction to the Kalman filter. In *ACM SIGGRAPH Intl. Conf. on Computer Graphics and Interactive Techniques*. LA, CA, USA.
- Wilson, D.I., Agarwal, M., and Rippin, D.W.T. (1998). Experiences implementing the extended Kalman filter on an industrial batch reactor. *Comp. Chem. Eng.*, 22(11), 1653 – 1672.
- Xie, T., McAuley, K.B., Hsu, J.C.C., and Bacon, D.W. (1994). Gas phase ethylene polymerization: Production processes, polymer properties, and reactor modeling. *Industrial Chemistry Research*, 33, 449 – 479.
- Yiannoulakis, H., Yiagopoulos, A., and Kiparissides, C. (2001). Recent developments in the particle size distribution modeling of fluidized-bed olefin polymerization reactors. *Chem. Eng. Sci.*, 56, 917 – 925.